

TLR4 NEUROINFLAMMATORY SIGNALING AND  
THE ANTI-INFLAMMATORY EFFECTS OF  
FENTANYL AND MORPHINE IN CHME-5  
MICROGLIAL CELLS

By

LEANDRA K. FIGUEROA-HALL

Bachelor of Science in Biology  
University of the Virgin Islands  
St. Thomas, USVI  
2008

Master of Science  
University of Maryland, School of Medicine  
Baltimore, MD  
2011

Submitted to the Faculty of the  
Graduate College of the  
Oklahoma State University  
in partial fulfillment of  
the requirements for  
the Degree of  
DOCTOR OF PHILOSOPHY  
July 2017

TLR4 NEUROINFLAMMATORY SIGNALING AND  
THE ANTI-INFLAMMATORY EFFECTS OF  
FENTANYL AND MORPHINE IN CHME-5  
MICROGLIAL CELLS

Dissertation Approved:

Dr. Randall L. Davis

---

Dissertation Adviser

Dr. Craig W. Stevens

---

Dr. J. Thomas Curtis

---

Dr. Kent Teague

---

Dr. Robert W. Allen

---

## ACKNOWLEDGEMENTS

First and foremost, I would like to thank God for giving me the strength and tenacity to achieve this lifelong goal. Without Him nothing is possible. Secondly, I would like to dedicate my dissertation to my grandmother, Petra Melendez (Mama), who passed last year July. I would always call Mama on my drive to and from school, and she would ask, “going home so late”, “you going in on the weekend, or “when are you finishing?” That always made me laugh. I know she is looking down and is very proud of what I have accomplished.

I would also like to thank my husband, Keith, for supporting me throughout all of these years. Thank you for doing the dishes, laundry, and taking care of Christian when I had to be at school late nights or on the weekends. Just know that this is not only my success, but also ours. Love you to the moon and back! A special thanks to my parents, Juan and Catherine Figueroa, and my brother, Juan Figueroa-Serville, and his family, for always believing in me and supporting me throughout all these years. I love you very much.

And finally, my acknowledgements would not be complete without thanking my Oklahoma State University family. Thank you Dr. Davis, for your dedication and advice throughout my time in your lab. Because of you I have matured as a critical thinker and scientist. I will always be proud to say that I received my Ph.D. under your mentorship. A special thank you to all of my committee members for your support and guidance: Dr. Craig W. Stevens, Dr. J Thomas Curtis, Dr. Robert W. Allen, and Dr. Kent Teague. Thank you to Michael Anderson, who collaborated with the immunocytochemistry studies. And last but not least, to Joni, Kelly, and Daniel, thank you for putting up with me during all these years. If it were not for you I probably would not have had such an easy breezy time at OSU! Love you guys!

Name: LEANDRA K. FIGUEROA-HALL

Date of Degree: JULY, 2017

Title of Study: TLR4 NEUROINFLAMMATORY SIGNALING AND THE ANTI-INFLAMMATORY EFFECTS OF FENTANYL AND MORPHINE IN CHME-5 MICROGLIAL CELLS

Major Field: BIOMEDICAL SCIENCES

**Abstract:** Microglia are instrumental in neuroinflammation, which is a key factor in neuronal damage in many neurological disorders. Pro-inflammatory mediators activate these cells, including bacterial lipopolysaccharide (LPS) that signals through toll-like receptor 4 (TLR4). In the field of neuroinflammation, identifying the specific effects of pharmacological agents and other factors on microglia is often problematic given the difficulty and expense in obtaining and culturing primary microglia. Thus, immortalized microglial cell lines are very useful. Therefore, characterization of LPS-induced TLR4 signaling in the CHME-5 microglial cell line was expected to be of value as an experimental model of inflammatory signaling in the central nervous system (CNS). Inflammatory signaling in response to *Escherichia coli* LPS induced I $\kappa$ B $\alpha$  and NF- $\kappa$ B p65 activation, NF- $\kappa$ B p65 binding activity, and *TNFA* gene expression. We confirmed the maintenance of microglial phenotype as seen with increased CD68 expression and the absence of GFAP-immunoreactivity. TLR4 expression was significantly increased after LPS treatment. Another family of receptors expressed in the CNS is the opioid receptors, which are guanine protein coupled receptors (GPCRs) and mediate their effects with the binding of opioids. Most notably, the *mu* opioid receptor (MOR) is expressed in many organ systems and binds opioid agonists, morphine and fentanyl, and antagonists, naloxone and naltrexone. Research shows that opioids modulate immune function, and therefore, our goal was to determine the effects of fentanyl and morphine on LPS-induced TLR4 signaling in CHME-5 cells. Co-treatment with LPS and fentanyl revealed a significant decrease in I $\kappa$ B $\alpha$  activation and NF- $\kappa$ B p65 binding activity, while morphine only decreased I $\kappa$ B $\alpha$  activation. Conversely, no differences in LPS-induced TLR4 or MyD88 expression were seen with co-treatment of fentanyl or morphine. Finally, treatment with naltrexone following LPS and fentanyl co-treatment did not reverse the opioid-mediated effect on NF- $\kappa$ B p65 binding activity. We have shown that CHME-5 microglial cell attributes are conserved, which makes these cells a beneficial tool for studying microglial inflammatory signaling. Additionally, results demonstrate that fentanyl, and to a lesser extent morphine, display anti-inflammatory effects through down-regulation of I $\kappa$ B $\alpha$  activation and NF- $\kappa$ B p65 binding activity, which may be instrumental during treatment of CNS-localized insults or neurodegeneration.

## TABLE OF CONTENTS

CHAPTER ONE: TLR4-NEUROINFLAMMATORY SIGNALING IN CHME-5 MICROGLIAL CELLS .....	1
LITERATURE REVIEW .....	2
TOLL-LIKE RECEPTORS .....	2
GRAM-NEGATIVE LPS .....	4
TLR4 RECOGNIZES GRAM-NEGATIVE LPS .....	4
MYD88-DEPENDENT SIGNALING .....	5
TRIF-DEPENDENT SIGNALING .....	6
TOLL-LIKE RECEPTORS EXPRESSED IN THE CENTRAL NERVOUS SYSTEM .....	7
NEUROINFLAMMATION IN THE CENTRAL NERVOUS SYSTEM.....	8
NEURODEGENERATION.....	9
IDENTIFICATION OF MICROGLIA .....	12
ORIGIN AND DEVELOPMENT.....	13
MICROGLIAL FUNCTION.....	15
NEUROPROTECTIVE VS. NEUROTOXIC .....	17
SURFACE ANTIGENS/RECEPTORS .....	17
CYTOKINES/CHEMOKINES.....	18
EXPERIMENTAL TOOL FOR THE STUDY OF MICROGLIA.....	18
PRIMARY CELLS.....	19
CELL LINES .....	19
METHODOLOGY .....	24
CELL CULTURE .....	24
LPS TREATMENT .....	24

MTT ASSAY.....	24
PROTEIN EXTRACTION .....	25
PROTEIN ASSAY.....	26
IMMUNOBLOT ANALYSIS.....	26
RNA EXTRACTION .....	28
RNA INTEGRITY .....	29
REVERSE TRANSCRIPTION.....	30
REVERSE TRANSCRIPTION-POLYMERASE CHAIN REACTION.....	30
IMMUNOCYTOCHEMISTRY .....	31
EPIFLUORESCENCE MICROSCOPY .....	32
CONFOCAL MICROSCOPY .....	32
NF- $\kappa$ B p65 BINDING ASSAY .....	33
STATISTICAL ANALYSIS.....	34
RESULTS .....	35
LPS-INDUCED ACTIVATION OF NF- $\kappa$ B p65 IN CHME-5 CELLS.....	35
LPS IS NOT TOXIC.....	35
LPS-MEDIATED ACTIVATION OF NF- $\kappa$ B p65 .....	35
ALPHA-TUBULIN AND HISTONE 3-IMMUNOREACTIVITY AS INTERNAL CONTROL.....	35
LPS-INDUCED CD68 EXPRESSION IN CHME-5 MICROGLIAL CELLS.....	36
<i>CD68</i> GENE EXPRESSION IN CHME-5 CELLS .....	36
CD68 PROTEIN EXPRESSION IN CHME-5 CELLS.....	36
CHME-5 CELLS ARE GFAP NEGATIVE .....	36
LPS-INDUCED TLR4 EXPRESSION IN CHME-5 CELLS .....	37
<i>TLR4</i> GENE EXPRESSION IN CHME-5 CELLS.....	37
LPS IS NOT TOXIC AT LATER TIME POINTS.....	37
TLR4 PROTEIN EXPRESSION IN CHME-5 CELLS.....	37
ANALYSIS OF CD68 AND TLR4 IMMUNOCYTOCHEMISTRY.....	37
QUANTITATIVE ANALYSIS OF CD68- AND TLR4-IMMUNOFLUORESCENCE IN CHME-5 CELLS.....	37
QUALITATIVE ANALYSIS OF CD68 AND TLR4 IMMUNOFLUORESCENCE.....	38
LPS-INDUCED I $\kappa$ B $\alpha$ ACTIVATION IN CHME-5 CELLS .....	38
LPS-INDUCED NF- $\kappa$ B p65 BINDING ACTIVITY .....	39
LPS-INDUCED NF- $\kappa$ B p65 ACTIVATION AT 90 MINUTES IN CHME-5 CELLS.....	39

LPS DOES NOT INDUCE P38 ACTIVATION IN CHME-5 CELLS.....	39
LPS-INDUCED <i>TNFA</i> GENE EXPRESSION.....	39
FIGURES .....	41
DISCUSSION .....	57
CHAPTER TWO: FENTANYL, AND TO A LESSER EXTENT MORPHINE, DISPLAY ANTI-INFLAMMATORY EFFECTS ON LPS-INDUCED TLR4 NEUROINFLAMMATORY SIGNALING .....	63
LITERATURE REVIEW .....	64
OPIOID RECEPTORS.....	64
OPIOID RECEPTORS IN THE PERIPHERY .....	65
<i>MU (M)</i> OPIOID RECEPTOR (MOR) .....	66
<i>DELTA (A)</i> OPIOID RECEPTOR (DOR).....	66
<i>KAPPA (K)</i> OPIOID RECEPTOR (KOR) .....	66
<i>NOCICEPTIN/ORPHANIN FQ</i> RECEPTOR PEPTIDE (NOP).....	67
OPIOID PEPTIDES AND DRUGS .....	67
OPIOID AGONISTS .....	68
MORPHINE .....	68
FENTANYL .....	69
OTHER OPIOIDS.....	70
OPIOID ANTAGONISTS .....	71
OPIOID RECEPTOR SIGNALING.....	74
OPIOID RECEPTOR SIGNALING REGULATION: INTERNALIZATION AND DOWN-REGULATION....	75
OPIOID TOLERANCE, DEPENDENCE, AND ADDICTION.....	76
OPIOID RECEPTORS AND IMMUNE FUNCTION .....	78
EXPRESSION OF MOR IN MICROGLIA .....	80
METHODOLOGY .....	83
CHME-5.....	83
LPS TREATMENT.....	83
OPIOID COMPOUNDS .....	83

RNA EXTRACTION WITH TRIZOL.....	84
RNA INTEGRITY WITH NORTHERNMAX-GLY KIT.....	84
REVERSE TRANSCRIPTION.....	85
REVERSE TRANSCRIPTION-POLYMERASE CHAIN REACTION.....	85
PROTEIN EXTRACTION.....	86
PROTEIN ASSAY.....	86
IMMUNOBLOT ANALYSIS.....	87
MTT ASSAY.....	88
NF- $\kappa$ B P65 BINDING ASSAY .....	88
STATISTICAL ANALYSIS.....	89
RESULTS .....	90
LPS-INDUCED <i>MU</i> OPIOID RECEPTOR (MOR) GENE EXPRESSION IN CHME-5 CELLS.....	90
FENTANYL-MEDIATED EFFECT ON LPS-INDUCED TLR4 EXPRESSION .....	90
FENTANYL-MEDIATED EFFECT ON LPS-INDUCED MYD88 EXPRESSION.....	90
FENTANYL-MEDIATED EFFECT ON LPS-INDUCED I $\kappa$ B $\alpha$ ACTIVATION.....	91
FENTANYL-MEDIATED EFFECT ON LPS-INDUCED NF- $\kappa$ B P65 BINDING ACTIVITY .....	91
EFFECT OF NALTREXONE ON FENTANYL-MEDIATED DOWN-REGULATION OF LPS-INDUCED NF- $\kappa$ B P65 BINDING ACTIVITY .....	91
MORPHINE-MEDIATED EFFECT ON LPS-INDUCED TLR4 EXPRESSION .....	92
MORPHINE-MEDIATED EFFECT ON LPS-INDUCED MYD88 EXPRESSION.....	92
MORPHINE-MEDIATED EFFECT ON LPS-INDUCED I $\kappa$ B $\alpha$ ACTIVATION.....	92
MORPHINE-MEDIATED EFFECT ON LPS-INDUCED NF- $\kappa$ B P65 BINDING ACTIVITY .....	92
FIGURES.....	94
DISCUSSION .....	108
CONCLUSION.....	114
REFERENCES .....	116



## LIST OF FIGURES

### CHAPTER ONE

Figure 1. <i>Escherichia coli</i> LPS O55:B5 and O111:B4 are not cytotoxic to CHME-5 cells .....	41
Figure 2. LPS-induced activation of NF- $\kappa$ B in CHME-5 cells .....	42
Figure 3. alpha-tubulin and histone 3-immunoreactivity in CHME-5 cellular fractions..	43
Figure 4. LPS-induced <i>CD68</i> gene expression in CHME-5 cells.....	44
Figure 5. LPS-induced CD68 protein expression in CHME-5 cells.....	45
Figure 6. CHME-5 cells are CD68-positive and GFAP-negative .....	46
Figure 7. LPS-induced <i>TLR4</i> gene expression in CHME-5 cells .....	47
Figure 8. LPS-induced TLR4 protein expression in CHME-5 cells.....	48
Figure 9. Quantitative analysis of LPS-induced CD68- and TLR4-immunofluorescence with epifluorescence microscopy.....	49
Figure 10. Visualization of LPS-induced CD68- and TLR4-immunofluorescence with confocal microscopy .....	51
Figure 11. LPS-induced I $\kappa$ B $\alpha$ activation increases at 10 minutes in CHME-5 cells .....	52
Figure 12. LPS-induced NF- $\kappa$ B p65 activation in CHME-5 cells.....	53
Figure 13. LPS-induced NF- $\kappa$ B p65 activation at 90 minutes in CHME-5 cells.....	54
Figure 14. LPS does not induce p38 activation in CHME-5 cells.....	55
Figure 15. LPS-induced TNF $\alpha$ gene expression in CHME-5 cells.....	56

### CHAPTER TWO

Figure 1. LPS-induced <i>mu</i> opioid receptor expression in CHME-5 cells.....	95
Figure 2. Fentanyl does not affect LPS-induced TLR4 expression in CHME-5 cells.....	96
Figure 3. Fentanyl does not affect LPS-induced MyD88 expression in CHME-5 cells ...	98
Figure 4. Fentanyl down-regulates LPS-induced I $\kappa$ B $\alpha$ activation in CHME-5 cells.....	99

Figure 5. Fentanyl down-regulates LPS-induced NF- $\kappa$ B activity in CHME-5 cells.....	100
Figure 6. Naltrexone has no effect on fentanyl-mediated effect in CHME-5 cells .....	101
Figure 7. Morphine does not affect LPS-induced TLR4 expression in CHME-5 cells..	103
Figure 8. Morphine does not affect LPS-induced MyD88 expression in CHME-5 cells .....	105
Figure 9. Morphine decreases LPS-induced I $\kappa$ B $\alpha$ activation in CHME-5 cells.....	106
Figure 10. Morphine does not affect LPS-induced NF- $\kappa$ B p65 activation in CHME-5 cells .....	107

## LIST OF ABBREVIATIONS

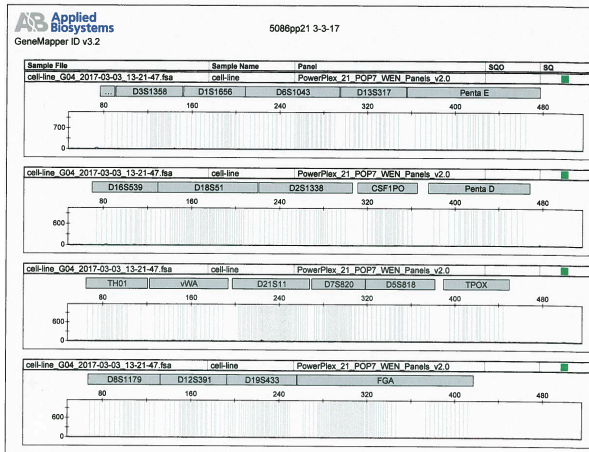
TLR4: toll-like receptor 4  
PCR: polymerase chain reaction  
LPS: lipopolysaccharide  
IkB $\alpha$ : inhibitor of kappa light chain alpha  
NF- $\kappa$ B: nuclear factor of kappa light chain enhancer of B cells  
GFAP: glial fibrillary astrocytic protein  
CNS: central nervous system  
TNF $\alpha$ : tumor necrosis factor alpha  
IL-1 $\beta$ : interleukin 1 beta  
MyD88: myeloid differentiation primary response gene 88  
PAMP: pathogen-associated molecular patterns  
DAMP: damage-associated molecular patterns  
DNA: deoxyribonucleic acid  
RNA: ribonucleic acid  
ATP: adenosine triphosphate  
A $\beta$ : amyloid beta  
LBP: LPS-binding protein  
CD14: cluster of differentiation 14  
MAL: MyD88 adapter-like  
TRIF: Toll-IL-1 domain containing receptor inducing interferon B  
TRAM: TRIF adaptor molecule  
IRAK: interleukin receptor-associated kinase  
TRAF6: TNF receptor-associated factor 6  
TAK1: transforming growth factor  $\beta$ -associated kinase  
MAPK: mitogen-associated protein kinase  
IKK: I kappa B kinase  
ERK: extracellular regulated kinase  
JNK: c-Jun N-terminal kinase  
AP-1: activator protein-1  
IRF: interferon regulatory factor  
IFN: interferon  
RIP: receptor-interacting protein  
TBK1: TANK binding kinase  
AD: Alzheimer's disease

PD: Parkinson's disease  
 MS: multiple sclerosis  
 MHC: major histocompatibility complex  
 ROS: reactive oxygen species  
 NO: nitric oxide  
 BBB: blood brain barrier  
 COX: cyclooxygenase  
 iNOS: inducible nitric oxide synthase  
 TGF $\beta$ : transforming growth factor beta  
 GM-CSF: granulocyte macrophage-colony stimulating factor  
 M-CSF: macrophage-colony stimulating factor  
 SV: simian virus  
 min: minutes  
 h: hours  
 sec: seconds  
 GM: growth media  
 DMEM: Dulbecco's Modified Eagle Medium  
 FBS: fetal bovine serum  
 MTT: 3-(4,5-dimethylthiazol-2-yl)-2,5-diphenyltetrazolium bromide  
 WCL: whole cell lysate  
 CBL: cell lysis buffer  
 LB1: Lysis buffer 1  
 LB2: Lysis buffer 2  
 PBS: phosphate-buffered saline  
 BCA: Bicinchoninic assay  
 BSA: bovine serum albumin  
 PVDF: polyvinylidene fluoride  
 TBST: Tris-buffered saline-tween  
 ECF: enhanced chemifluorescence  
 PFA: paraformaldehyde  
 DAPI: 4,6-diamidino-2-phenylindole  
 RT-PCR: real-time polymerase chain reaction  
 mRNA: message ribonucleic acid  
 NCBI: National Center for Biotechnology Information  
 NIH: National Institutes of Health  
 ANOVA: analysis of variance  
 NHA: normal human astrocytes  
 GI: gastrointestinal  
 GPCR: G-protein coupled receptor  
 MOR: *mu* opioid receptor

DOR: *delta* opioid receptor  
KOR: *kappa* opioid receptor  
NOP: *nociception orphanin* peptide  
 $\beta$ -FNA:  $\beta$ -funaltrexamine  
DA: dopamine  
cAMP: cyclic adenosine monophosphate  
GRK: GPCR kinase  
PKA: protein kinase A  
PKC: protein kinase C  
GASP: G-protein coupled receptor-associated protein  
VTA: ventral tegmental area  
AC: adenylyl cyclase  
LC: locus coeruleus  
HPA: hypothalamic-pituitary-adrenal

## ADDENDUM

A few months before my final dissertation defense, a research group from Case Western University published an article (Garcia-Mesa et al., 2017), which claimed that CHME-5 cells are no longer of human origin. In the study, they performed genotyping by macrosatellite analysis, and investigated the CYCT1 gene expression in CHME-5 cells using both human and rat primers, and showed rat CYCT1 gene expression, but not the human counterpart in these cells (Garcia-Mesa et al., 2017). To our knowledge, the non-human origin of CHME-5 cells, currently in use among numerous labs, has yet to be validated by a second lab. Here we provide further evidence that CHME-5 cells are no longer of human origin. To validate this claim, human short tandem repeats genotyping was performed on CHME-5 cells, which confirmed that these cells are not of human origin (see data below). This recent turn of events in no way invalidates my research in this dissertation. I verified that all antibodies were cross-reactive with rat, and real-time PCR primers were re-designed using rat mRNA sequence. The data presented throughout this dissertation supports my conclusion that CHME-5 cells are still a useful tool to study microglia, particularly neuroinflammatory signaling.



## STR Genotyping for CHME-5 Cells

Genotyping in CHME-5 cells revealed the absence of short tandem repeats. Genotyping was performed by Dr. Jun Fu, in the laboratory of Dr. Robert W. Allen; OSU-CHS Forensics Department.

## INTRODUCTION

Microglia are the “macrophages” of the central nervous system (CNS) and are responsible for homeostatic maintenance, neuronal support, and recognition and clearance of injury or infectious agents, which is achieved through production and up-regulation of various proteins. When insults or injury occur in the CNS, microglia become activated and release several mediators thereby creating an inflammatory environment known as neuroinflammation.

One receptor family expressed in microglia is toll-like receptors (TLRs), which are pattern recognition receptors (PRRs) that recognize a variety of patterns produced by bacteria, viruses, and fungi. TLR4 recognizes bacterial lipopolysaccharide (LPS), which initiates two distinct signaling cascades leading to production of various inflammatory cytokines including tumor necrosis factor alpha (TNF $\alpha$ ), interleukin-1 beta (IL-1 $\beta$ ), IL-6, IL-8, and several others.

The LPS-induced signaling mechanisms are well defined in peripheral immune cells, but less so in cells within the CNS. Thus, it is important to elucidate the signaling mechanisms that occur through the TLR4-myeloid differentiation primary response gene 88 (MyD88)-dependent pathway. These findings will allow us to determine the extent to which TLR4-mediated responses in microglia are similar to those observed in macrophages and dendritic cells. These insights will further our understanding of the mechanisms through which microglia respond to neurological conditions, injury, or



infection. Together these findings will be particularly informative in ongoing efforts to devise new therapeutic strategies for neurological disorders.

Creating new therapies is at the forefront of biomedical research but it always begins with basic science. For this reason, we also wanted to investigate the effects of two opioid agonists, fentanyl and morphine, on LPS-induced TLR4 neuroinflammatory signaling in CHME-5 microglial cells. Opioids are known for their anti-nociceptive effects, but research shows they also have the potential to modulate immune function in both the peripheral and central nervous systems. This discovery can have broader implications on the way opioids are used to treat patients. It is important to investigate these opioid-mediated effects on inflammation because patients with inflammatory conditions or neurodegeneration are being treated with opioids to relieve pain symptoms.

Therefore we need to better understand the impact of opioids on non-neuronal cells, including microglia. Interestingly, some research indicates that opioid agonists are pro-inflammatory and initiate TLR4 signaling. Conversely, our laboratory and others show that opioid agonists, along with antagonists, display anti-inflammatory potential on inflammatory signaling in astrocytes and other cells expressed in the CNS. Additionally, our research demonstrates that fentanyl exerts its effect via a non-classical opioid site. In this study we look to define the molecular mechanisms by which fentanyl and morphine affect key signaling molecules that are activated in response to LPS-induced TLR4 signaling in a microglial cell line, CHME-5.

## CHAPTER ONE

### TLR4-NEUROINFLAMMATORY SIGNALING IN CHME-5 MICROGLIAL CELLS

## **LITERATURE REVIEW**

### **Toll-like Receptors**

Toll-like receptors (TLRs) are pattern recognition receptors of the innate immune system, and to date, ten human and twelve rodent TLRs have been described (Kawai & Akira, 2007). TLRs are type I transmembrane glycoproteins with an extracellular domain responsible for ligand recognition, and, a cytoplasmic domain categorized by the toll-IL-1 resistance (TIR) domain (Uematsu & Akira, 2008). TLRs recognize a variety of bacterial, viral, and fungal patterns, known as pathogen-associated molecular patterns (PAMPs), which include evolutionary conserved motifs such as lipids, lipopeptides, and proteins (Hanisch et al., 2008; Kawai et al., 2007). TLRs also have the ability to recognize endogenous molecules known as damage-associated molecular patterns (DAMPs), which include heat shock proteins (HSPs), deoxyribonucleic acid (DNA), adenosine triphosphate (ATP), high-mobility group box 1 (HMGB1), and low-density lipoproteins (LDL), released from apoptotic and necrotic cells (Hanisch et al., 2008).

TLRs are differentially expressed throughout the plasma membrane and endosomes. TLRs 1,2,4,5,6, and 10 are surface TLRs and bind products produced by extracellular bacteria, while TLRs 3,7,8, and 9 recognize viral and intracellular bacterial proteins, and therefore, are located intracellularly in endosomal membranes (Barton & Kagan, 2009; Kawai et al., 2007). Despite their location, PAMP recognition is analogous and occurs in the receptor's ectodomain in structures called leucine-rich-repeats

(Uematsu et al., 2008). LRRs are comprised of 19-25 tandem motifs, each containing 24-29 amino acids in length, which form horseshoe structures with ligand binding occurring on the concave surface (Uematsu et al., 2008). The TLR ECD also contains a N-terminus and C-terminus cap, denoted as LRR-NT and LRR-CT, which are thought to participate in stabilization of the protein structure and signaling, respectively (Bell et al., 2003).

Besides ligand binding, LRRs also form protein-protein interactions making them capable of forming homodimers or heterodimers, depending on the ligand. For example, TLR2 forms a heterodimer with TLR1, to recognize bacterial triacylated lipopeptides, or with TLR6, to recognize bacterial diacylated lipopeptides, lipotechoic acid, and fungal zymosan (Jin et al., 2007; Kang et al., 2009). TLR10 heterodimerizes with TLR1 or TLR2 to recognize diacylated and triacylated lipopeptides, respectively (Govindaraj et al., 2010; Guan et al., 2010; Hasan et al., 2005). TLR4 and TLR6 also heterodimerize to recognize oxidized low-density lipoproteins and amyloid beta (A $\beta$ ) plaques (Godfroy et al., 2012; Kawai et al., 2007; Stewart et al., 2010). Also, TLR8 can dimerize with TLR7 and TLR9 (J. Wang et al., 2006).

All other TLRs homodimerize to recognize their corresponding ligands: TLR2-fungal phospholipomannan, and herpes simplex virus I (Kurt-Jones et al., 2004), TLR3-viral double-stranded RNA (Alexopoulou et al., 2001), TLR4-Gram-negative LPS, F protein from respiratory syncytial virus (Kurt-Jones et al., 2004), and fungal mannan, TLR5-bacterial flagellin of Gram-negative bacteria (Hayashi et al., 2001), TLR7 and TLR8-single-stranded RNA (Diebold et al., 2004; Heil et al., 2004), TLR9-bacterial and viral unmethylated cytidine-phosphate-guanosine DNA motifs, and TLR10-diacylated

lipopeptide. The *TLR11* gene contains several stop codons, which prevent expression of full-length protein (Lauw et al., 2005; D. Zhang et al., 2004).

### **Gram-negative LPS**

LPS, the prototypical ligand for TLR4, is located on the outer membrane of the Gram-negative bacterial cell wall, and because of its potent toxic potential, LPS is termed endotoxin (Westphal et al., 1981). The importance of LPS is denoted by the amount of molecules ( $3.5 \times 10^6$ ) per bacterial cell and their ability to maintain bacterial viability (Rietschel et al., 1994).

The LPS structure consists of Lipid A, inner and outer core oligosaccharides, and the O-antigen. Lipid A, a phosphoglycolipid with six or seven fatty acid chains attached, (Volpi, 2003), is highly conserved across Gram-negative bacteria, is cytotoxic, and activates the complement system via the classical pathway (Peterson & McGroarty, 1985). The inner core structure is composed of 2-keto-3-deoxyoctonate and heptose residues, while the outer core consist of a N-acetyl-glucosamine dimer (Rietschel et al., 1994; Volpi, 2003). The O-antigen is covalently linked to the Lipid A core and consists of an oligosaccharide chain that varies in length up to 40 repeat units (Rietschel et al., 1987). The O-specific chain is antigenic and activates the complement system via the alternate pathway (Peterson et al., 1985).

### **TLR4 recognizes Gram-negative LPS**

The binding of LPS occurs with the aid of several proteins including the LPS binding protein (LBP), cluster of differentiation 14 (CD14), and lymphocyte antigen 96 (also known as MD2) which are all necessary for binding to and activation of TLR4 (Dziarski & Gupta, 2000; Schumann et al., 1990; Shimazu et al., 1999; Tobias et al., 1988; Wright

et al., 1990). LBP, an acute phase protein produced in the liver, binds LPS multimers and monomerizes them, which allows for recognition of LBP-LPS by CD14 and the other LPS acceptors, MD2 and TLR4 (Lynn & Golenbock, 1992; Weiss, 2003). CD14, a glycosylphosphatidyl inositol-anchored protein, binds LBP-LPS to the cell surface, allowing binding to the MD2 hydrophobic pocket (Lynn et al., 1992; Park et al., 2009). Following LPS binding to the TLR4-MD2 complex, dimerization with another TLR4-MD2-LPS complex occurs, leading to a conformational change that brings TIR domains into contact, a step that is necessary for signaling to begin (Park et al., 2009).

Additionally, adaptor and bridging molecules, myeloid differentiation primary response gene 88 (MyD88) and MyD88 adaptor-like (MAL) are recruited for initiation of MyD88-dependent signaling. TLR4 also signals through another set of adaptor and bridging molecules known as Toll-IL-1 receptor domain-containing adaptor inducing interferon beta (TRIF) and TRIF-related adaptor molecule (TRAM), which are recruited after endocytosis of the TLR4-MD2-LPS complex (Barton et al., 2009).

### **MyD88-dependent Signaling**

MyD88-dependent signaling, which is used by all TLRs except TLR3, occurs after ligand binding and recruitment of MyD88 and MAL (only for TLR2 and TLR4 signaling) adaptors (O'Neill, 2006). After initiation of the signaling cascade, recruitment and activation of several downstream signaling proteins occurs, leading to transcription of pro-inflammatory genes including  $\text{TNF}\alpha$ ,  $\text{IL-1}\beta$ , and  $\text{IL-6}$  (Takeuchi & Akira, 2001). First is the formation of the Myddosome consisting of 6 MyD88s, 4 interleukin 1-receptor associated kinase 4s (IRAK4s), and 2 IRAK2s, which are all critical mediators for TLR signaling (Lin et al., 2010). After recruitment of MyD88 molecules to the

receptor complex, IRAK4 is recruited to MyD88 through death domains, followed by IRAK1 and IRAK2. After activation of IRAK molecules TNF receptor-associated factor 6 (TRAF6) is recruited to the complex (Cao et al., 1996; Takeuchi & Akira, 2010). TRAF6, an E3 ubiquitin ligase, is phosphorylated and associates with TAB2 and TAB3, which are the regulatory components of transforming growth factor- $\beta$  associated kinase (TAK1), and are also responsible for activation of TAK1 (Kawai et al., 2007; Palsson-McDermott & O'Neill, 2004). TAK1, a mitogen-activated protein kinase kinase kinase, activates the I $\kappa$ B kinase (IKK) complex, specifically IKK $\beta$ , and simultaneously activates MAPKs, extracellular-signal regulated kinase (ERK)1/2, p38, and c-Jun N-terminal kinase (JNK), leading to activation of various transcription factors, such as activator protein-1 (AP-1) (Irie et al., 2000; Kawai & Akira, 2011; Sato et al., 2005). IKK $\beta$  in turn activates inhibitor of kappa B alpha (I $\kappa$ B $\alpha$ ), the negative regulator of nuclear factor of kappa-light-chain-enhancer of activated B cells (NF- $\kappa$ B) (Karin, 1999). I $\kappa$ B $\alpha$ 's phosphorylation-induced degradation leads to the release of the transcription factor NF- $\kappa$ B, which then translocates into the nucleus and binds DNA promoter regions for transcription of pro-inflammatory cytokines (Arenzana-Seisdedos et al., 1997). TLR7, 8, and 9 also use the MyD88 adaptor molecule along with IRAK4, IRAK1, TRAF6, and TRAF3, which leads to activation of several interferon regulatory factors (IRFs) (IRF1, 5, 7, 8), and NF- $\kappa$ B, for the production of Type I interferons (IFN- $\beta$ , IFN- $\alpha$ ) and pro-inflammatory cytokines, respectively (Kawai et al., 2007; O'Neill & Bowie, 2007).

### **TRIF-dependent Signaling**

TRIF-dependent signaling only occurs after endocytosis of the TLR4-MD2-LPS complex and is considered the late-phase activation of TLR4 signaling (Kagan et al., 2008; Lu et

al., 2008; Palsson-McDermott et al., 2004). Once MyD88-dependent signaling is activated, the TLR4-MD2-LPS complex is coupled to the adaptor molecule TRAM at the plasma membrane and becomes endocytosed, ultimately recruiting TRIF to the endosomal membrane (Kagan et al., 2008; Yamamoto et al., 2002). The TRAM bridging molecule is TLR4-specific and necessary for late-activation of NF- $\kappa$ B, as well as for IRF3 activation (O'Neill et al., 2007). TRIF has the potential to interact with three molecules, receptor-interacting protein 1 (RIP1), TRAF6, and TRAF3 (Lu et al., 2008; O'Neill, 2006). TRIF forms a multi-protein signaling complex with RIP1, TRAF6, and the adaptor molecule tumor necrosis factor receptor type I-associated death domain, leading to activation of TAK1, mitogen-activated protein kinase (MAPK), AP-1, and NF- $\kappa$ B, ultimately leading to production of pro-inflammatory cytokines (Kawai et al., 2007; Lu et al., 2008). TRAF3 associates with TRAF family member-associated NF- $\kappa$ B activator, TANK binding kinase 1 (TBK1), and IKK iota for the activation and dimerization of interferon regulatory factor 3, and production of Type I interferons and co-stimulatory molecules including, CD40, CD80 and CD86 (Hoebe et al., 2003; Lu et al., 2008). Along with TLR4, TLR3 is the only other TLR that uses the TRIF-dependent signaling pathway. Once activated, TLR3 recruits the TRIF adapter molecule to endosomes and activates NF- $\kappa$ B (IKK complex), IRF3, and IRF7 (TRAF3, TRAF6, and TBK1)(Kawai & Akira, 2010; Suh et al., 2009).

### **Toll-like Receptors expressed in the Central Nervous System**

Investigation of TLR expression in the CNS has established the presence of TLRs 1-9, most notably in microglia (TLRs 1-9) and to a lesser extent in neurons (TLRs 2-4,7,8), astrocytes (TLRs 2-4,7-9), and oligodendrocytes (TLRs 2 and 3) (Bsibsi et al., 2002; Jack



et al., 2005; Kettenmann et al., 2011). TLRs have also been implicated in several CNS diseases including Alzheimer's (AD), Parkinson's (PD), neurodegeneration, and trauma, leading to activation of microglia and production of pro-inflammatory cytokines and chemokines, such as TNF $\alpha$  and IL-6 (Kettenmann et al., 2011; Okun et al., 2011). The "pathogen-necrosis-autoantigen triad" is thought to explain the exaggerated inflammatory response that occurs during CNS disorders, namely, TLRs are thought to play a dual role in ligand recognition: 1) facilitation of initial response to pathogens and 2) recognition of newly released self-antigens due to necrotic/apoptotic death (Hanke & Kielian, 2011).

### **Neuroinflammation in the Central Nervous System**

Inflammation in the CNS, known as neuroinflammation, can result from 1) production of various inflammatory molecules, including cytokines, chemokines and lipid mediators derived from arachidonic acid, such as prostaglandins and leukotrienes, 2) during tissue injury or infection, or 3) may result from neurodegenerative disorders that can impart an inflammatory component as in the case of multiple sclerosis (MS), AD, and PD (Pasare & Medzhitov, 2004; Pedras-Vasconcelos et al., 2009; Rivest, 2009).

Classical hallmarks of CNS inflammation include microglial activation, pro-inflammatory cytokine production, and up-regulation of adhesion molecules that allow entry of peripheral immune cells into the CNS (Matyszak, 1998). Microglial activation is characterized by expression of receptors responsible for sensing danger signals in response to pathogens, or cellular/tissue damage from infection or disease states, up-regulation of molecules necessary for immune response such as chemokines and the major histocompatibility complex (MHC), and induction of NF- $\kappa$ B-dependent genes (Glass et al., 2010). This activation leads to production of pro-inflammatory cytokines

and neurotoxic factors including  $\text{TNF}\alpha$ ,  $\text{IL-1}\beta$ , nitric oxide (NO) and reactive oxygen species (ROS) that can activate astrocytes and also have detrimental effects on neurons (Glass et al., 2010). Exposure of cerebral endothelial cells to cytokines or activating stimuli during infection or disease results in expression of adhesion molecules including intracellular and vascular cell adhesion molecule, which bind selectins expressed on monocytes, neutrophils, eosinophils and T-lymphocytes (Libby, 2007; Rivest, 2009). These interactions, along with chemical signals (chemokines) released from microglia and astrocytes, allow immune cells to migrate through tight junctions for entry into the CNS (Libby, 2007; Rivest, 2009).

Neuroinflammation can impose beneficial outcomes including neuroprotection, axonal regeneration, neurogenesis and remyelination; or detrimental outcomes, such as, injury to neural elements, death to neurons and oligodendrocytes, and inhibition of regenerative processes (Wee Yong, 2010). The “Strength of Signal” hypothesis is the concept that microglia can be neuroprotective or detrimental depending on the concentration of the insult (e.g. TLR ligands) present in the CNS (Kielian, 2009).

### **Neurodegeneration**

Neuroinflammation resulting from neurodegeneration can be a direct effect of the inducers causing the offending condition or as a secondary consequence from neurotoxic factors released from surrounding immune cells, as seen in many CNS disorders, including MS, AD and PD (Glass et al., 2010; Pedras-Vasconcelos et al., 2009). For example,  $\text{IL-1}\beta$  can have indirect neurotoxic effects by binding CNS immune cells, microglia, astrocytes and oligodendrocytes, which leads to induction of inflammatory mediators, such as ROS, cytokines and chemokines (Zipp & Aktas, 2006).  $\text{IL-1}\beta$  can also

block glutamate uptake by astrocytes, promote the formation of NO and increases levels of matrix metalloproteinases (MMPs) to neurotoxic levels (Wee Yong, 2010).

Multiple sclerosis is an autoimmune disease of the CNS displaying chronic neuroinflammatory pathology which causes widespread inflammation, demyelination and progressive axonal degeneration, leading to clinical manifestations characterized by neurological deficits in sensation and in the motor, autonomic, visual, and cognitive systems (Glass et al., 2010; Hanke et al., 2011; Lampron et al., 2013; Zipp et al., 2006). For investigational study of MS, the experimental autoimmune encephalomyelitis mouse model is used, which can be induced by immunization with myelin components or activated myelin-specific T lymphocytes (Lampron et al., 2013; Zipp et al., 2006).

Myelin and oligodendrocytes are the main targets of myelin-reactive T lymphocytes, macrophages, and antibody-producing plasma cells, which infiltrate the CNS through the blood brain barrier (BBB) (Glass et al., 2010; Lampron et al., 2013; Zipp et al., 2006). Breakdown of the BBB occurs from microglial activation and production of pro-inflammatory cytokines, IL-1 $\beta$ , IL-6 and TNF $\alpha$ , which lead to up-regulation of adhesion molecules and chemokines, CCL2, CCL3 and CCL5, for the recruitment and attachment of immune cells (Graeber & Streit, 2010; Lampron et al., 2013). Metallomatrix proteases also play a role in leukocyte infiltration, in particular, MMP-9, which degrades extracellular matrix proteins and creates ducts in perivascular space for entry of leukocytes (Lampron et al., 2013).

Alzheimer's disease is an age-related neurodegenerative disease characterized by the loss of memory, progressive impairment of cognition and various behavioral and neuropsychiatric disturbances (Glass et al., 2010). Classical hallmarks of AD include

amyloid beta (A $\beta$ ) peptides, cleaved from the amyloid precursor protein, and neurofibrillary tangles generated from hyper-phosphorylated tau proteins (Akiyama et al., 2000; Glass et al., 2010). Numerous studies have shown evidence for A $\beta$ -mediated inflammatory response in AD, including microglial activation as defined by change in morphology, from ramified to amoeboid, production and release of inflammatory mediators, such as cytokines, chemokines, reactive oxygen intermediates, proteases and excitatory amino acids, and induction of chemokines with the ability to recruit astrocytes to sites surrounding A $\beta$  plaques. Additionally, astrogliosis is manifested by an increase in the number, size, and motility of astrocytes, the ability to express complement receptors and components, and, produce IL-1 $\beta$ , IL-6, prostaglandins, cyclooxygenase (COX)-2 and inducible nitric oxide synthase (iNOS) in response to plaques (Akiyama et al., 2000; Glass et al., 2010).

Uptake of A $\beta$  plaques by microglia and astrocytes is possible through several routes including macro-pinocytosis, phagocytosis, and receptor-mediated endocytosis both *in vivo* and *in vitro* (Glass et al., 2010; Graeber et al., 2010). Several cell surface and cytoplasmic receptors are implicated in the ability of microglia and astrocytes to detect and engulf A $\beta$  peptides including TLRs (TLR4-TLR6, in conjunction with CD36), receptor for advanced glycoxidation end-products, that belongs to the immunoglobulin superfamily, and Nod-like receptors (Glass et al., 2010; Mandrekar et al., 2009; Stewart et al., 2010).

Parkinson's disease is a neurodegenerative disease and the most common movement disorder. It is characterized by motor symptoms, such as, bradykinesia, tremor, rigidity, and postural instability, and non-motor related symptoms including

olfactory deficits, autonomic dysfunction, depression, cognitive deficits and sleep disorders (Glass et al., 2010). The onset of PD occurs from the loss of dopaminergic neurons in the substantia nigra and accumulation and aggregation of misfolded  $\alpha$ -synuclein and ubiquitinated proteins, known as Lewy bodies (Glass et al., 2010). Alpha-synuclein aggregates are intraneuronal, which become neurotoxic, thereby causing neuronal loss and release of proteins into extracellular compartments, leading to microglial activation (Khandelwal et al., 2011; Roodveldt et al., 2008).

Investigators have been trying to correlate PD with inflammatory mechanisms mediated by microglia, but that theory is controversial, so the question remains whether microglia play an active disease-promoting role in PD pathogenesis (Graeber et al., 2010; Khandelwal et al., 2011). In keeping with this theory, several studies suggest that  $\alpha$ -synuclein-mediated neurotoxicity is enhanced by microglial activation through a TLR-dependent mechanism leading to the release of pro-inflammatory cytokines, such as, IL- $1\beta$  and TNF $\alpha$ . Also, a TLR-independent mechanism of  $\alpha$ -synuclein phagocytosis and NADPH-mediated ROS/RNS production has been suggested (Glass et al., 2010; Hirsch & Hunot, 2009; Khandelwal et al., 2011; W. Zhang et al., 2005a). Neurodegeneration encompasses a wide field and under no circumstance is this field confined to these three diseases mentioned above, but can also include stroke, cerebral palsy, traumatic brain injury, and brain tumors. In looking forward, strategies and therapeutics need to be investigated for the treatment of neuropathologies.

### **Identification of Microglia**

Microglia are considered the innate immune cells of the CNS that comprise about 10-20% of the total CNS cell population (Vaughan & Peters, 1974). Microglia were first

recognized by Franz Nissl in 1899, who used the term “rod cells” to describe a type of glial cell that reacted to brain pathology (Kettenmann et al., 2011). Thereafter, metallic-staining techniques allowed Santiago Ramon y Cajal, and Pio del Rio-Hortega to visualize and categorize three neuronal supporting cells as oligodendrocytes, astrocytes, and microglia (Kettenmann et al., 2011).

### **Origin and Development**

During development, amoeboid microglia derived from migrating monocytes, play a macrophagic role in the CNS, which has been studied using both carbon labeling and rhodamine isothiocyanate fluorescence studies (Leong & Ling, 1992; Ling, 1979; Ling & Wong, 1993). Microglia enter the CNS from the middle of the 1<sup>st</sup> trimester until the 2<sup>nd</sup> trimester (Monier et al., 2006). During early entry (4.5 weeks gestation), microglia penetrate the cerebral cortex and white matter through the ventricles, meninges, and the choroid plexus (Monier et al., 2007). These cells display amoeboid forms with large cell bodies and absence of processes (Monier et al., 2007). These microglia are representative of fetal macrophages originating from the yolk sac myeloid progenitors (Monier et al., 2007; Orihuela et al., 2016). Amoeboid microglia express several prototypical macrophagic markers, including Iba-1, CD68, and CD45, nonspecific esterase activity, and are actively phagocytic; characteristics that are down-regulated with the evolution into the resting microglia (Lawson et al., 1992; Ling et al., 1993).

There are numerous factors that influence morphological transformation of microglia from amoeboid to ramified morphology after entry into the CNS. This process occurs from the middle of the second trimester onward, in which microglia colonize the entire cerebral parenchyma and down-regulate surface antigens (Monier et al., 2006).

Several studies have shown that factors such as ATP, purines, cytokines released from astrocytes, transforming growth factor  $\beta$  (TGF- $\beta$ ), granulocyte macrophage-colony stimulating factor (GM-CSF), macrophage-colony stimulating factor (M-CSF), and chloride channels all influence transformation (Giulian & Ingeman, 1988; Schilling et al., 2001; Suzumura et al., 1990; Wollmer et al., 2001).

Furthermore, Suzumura et al. 1991, observed morphological transformation of microglia and biological activity displayed by amoeboid, ramified (resting), and rod-like microglia, in which it was concluded that morphological transformation is reversible between amoeboid and ramified morphologies. Amoeboid microglia could be induced by LPS, interferon gamma (IFN- $\gamma$ ), or 12-*O*-tetradecanoylphorbol-13-acetate, and displayed enzymatic activity and superoxide anion production indicating an activated form (Suzumura et al., 1991). GM-CSF induced microglia to become rod-like, which showed no activity, but had bromodeoxyuridine uptake, indicating proliferation. Also, conditioned from LPS-stimulated astrocytes transformed microglia into ramified morphology, with no enzymatic activity, indicating non-activated microglia (Suzumura et al., 1991).

In the healthy mature CNS, microglia display ramified morphology, small somas, and small cellular processes (Kettenmann et al., 2011). The resident adult population is maintained through local cell division and through recruitment of circulating peripheral blood monocytes as described by several investigators (Bruttger et al., 2015; Korzhevskii & Kirik, 2015; Lawson et al., 1992; Varvel et al., 2012). Following damage to the BBB, for example during pathological conditions, monocytes differentiate and populate the CNS (Korzhevskii et al., 2015).

## **Microglial Function**

Under physiological conditions, microglia maintain a quiescent surveillance phenotype, which is accomplished with several neuronal and astrocytic signals that are recognized by corresponding microglial receptors (Orihuela et al., 2016). Under pathological conditions, signal blockade can also contribute to down-regulation of microglial responses. For instance, CD45 crosslinking resulted in negative regulation through decrease in TNF $\alpha$  and NO production in A $\beta$ -treated microglia via inhibition of the p44/p42 MAPK pathway (Tan et al., 2000). Additionally, microglia express high levels of micro ribonucleic acid (RNA) (miRNA)-124, which reduces the expression of CD46, MHC II, and CD11b (Conrad & Dittel, 2011).

Microglia should not only be considered the immune cell of the brain but also a regulator of the environment. Microglia communicate with neurons and other glia for homeostasis as well as maintenance of cell populations and cellular components, such as astrocyte differentiation and axon regeneration, respectively (Lawson et al 1992). Microglia are also involved in regulatory processes critical for tissue development, maintenance of neural environment, response to injury, and subsequent remodeling and repair (Orihuela et al., 2016).

Microglia are the phagocytes of the brain, a function that is not only important during pathological insults and tissue injury (molecules and debris), but also during development (removal of apoptotic cells, synapse removal, and pruning during post-natal development) and normal brain function (Kettenmann et al., 2011; Napoli & Neumann, 2010; Neumann et al., 2009). Several factors increase phagocytic activity in microglial



cells including M-CSF and glial-cell line derived neurotrophic factor (GDNF) (Mitrasinovic et al., 2003).

Microglia are polarized to a M1 (pro-inflammatory) or M2 (anti-inflammatory) phenotype depending on the signals received in the environment. M1 phenotype can be induced in response to tissue injury or exposure to pathogenic-derived products, leading to production of cytokines, presentation of antigen, and expression of high levels of iNOS, allowing for clearance of pathogens and induction of adaptive immune responses (Gordon & Taylor, 2005). In the absence of the pathogenic stimuli, polarization to the M1 phenotype can also be induced by trauma or ischemic reperfusion (Orihuela et al., 2016). Much of the work looking at extensive transcription profiles of M1 markers in response to LPS or IFN- $\gamma$  has been done in rodent microglia, which include *IL-1 $\beta$* , *IL-6*, *IL-12*, *TNF $\alpha$* , chemokines, and co-stimulatory molecules (Hanisch & Kettenmann, 2007). Furthermore, a study using adult human microglia also showed the M1 phenotype upon stimulation with LPS and IFN- $\gamma$  (Durafour et al., 2012).

Alternatively, there are three immunophenotypes that characterize M2 activation: M2, M2b, and M2c. Microglia adopt the M2 phenotype in response IL-4, and produce anti-inflammatory cytokines such as IL-10 and TGF- $\beta$  (Orihuela et al., 2016; Perry & Teeling, 2013; M. Stein et al., 1992). Next, M2b is considered the regulatory phase, where microglia undertake wound healing, tissue repair, collagen formation, and recruitment of T helper 2 (Th2) cells (Perry et al., 2013). Finally, M2c is the deactivated state in response to IL-10, TGF- $\beta$ , or ingestion of apoptotic cells, leading to down-regulation of pro-inflammatory cytokines and up-regulation of scavenger receptors such as CD163 (Perry et al., 2013).

## **Neuroprotective vs. Neurotoxic**

There has been great debate as to the beneficial and cytotoxic roles of microglia in the CNS. The properties that label microglia either neurotoxic or neuroprotective refer to the influence that microglia have on neurons or vice versa (Luo & Chen, 2012). For example, crosstalk that occurs between neurons and microglia consists of “off” and “on” signals that influence microglial activation, including interactions between CD200 (neuron) and CD200R (microglia), and release of soluble factors such as anti-inflammatory molecules and neurotrophins that attenuate microglial responses (Hoek et al., 2000; Kreutzberg, 1996; Luo et al., 2012; Neumann, 2001; Wei & Jonakait, 1999).

Neuroprotective and beneficial aspects of microglia include neuronal differentiation and apoptosis regulation in the developing brain, axonal regeneration, tissue repair, removal and down-regulation of cytokines, production of anti-inflammatory cytokines, and return to, and, maintenance of, homeostasis in the adult brain (Kreutzberg, 1996). The underlying significance is that control of microglial activation is necessary to prevent microglial-mediated cytotoxicity.

## **Surface Antigens/Receptors**

Microglia constitutively express cell surface markers and proteins during ramified and activated states, which allow for immuno-histological/cytochemical identification.

During the surveillance stage, microglia express CD11b and CD45<sup>lo</sup>, and up-regulate MCH II, CD4, CD40 and CD86 in response to CNS insults and infection. Additionally, GLUT5, CD163, CCR2 and nestin, have also been identified as additional microglial markers (Graeber et al., 2010; Y. B. Lee et al., 2002; Ponomarev et al., 2006; Rock et al., 2004; Sedgwick et al., 1991). Lee et al. 2002, demonstrated that normal, unstimulated

human microglia constitutively express mRNA transcripts for *IL-1 $\beta$* , *IL-6*, *-8*, *-10*, *-12*, *-15*, *TNF $\alpha$* , monocyte chemoattractant protein (*MCP*)-1 and macrophage inflammatory protein (*MIP*)-1 $\alpha$  and  $\beta$ , while stimulation with LPS or A $\beta$  peptides induced increased expression of IL-8, IL-10, IL-12, MIP-1 $\alpha$  and  $\beta$ , MCP-1 and TNF $\alpha$  (Y. B. Lee et al., 2002). Activated microglia also express and up-regulate scavenger, complement, and cytokine/chemokine receptors (Rock et al., 2004).

### **Cytokines/Chemokines**

Chemokines are secreted proteins that were initially described as activators of leukocyte migration to areas of infection and inflammation (Cartier et al., 2005; Kettenmann et al., 2011; Khandaker et al., 1998). It is now understood that chemokines are multifunctional proteins that act on a various cell types and take part in inflammatory (CXCL10, CXCL8) and homeostatic functions (CX3CL1, CXCL12), including cytokine secretion, modulation of cell adhesion, phagocytosis, cell proliferation, apoptosis, and angiogenesis (Cartier et al., 2005). Based on the number and spacing of their conserved cysteine residues, chemokines are classified into four subfamilies, CC, CXC, XC, or CX3C, and exert their biological activity via members of the G-protein coupled receptor (GPCR) family (Cartier et al., 2005).

Chemokines including IP-10 (CXCL10), IL-8 (CXCL8), RANTES (CCL5), are not constitutively expressed in the CNS, but are up-regulated by microglia in response to pathological aberrations and mediate their effects through binding to inducible chemokine receptors, including CCR2, CXCR3, CXCR1, and CCR5, respectively (Cartier et al., 2005).

### **Experimental tool for the study of microglia**

## **Primary Cells**

There are several experimental tools available for studying microglia that include primary cells, as well as immortalized cell lines. Primary cells are certainly advantageous in that they can be obtained from *in vivo* model systems, but also devoid of genetic manipulations. Yet, there are some disadvantages including 1) difficulty in obtaining absolute pure cultures, 2) difficulty in obtaining a sufficient number of cells, and 3) derivation from neonatal brains; less representative of adult population (Henn et al., 2009).

Several reports on microglial inflammatory responses have been published with human, mouse, or rat primary cells. The use of human primary cells is often preferred, but the ability to obtain these cells is difficult due to both practical and ethical issues. Even so, there are studies that used human primary microglial cultures to assess inflammatory responses. One study showed increased IL-1 $\beta$  and IL-6 mRNA and protein expression in response to LPS (Sebire et al., 1993). Primary cultures of rodent microglia express TNF $\alpha$ , IL-6, and IL-1 $\beta$  in response to LPS, depending on the stage of embryonic development (Giulian, 1987).

## **Cell lines**

Immortalized cell lines, especially CNS cultures, are useful tools for conducting biomedical research. The benefits include external propagation of culture leading to increased yields. Thus, a myriad of elements such as activation states, releasable factors, and other components, which are crucial to microglial inflammatory responses that can be studied in an efficient and timely manner (Stansley et al., 2012). However, cell lines

contain oncogenes, which increase cell proliferation, adherence, and variable morphology, as compared to primary cells (Stansley et al., 2012).

BV-2 murine cells, immortalized using the v-raf/v-myc oncogene carrying the J2 virus, are likely the most commonly used and best characterized microglial cell line (Blasi et al., 1990). BV-2 cells are well characterized in terms of 1) non-specific esterase and phagocytic activity, 2) release of IL-1 $\beta$  and lysozyme upon stimulation, 3) expression of macrophage-1 antigen (Mac-1) and Iba-1, and 4) absence of glial fibrillary astrocytic protein (GFAP) and galactocerebroside, astrocyte and oligodendrocyte markers, respectively (Blasi et al., 1990). One report examined similarities between primary microglia and BV-2 cells, in which 90% of the genes induced by LPS in primary microglia including MIP-1 $\alpha$ , IL-1 $\beta$ , and I $\kappa$ B $\alpha$  were induced in BV-2 cells, but to a lesser degree (Dai et al., 2015; Henn et al., 2009). Additionally, Dai et al, 2015 showed increased expression of TLR4, MyD88, NF- $\kappa$ B, p-I $\kappa$ B $\alpha$ , and IL-1 $\beta$ , 24 hours after stimulation with LPS (10-30  $\mu$ g/ml) (Dai et al., 2015).

Another commonly used rat cell line, N9 microglial cells, were immortalized with the v-myc oncogenes of the avian retrovirus MH2, which displayed non-esterase and phagocytic activity and expressed several surface markers including FcR, F4/80, and Mac-1 (Righi et al., 1989; Stansley et al., 2012). N9 microglial cells produce TNF $\alpha$ , IL-6, and IL-1 $\beta$  in response to LPS (Righi et al., 1989).

The Highly Aggressive Proliferating Immortalized (HAPI), rat microglial cell line is not genetically modified but is considered highly proliferative (Cheepsunthorn et al., 2001). HAPI microglial cells are phagocytic and up-regulate TNF $\alpha$  mRNA and protein,

and NO in response to LPS stimulation (Cheepsunthorn et al 2001). HAPI cells express the microglial marker, OX-42 (Stansley 2012).

A human microglial cell line, HMO6, was immortalized from human primary embryonic microglial cultures using the PASK 1.2 retroviral vector containing the v-myc oncogene. HMO6 microglial cells display phagocytic activity, a rapid doubling time, and express the microglial-specific antigens, Mac-1, CD68, and CD86. HMO6 also up-regulated *IL-1 $\beta$* , *IL-6*, *IL-8*, *IL-12*, and *MCP-1* mRNA expression, as well as TNF $\alpha$  and IL-8 protein expression in response to LPS, similar to human primary microglia (Nagai et al., 2005; Nagai et al., 2001).

CHME-5 cells were originally reported to be immortalized using human primary microglial cells obtained from human embryonic tissue using a plasmid containing the simian virus (SV) 40 large T-antigen (Janabi et al., 1995; Peudenier et al., 1991). CHME-5 cells were reported to express MHC1, CD11b, and CD68, display non-esterase activity, and phagocytose zymosan particles. CHME-5 cells are widely used as an acceptable human microglial model to study Alzheimer's disease, human immunodeficiency virus (HIV), and cellular heat stress. Very recently, it was reported that CHME-5 cells are not human, but of rat origin as determined through sequencing and genotyping (Garcia-Mesa et al., 2017). The modification of CHME-5 cells from human to rat may be the reason why a publication characterizing primary human microglia revealed inconsistencies in microglial and inflammatory genes between primary human microglia and microglial cell lines, including CHME-5 cells (Melief et al., 2016). Knowing what we do now about the non-human origin of CHME-5 cells from Garcia-Mesa et al. 2017, the inability to detect gene expression might have been due to the use of human primers.

Garcia-Mesa et al. (2017) recently obtained human microglial cells from ScienCell (catalog #1900) and immortalized them by infecting them with vesicular stomatitis virus G envelope SV40 large T-antigen by spinoculation (Garcia-Mesa et al., 2017). These immortalized human microglial cells (hμglia) express CD68 and CD14, and secrete IL-6, TNFα, and IL-8 following stimulation with TNFα (Garcia-Mesa et al., 2017).

## **PURPOSE**

TLR4 signaling is well defined in peripheral immune cells, but less so in cells of the CNS. Additionally, the ability to study human microglial responses is difficult due to their location within the CNS, and accordingly, research is primarily pursued in rat and mouse models. To a lesser extent, human primary microglia are used but obtaining these cultures is complicated by ethical issues, culture techniques, high cost, and often, commercial unavailability. To this end, this aim was to characterize CHME-5 cells for microglial attributes with the expectation that this cell line remains a useful tool in the study of microglial responses, particularly as related to neuroinflammation.

## **Aim I**

The first aim was to characterize LPS-induced TLR4 inflammatory signaling in a microglial cell line, CHME-5.

## **Hypothesis (H<sub>1</sub>)**

Since microglia are considered “macrophages” of the CNS, it was hypothesized that CHME-5 microglial cells respond to LPS and induce expression of key signaling and inflammatory molecules in the TLR4 MyD88-dependent signaling pathway, as seen in peripheral immune cells.

## **Null Hypothesis (H<sub>0</sub>):**

CHME-5 cells are not activated and do not induce key signaling and inflammatory molecules in the TLR4 MyD88-dependent signaling pathway in response to LPS stimulation.



## **METHODOLOGY**

### **Cell Culture**

CHME-5 growth media (GM) consisted of Dulbecco's Modified Eagle Medium (DMEM) with 4.5 g/L glucose and sodium pyruvate without L-glutamine (Mediatech, Inc., Corning Subsidiary, Manassas, VA), fetal bovine serum (FBS) (Atlanta Biologicals, Flowery Branch, GA), 200 mM L-glutamine (Mediatech, Inc.), penicillin-streptomycin (100 U/ml potassium penicillin, 100 µg/ml streptomycin sulfate (Fischer Scientific, Pittsburgh, PA), and 250 µg/ml amphotericin B (Mediatech, Inc.). CHME-5 cells were maintained in GM at 37°C, with 5% CO<sub>2</sub>. Growth media was replaced every 48 h and for experimental assays, GM was replaced with serum free media (SFM), for no less than 16 h at 37°C.

### **LPS Treatment**

Lipopolysaccharide from *Escherichia coli* O111:B4 (L4391) was purified by gel-filtration chromatography and *E. coli* O55:B5 (L2880) was purified by phenol extraction (Sigma-Aldrich, Saint Louis, MO). The lyophilized powders were reconstituted in HyPure cell culture grade water (#SH30529.03, Hyclone-Thermo Scientific, Rockford, IL) and sterile filtered to a stock concentration of 1.0 mg/ml and 1.2 mg/ml, respectively.

### **MTT assay**

MTT (3-(4,5-dimethylthiazol-2-yl)-2,5-diphenyltetrazolium bromide) assays were performed to verify cell viability of CHME-5 cells after treatment. CHME-5 cells were seeded in 12-well plates at a density of 40,000 cells/well. Cells were incubated overnight in SFM. After corresponding treatments, fresh SFM (1 ml) was added to each well followed by addition of 111  $\mu$ l MTT. Cultures were then incubated at 37°C for 45 min. Media was aspirated from each well and 1.5 ml dimethyl sulfoxide (DMSO) added for 30 min, rocking at 25°C. Absorbance was read at 492 nm with the Synergy 2 plate reader (Biotek Instruments).

### **Protein extraction**

Whole cell lysates (WCLs) were extracted with cell lysis buffer (CBL) from Cell Signaling, (Danvers, MA) containing 20 mM Tris-HCl (pH 7.5), 150 mM NaCl, 1 mM EDTA, 1 mM EGTA, 1% Triton, 2.5 mM sodium pyrophosphate, 1 mM  $\beta$ -glycerophosphate, 1 mM  $\text{Na}_3\text{VO}_4$ , and 1  $\mu$ g/ml leupeptin. For cytoplasmic and nuclear protein extraction, Lysis Buffer 1 (LB1) and Lysis Buffer 2 (LB2) were used. LB1 was diluted to a concentration of 1 $\times$  for a final concentration of 10 mM HEPES (pH 7.9), 10 mM KCl, 0.10 mM EDTA, 0.10 mM EGTA, 1 mM DTT, 0.5 mM PMSF, 10  $\mu$ g/ml leupeptin, and 10  $\mu$ g/ml aprotinin. Octylphenoxypolyethoxyethanol (Igepal) was added to cells after incubation. LB2 was diluted 1 $\times$  for a final concentration of 20 mM HEPES, 400 mM NaCl, 1 mM EDTA, 1 mM EGTA, 1 mM DTT, 1 mM PMSF, 1 mM leupeptin, 10  $\mu$ g/ml aprotinin. For WCLs, cells were washed with ice-cold phosphate-buffered saline (PBS) and then 400  $\mu$ l of CBL was added to each 100-mm dish. Following a 5 min incubation at 4°C, lysates were collected and centrifuged at 14,000  $\times$  g (4°C) for 10 min.

The supernatant was collected and stored at -20°C. For cytoplasmic and nuclear extracts, cells were washed with and collected in 1 ml ice-cold PBS. Cells were centrifuged at  $129 \times g$  (4°C) for 5 min. The supernatant was aspirated and combined with 400  $\mu$ l LB1 and vortexed vigorously for 10 sec, followed by incubation on ice for 15 min. Next, 100  $\mu$ l 5.4% Igepal was added, samples were vortexed for 10 sec, then centrifuged at  $14,000 \times g$  (4°C) for 5 min. The supernatant was collected and stored at -20°C; then 100  $\mu$ l LB2 was added to the remaining pellet. The samples were vortexed for 15 min at 4°C and then centrifuged at  $14,000 \times g$  (4°C) for 22 min. The supernatant was collected and stored at -20°C.

### **Protein assay**

Pierce Bicinchoninic Assay (BCA) Reagent A and Reagent B (Thermo Scientific) were used to determine protein concentrations in cell extracts. Protein concentrations for WCLs and cytoplasmic/nuclear extracts were measured using BCA. First, a standard curve was prepared from lysis buffer, 1 mg/ml bovine serum albumin (BSA), and water to reflect the following concentrations: 0, 2, 4, 6, 8, 10, 12  $\mu$ g/ml. Standards and samples (10  $\mu$ l), in duplicate, were pipetted into a 96-well plate. The working solution (Reagent A + Reagent B) (200  $\mu$ l) was added to each well, incubated at 37°C for 1 h, and absorbance read at 570 nm.

### **Immunoblot analysis**

**Gel Casting:** ACRYL/BIS solution-Ultra Pure, 30% (AMRESCO LLC-Solon, OH), TEMED (J.T. Baker-Center Valley, PA), 10% Ammonium Persulfate (APS) (#802811,

MP Biomedicals, Inc., Solon, OH), resolving buffer (1.5 M Tris, pH 8.8, 0.4% sodium dodecyl sulfate (SDS) (J.T. Baker), and stacking buffer (0.5 M Tris pH 6.8, 0.4% SDS) were used to cast gels.

**Electrophoresis:** 5× loading dye (0.25 mM Tris pH 6.8, 10% SDS, 10 mM DTT, 30% glycerol, 0.05% bromophenol blue, β-mercaptoethanol), running buffer (0.25 mM Tris, 250 mM Glycine, 0.1% SDS), and multicolor broad range protein ladder (#26634-Spectra, ThermoFisher Scientific) were used for electrophoresis.

**Transfer:** Immobilon-P Transfer Membrane, pore size: 0.45 μm (Merck Millipore Ltd.), (PVDF) membrane, 3MW Blotting Paper (MIDSCI, St. Louis, MO), and Transfer buffer (25 mM Tris pH 8.0, 195 mM Glycine, 20% methanol), were used to transfer gels.

**Blocking:** BSA (AMRESCO, LLC), and Tris buffered saline (25 mM Tris pH 8.0, 150 mM NaCl, 2 mM KCl) were used to block PVDF membranes.

**Wash:** Tris buffered saline-tween (TBST) (TBS 0.1% Tween-20 (AMRESCO, LLC) was used to wash PVDF membranes.

**Antibodies:** Several antibodies were obtained from Santa Cruz Biotechnology (Dallas, TX) including p-IκBα-Ser32/36 (sc-847), total IκBα (sc-101713), total NF-κB p65 (sc-372), TLR4 (sc-293072), CD68 (H-255) (sc-9139), alpha-tubulin (sc-5546), and β-tubulin (sc-9104). Antibodies purchased from Cell Signaling included phospho NF-κB p65-Ser536 (3033S), MyD88 (4283S), His3 (4499S), anti-rabbit (7054S), and anti-mouse (7056S). Anti-Glial Fibrillary Acidic Protein clone GA5 (MAB360) was purchased from Millipore.

**Imaging:** Enhanced Chemifluorescence substrate (#RPN5785) and a Typhoon Scanner 9410 (GE Healthcare Bio-Sciences, Pittsburgh, PA) were used to visualize proteins.

Protein lysates were subjected to SDS-page electrophoresis and immunoblot analysis. Acrylamide gels (10-well) were made ranging from 7-13% (depending on the protein being measured) and placed in 4°C, overnight. Protein extracts (50 µg) were prepared using loading dye (0.25 mM Tris, pH 6.8, 10 mM DTT, 30% glycerol, 10% SDS, 0.05% bromophenol blue, and 50 µl/ml β-mercaptoethanol). Samples were boiled for 10 min and brought to a standing temperature of 37°C. Samples were loaded into gels with running buffer and electrophoresed at 100 V for 15 min, and then increased to 125 V for 145 min for an overall running time of 2 h. Proteins were transferred onto PVDF membranes in transfer buffer and electrophoresed at 100 V for 90 min. After transfer, PVDF membranes were rinsed and blocked in BSA TBS-Tween (2% BSA for CD68 and 5% BSA for all other antibodies) for 2 h at 25°C with rocking. Primary antibodies (1:500-1:2000) diluted in 2-5% BSA-TBST, were added to membranes and rocked overnight at 4°C. The following day, membranes were washed three times with TBST for 5 min. AP-linked secondary antibodies (1:1000-1:5000) diluted in 2-5% BSA-TBST (2% for CD68 and 5% for all other antibodies) were added to membranes and rocked for 2 h at 25°C and then washed three times with TBST for 20 min. ECF fluorescent substrate (#45-000-947, GE Healthcare Amersham) was used to image blots using the Typhoon Scanner 9410. Image J software (NIH) was used to obtain the mean grey intensity for the bands of interest.

### **RNA extraction**

Trizol reagent (#15596018, Ambion, Inc., Austin, TX) was used for RNA extraction. Reagents used for extraction included chloroform, 100% isopropanol, 75% molecular

grade ethanol, and nuclease-free or diethylpyrocarbonate-treated water. Following cell stimulation, cells were washed three times with ice-cold PBS, incubated in Trizol (1 ml/100 mm dish) at 25°C for 5 min, and then lysates were collected in nuclease-free tubes. Chloroform (0.2 ml) was added to lysates followed by manual shaking of tubes for 15 sec. Lysates were then incubated at 25°C for 3 min, centrifuged at  $12,000 \times g$  for 15 min (4°C) and then the upper aqueous phase was collected. Isopropanol (0.5 ml) was added to the aqueous phase, followed by incubation at 25°C for 10 min, and centrifuged at  $12,000 \times g$  for 10 min (4°C). Next, the supernatant was removed and RNA pellets washed with ethanol, and centrifuged at  $7,500 \times g$  for 2 min (4°C). This ethanol wash step was repeated twice. RNA pellets were dried at 25°C for 15 min, followed by the addition of 35  $\mu$ l nuclease-free water. RNA samples were incubated in a 65°C water bath for 10 min and then stored at -80°C. To obtain RNA concentrations, RNA was thawed on ice and ng/ml determined with a Nanodrop Spectrophotometer 1000 (ThermoScientific), and validated with the 260/280 and 260/230 ratios greater than 1.80.

### **RNA Integrity**

NorthernMax-Gly Gel Prep/Running Buffer (#AM8678, Ambion), glyoxal sample load dye (#AM8551, Ambion), agarose (#BE-A500, MIDSci), 10,000 $\times$  SYBR Safe DNA Gel Stain (#S33102, Invitrogen), RNase ZAP (#9780, Ambion), and nuclease-free or DEPC-treated water were used to verify RNA integrity. RNA gels were prepared with NorthernMax-Gly Reagents to check RNA integrity. A 1% agarose gel was prepared with NorthernMax-Gly buffer. To prepare samples, 3  $\mu$ l RNA, 3  $\mu$ l nuclease-free water and 6  $\mu$ l glyoxal sample loading dye (equal parts) were incubated at 50°C for 30 min. Samples

were loaded and electrophoresed at 100 V for 45 min. RNA gels were stained with SYBR Safe (3  $\mu$ l/50 ml in 1 $\times$  NorthernMax-Gly buffer) and rocked on a Multimixer (Lab-Line Instruments, LLC-Melrose Park, IL) for 30 min. To visualize the 28S and 18S bands, RNA gels were imaged on Typhoon Scanner 9410 at 450 V.

### **Reverse Transcription**

Reverse transcription was achieved using the SuperScript<sup>TM</sup> IV VILO<sup>TM</sup> Master Mix with ezDNase<sup>TM</sup> Enzyme (Invitrogen, #11766050). The kit included Superscript IV VILO master mix, Superscript IV VILO master mix “no RT” control, ezDNase enzyme, ezDNase buffer, and nuclease-free water. First 10 $\times$  ezDNase buffer and ezDNase enzyme were added to 2  $\mu$ g RNA, and nuclease-free water was added up to 10  $\mu$ l total volume. Samples were mixed gently and incubated at 37°C for 2 min. Samples were placed on ice and Superscript master mix (4  $\mu$ l) or “no RT” control (4  $\mu$ l) was added to each sample and water added up to 20  $\mu$ l total volume. Samples were gently mixed and incubated at 25°C for 10 min, 50°C for 10 min, and 85°C for 5 min. Samples were diluted with nuclease-free water up to 100  $\mu$ l volume, for a final concentration of 20 ng/ml.

### **Reverse Transcription-Polymerase Chain Reaction**

cDNA (100 ng/ml) was used to perform reverse-transcription polymerase chain reaction (RT-PCR) for genes of interests. The primer for CD68 was designed using rat CD68 messenger RNA (mRNA) from the National Institute of Health's (NIH) National Center for Biotechnology Information website and ordered from IDT Technologies. The primers for TLR4 and TNF $\alpha$  were obtained from IDT Technologies. RT-PCR mix included 2 $\times$

PowerUp SYBR Green, 0.5  $\mu$ M forward primer, 0.5  $\mu$ M reverse primer, and nuclease-free water up to 15  $\mu$ l. Thermocycler settings were as follows: 50°C-2 min, 95°C-2 min, (95°C-15 sec, 60°C-1 min for 40 cycles), 95°C-15 sec, 60°C-1 min, 95°C-15 sec. Primer sequences are as follows: *TLR4*-forward: 5'-GAA GCT ATA GCT TCA CCA ATT TCT CAC AA-3', 60.2°C; reverse: 5'-GAT AGG GTT TCC TGT CAG TAC CAA GGT TG-3', 60.1°C, *CD68*-forward: 5'- CTC AGC AGC TCT ACC ATG AGG TTC -3', 59°C; reverse: 5'- CTT CCG GTG GTT GTA GGT GTC TC -3', 59.2°C, *TNF $\alpha$* -forward: 5'- CAG ATC ATC TTC TCA AAA CTC GAG TGA CA-3', 60.3°C; reverse: 5'-GTT GGT TGT CTT TGA GAT CCA TGC CAT TG'3', 60.1°C, and  *$\beta$ -actin*-Forward: 5'-GAA GGA TTC CTA TGT GGG CGA CGA-3', 60.5°C ; Reverse: 5'-GAG CCA CAC GCA GCT CAT TGT AG-3', 60.3°C.

### **Immunocytochemistry**

CHME-5 cells were prepared for fluorescence imaging using epifluorescence and confocal microscopy. Paraformaldehyde (PFA) (#30525-89-4, ACROS-New Jersey), BSA (#0332-500G, AMRESCO-Solon, OH) with Triton-X (#A16046, Alfa Aesar), primary antibodies (1:1000), fluorescently-labeled secondary antibodies (1:1000, 647-#A31573; 555-#A31570, Invitrogen), Prolong Gold anti-fade reagent (#P10144, Life Technologies; Eugene, OR), Gold Seal cover slips (#3306, Thermo Scientific), Premium microscope slides (#12-544-7, Fisher Scientific), and 4,6-diamidino-2-phenylindole (DAPI) nuclear staining were used to prepare samples. Cells were exposed to SFM with or without LPS (1  $\mu$ g/ml) for 10 min at 37°C. After stimulation, cells were gently washed three times with ice-cold PBS and fixed with 4% PFA for 10 min at 25°C. Cells were



washed three times with ice-cold PBS and permeabilized with 0.01% Triton-X in PBS for 10 min at 25°C. Next, cells were washed as described above and primary antibodies (TLR4-mouse, 1:1000) or CD68-rabbit, 1:1000) in PBS added to each appropriate well and rocked overnight at 4°C. The next day, cells were washed three times with TBST and incubated with fluorescently labeled secondary antibodies (anti-rabbit-AlexaFluor-647, 1:1000 or anti-mouse-AlexaFluor-555, 1:1000), while rocking for 2 h at 25°C. Negative control cells were only treated with secondary antibodies. Cells were washed three times with TBST and labeled with DAPI-PBS for 10 min, rocking at 25°C. Finally, cells were washed three times with TBST, cover slips removed from wells, and mounted on slides using anti-fade gold mounting media. Slides were allowed to dry overnight and imaged the following day.

### **Epifluorescence Microscopy**

TLR4 and CD68 immunofluorescence was imaged with an epifluorescence microscope (Olympus BX51) using Spot 5.1 software. Images were captured with the 40× objective using fluorescent channels for DAPI (350 nm), TLR4 (TRITC-555 nm), and CD68 (Cy5-647 nm). Images were processed with CellProfiler cell image analysis software (Carpenter et al., 2006), and quantified in GraphPad Prism 7.0. For verification, cells were traced with the Wacom in Image J Software and then quantified in GraphPad Prism 7.0.

### **Confocal Microscopy**

The Leica SPE Scanhead RYBV confocal microscope was used to capture images for bright field, and immunofluorescence and all images were processed in Leica Application Suite Advanced Fluorescence (LAS-AF). For bright field imaging, the 488 laser (55%) was used to capture images with the 100× oil objective in unstimulated and LPS-stimulated cells, which were fixed with 4% PFA for 10 min at 25°C. For fluorescent imaging, cells were prepared as described in the immunocytochemistry section and images captured with the 100× oil objective using fluorescent channels for DAPI (350 nm), TLR4 (Rhodamine-555 nm), and CD68 (Texas Red-647 nm). The TLR4 channel (red) gain and laser was set to 925 and 33%, the CD68 channel (green) gain and laser was set to 975 and 33%, and the DAPI channel (blue) gain and laser was set to 839 and 15%. These settings were applied to all confocal images.

### **NF-κB p65 binding assay**

A NF-κB p65 Transcription Factor Kit (#89859, Thermo Scientific) was used to analyze CHME-5 nuclear extracts. This kit included a 96-well assay plate coated with NF-κB consensus sequence, (5× NF-κB Binding buffer, 20× Poly dI-IC, MilliQ H<sub>2</sub>O), 10× wash buffer, antibody dilution buffer, NF-κB p65 primary antibody, HRP-conjugated secondary antibody, Luminol/Enhancer solution, Stable peroxide solution, and TNFα-activated HeLa cell nuclear extract (positive control). Initially, binding buffer (50 µl) was added to each well, which contained the NF-κB consensus sequence. Then, 10 µl of nuclear extracts or positive control, TNFα-activated HeLa cells, were added to each well, in duplicate. Extracts were incubated for 1 h with mild agitation. Wells were then washed three times with 200 µl of wash buffer, 100 µl of primary antibody (1:1000) was then

added to each well, followed by incubation for 1 h at 25°C, without agitation. Wells were then washed three times with 200 µl of wash buffer, 100 µl of secondary antibody (1:10,000) was then added, followed by incubation for 1 h at 25°C, without agitation. Wells were then washed four times with 200 µl of wash buffer, and 100 µl of chemiluminescence substrate (equal parts Luminol/Enhancer and Stable peroxide solution) added to each well. Chemiluminescence was read immediately with a Synergy 2 plate reader. Binding activity was quantified with protein concentrations obtained with BCA protein assay.

### **Statistical Analysis**

Image J Software was used to obtain the mean grey intensity of all immunoblots and the mean was taken for each time point. Protein expression was normalized to the  $\beta$ -tubulin housekeeping gene, or to total protein (phosphorylation blots). GraphPad Prism 7.0 was used for transformation, quantification, and graphing of all data. For statistical analysis, one-way analysis of variance (ANOVA) with Dunnett's or Tukey's multiple comparison tests were used, unless otherwise stated in the results section. Significance was determined at  $p < 0.05$ .

## RESULTS

### *LPS-induced activation of NF- $\kappa$ B p65 in CHME-5 cells*

#### **LPS is not toxic**

The MTT assay was used to determine the extent to which LPS stimulation affects cell viability. Statistical analysis revealed that LPS did not significantly affect viability of CHME-5 cells, ( $p=1.00$ , **Figure 1A**) or ( $p=0.90$ , **Figure 1B**).

#### **LPS-mediated activation of NF- $\kappa$ B p65**

Phosphorylation of NF- $\kappa$ B p65 activation (p-NF- $\kappa$ B p65) was used to measure of NF- $\kappa$ B activation (**Figure 2A**). Statistical analysis revealed that LPS O55:B5 (1  $\mu$ g/ml) significantly increased nuclear levels of phospho-NF- $\kappa$ B p65 compared to unstimulated cells,  $p<0.05$  (**Figure 2B**).

#### **Alpha-tubulin and Histone 3-immunoreactivity as internal control**

Alpha-tubulin and histone 3 expressions were measured as an internal control to confirm purity of cellular compartmentalization in cytoplasmic and nuclear fractions (**Figure 3A**). Statistical analysis revealed significant differences in alpha-tubulin immunoreactivity in cytoplasmic extracts compared to nuclear samples ( $p<0.01$ - $p<0.0001$ ) and significant differences in histone 3-immunoreactivity in nuclear extracts as compared to cytoplasmic

samples ( $p < 0.0001$ ) (**Figure 3B, 3C**).

### ***LPS-induced CD68 expression in CHME-5 microglial cells***

#### **CD68 gene expression in CHME-5 cells**

Quantification of CD68 with  $\beta$ -actin revealed a significant up-regulation of *CD68* gene expression at 3 ( $p < 0.0001$ ) and 6 ( $p < 0.01$ ) h compared to unstimulated cells, while expression returned to basal levels by 18 h (**Figure 4A**). As an internal control, RNA integrity was verified by visualizing the 28S and 18S ribosomal RNA (rRNA) bands (**Figure 4B**).

#### **CD68 protein expression in CHME-5 cells**

CD68 protein expression was analyzed after LPS stimulation in whole cell lysates (**Figure 5A**). CD68 expression was significantly greater in LPS-stimulated cells at 10 min compared to unstimulated cells,  $p < 0.001$  (**Figure 5B**). Multiple CD68 protein bands were detected in LPS-treated cells, most prominently at 68, 90, and 110 kilodaltons (kDa).

#### **CHME-5 cells are GFAP negative**

For further confirmation that CHME-5 cells are microglia and not astrocytes, GFAP was measured using NHA whole cell lysates as a positive control (**Figure 6A**). Tukey's multiple comparison tests revealed a significant fold-change in GFAP expression in unstimulated ( $p < 0.001$ ) and LPS-stimulated ( $p < 0.0001$ ) NHA compared to CHME-5 cells, indicating an absence of GFAP-immunoreactivity in CHME-5 cells (**Figure 6B**).

### ***LPS-induced TLR4 expression in CHME-5 Cells***

#### **TLR4 gene expression in CHME-5 cells**

LPS induces the innate immune response through binding TLR4 and initiating intracellular signal transduction. TLR4 mRNA expression was significantly elevated 3 ( $p<0.0001$ ) and 6 ( $p<0.01$ ) h after LPS treatment; by 18 h expression was similar to unstimulated control (**Figure 7A**).

#### **LPS is not toxic at later time points**

The MTT assay revealed that LPS was not cytotoxic, rather it resulted in a minimal increase in cell viability at 6 h,  $p<0.05$  (**Figure 7B**).

#### **TLR4 protein expression in CHME-5 cells**

We also determined the extent to which LPS modulates TLR4 protein expression in CHME-5 cells. Immunoblot analysis revealed significant increases in TLR4 protein expression at 90 ( $p<0.01$ ) and 270 ( $p<0.01$ ) min after LPS treatment (**Figure 8A, 8B**).

### ***Analysis of CD68 and TLR4 immunocytochemistry***

#### **Quantitative analysis of CD68- and TLR4-immunofluorescence in CHME-5 cells**

Epifluorescence microscopy was employed to visualize and quantify CD68- and TLR4-immunofluorescence in unstimulated and LPS-stimulated CHME-5 cells (**Figure 9A, 9C**). Even though there was significant basal CD68-immunofluorescence in unstimulated cells, there was a greater increase in CD68-immunofluorescence in LPS-stimulated cells compared to unstimulated cells and negative controls, as assessed with Kruskal-Wallis

and Dunn's multiple comparison tests,  $p < 0.0001$  (**Figure 9B**). Multiple comparison tests also revealed a significant, increase in TLR4-immunofluorescence in LPS-stimulated cells compared to unstimulated cells and negative controls,  $p < 0.0001$  (**Figure 9D**). Handtracing also revealed significant increases in CD68- and TLR4-immunofluorescence in LPS-stimulated cells compared to unstimulated cells,  $p < 0.001$  (**Figure 9E, 9F**).

### **Qualitative analysis of CD68 and TLR4 immunofluorescence**

Next, we captured images of unstimulated and LPS-stimulated cells with bright field and fluorescent imaging, using confocal microscopy, to observe protein expression and localization. Overall, untreated cells displayed elongated cell bodies with longer processes than those treated with LPS, which exhibited rounded or swollen cell bodies with shorter processes (**Figure 10A**). In addition, TLR4-immunofluorescence in unstimulated cells was localized predominantly to the cell membrane, as opposed to LPS-treated cells, where TLR4 was present in both cytoplasmic and nuclear compartments (**Figure 10B**). CD68-immunofluorescence was widely distributed in the unstimulated cells, compared to LPS-stimulated cells, where CD68 was localized to the cytoplasm (**Figure 10C**). In unstimulated cells, CD68 and TLR4 were co-localized to the plasma membrane, while in LPS-stimulated cells co-localization was retained in the cytoplasmic compartment (**Figure 10D**).

### **LPS-induced I $\kappa$ B $\alpha$ activation in CHME-5 cells**

Phosphorylation of I $\kappa$ B $\alpha$  was used as a measure of I $\kappa$ B $\alpha$  activation in cytoplasmic lysates (**Figure 11A**). Statistical analysis revealed that LPS significantly increased I $\kappa$ B $\alpha$

activation at 10 min following stimulation,  $p < 0.05$  (**Figure 11B**). At 30-270 min, stimulation levels of p-I $\kappa$ B $\alpha$  were comparable to control cells.

#### **LPS-induced NF- $\kappa$ B p65 binding activity**

NF- $\kappa$ B p65 activation was also determined by assessing NF- $\kappa$ B p65 binding activity in nuclear extracts. NF- $\kappa$ B p65 binding activity was significantly increased at 10 ( $p < 0.05$ ) and 90 ( $p < 0.01$ ) min (**Figure 12**). Interestingly, binding activity at 30 and 180 minutes remained at basal levels.

#### **LPS-induced NF- $\kappa$ B p65 activation at 90 minutes in CHME-5 cells.**

Phosphorylation of NF- $\kappa$ B p65 was used as a measure of NF- $\kappa$ B p65 activation in nuclear extracts at 90 min (**Figure 13 A**). ANOVA and Dunnett's multiple comparison tests revealed significant increases in NF- $\kappa$ B p65 activation at 0.1 ( $p < 0.05$ ), 1 ( $p < 0.001$ ), and 10 ( $p < 0.01$ )  $\mu$ g/ml (**Figure 13 B**).

#### **LPS does not induce p38 activation in CHME-5 cells**

Phosphorylation of p38 was used as a measure of p38 activation in cytoplasmic lysates (**Figure 14A**). ANOVA revealed no significant differences in p38 activation as compared to unstimulated cells,  $p = 0.80$  (**Figure 14B**).

#### **LPS-induced TNF $\alpha$ gene expression**

Once NF- $\kappa$ B p65 is phosphorylated and translocated into the nucleus, it binds to pro-inflammatory consensus sequences for initiation of gene transcription of mediators, such



as  $\text{TNF}\alpha$ . Compared to unstimulated cells, stimulation with LPS significantly increased *TNF $\alpha$*  gene expression at 3 ( $p<0.01$ ), 6 ( $p<0.05$ ), and 18 ( $p<0.01$ ) h (**Figure 15**).

## FIGURES

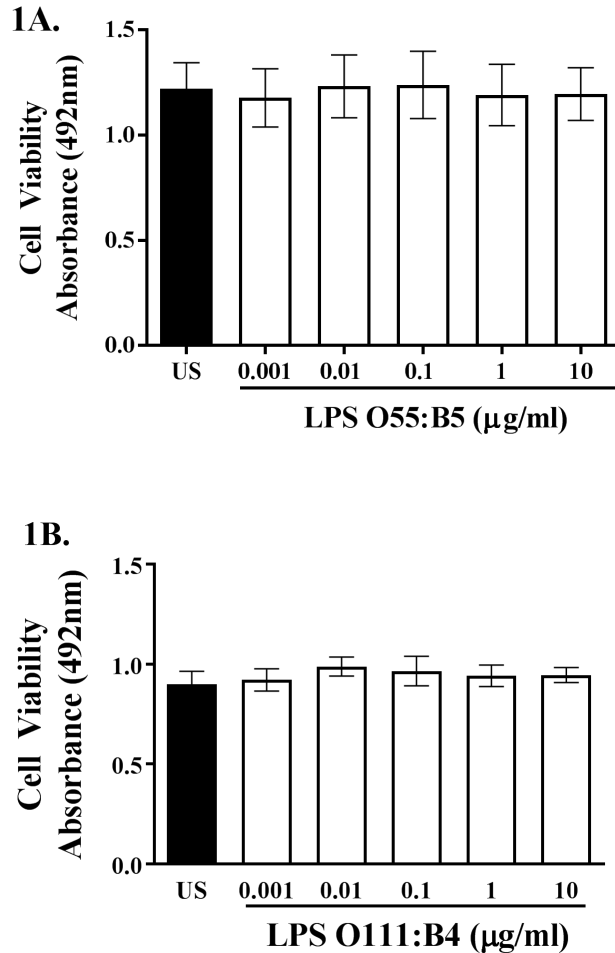


**Figure 1. *Escherichia coli* LPS O55:B5 and O111:B4 are not cytotoxic to CHME-5 cells**  
CHME-5 cells were stimulated with increasing doses of LPS (**A**) O55:B5 or (**B**) O111:B4 and incubated at 37°C for 30 min. MTT cell viability absorbance was measured at 492 nm. ANOVA and Dunnett's multiple comparison tests revealed no significant differences between control and LPS-treated cells, (**A**)  $p=0.100$  and (**B**)  $p=0.91$ . Three independent experiments were performed in duplicate ( $n=3$ ) for each treatment group. Bars are presented as mean  $\pm$  SEM.

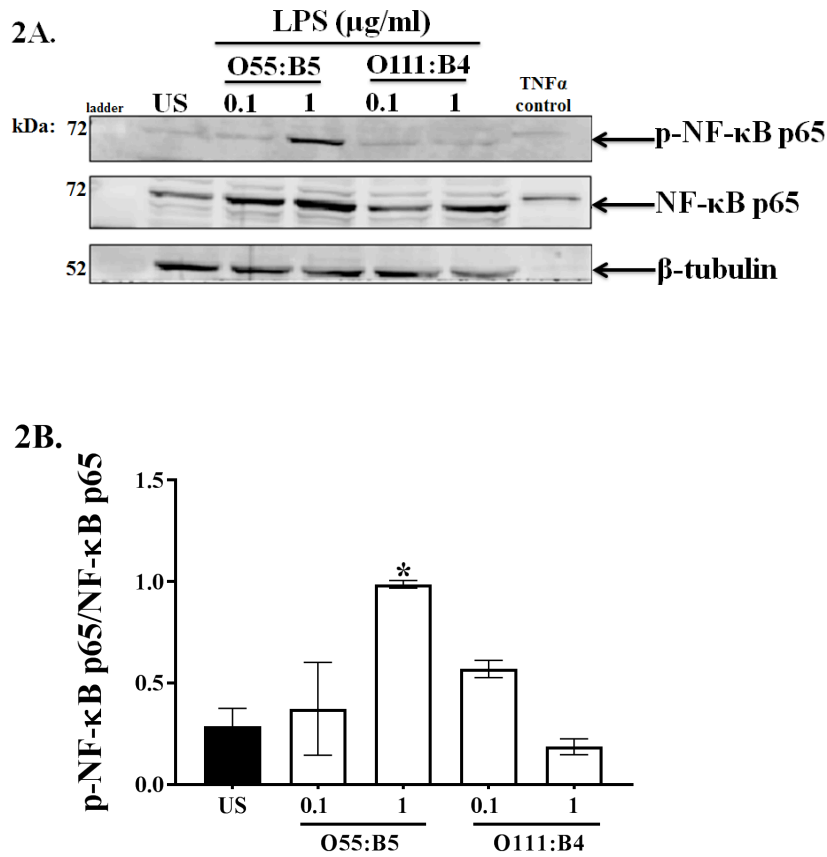


**Figure 2. LPS-induced activation of NF- $\kappa$ B in CHME-5 cells**

CHME-5 cells were treated with LPS O55:B5 and O111:B4 and incubated at 37°C for 30 min. **A.** Nuclear lysates were subjected to SDS-page electrophoresis and immunoblotted with phospho-NF- $\kappa$ B p65 (1:1000), NF- $\kappa$ B p65 (1:1000), and  $\beta$ -tubulin (1:1000) antibodies. **B.** phospho-NF- $\kappa$ B p65 was quantified with total NF- $\kappa$ B p65 and ANOVA and Dunnett's multiple comparison tests revealed a significant increase in phospho-NF- $\kappa$ B p65 with LPS O55:B5 (1  $\mu\text{g/ml}$ ). Images are representative of three independent experiments (n=3) for each treatment group. Bars are presented as mean  $\pm$  SEM.

\*  $p < 0.05$  vs. unstimulated cells

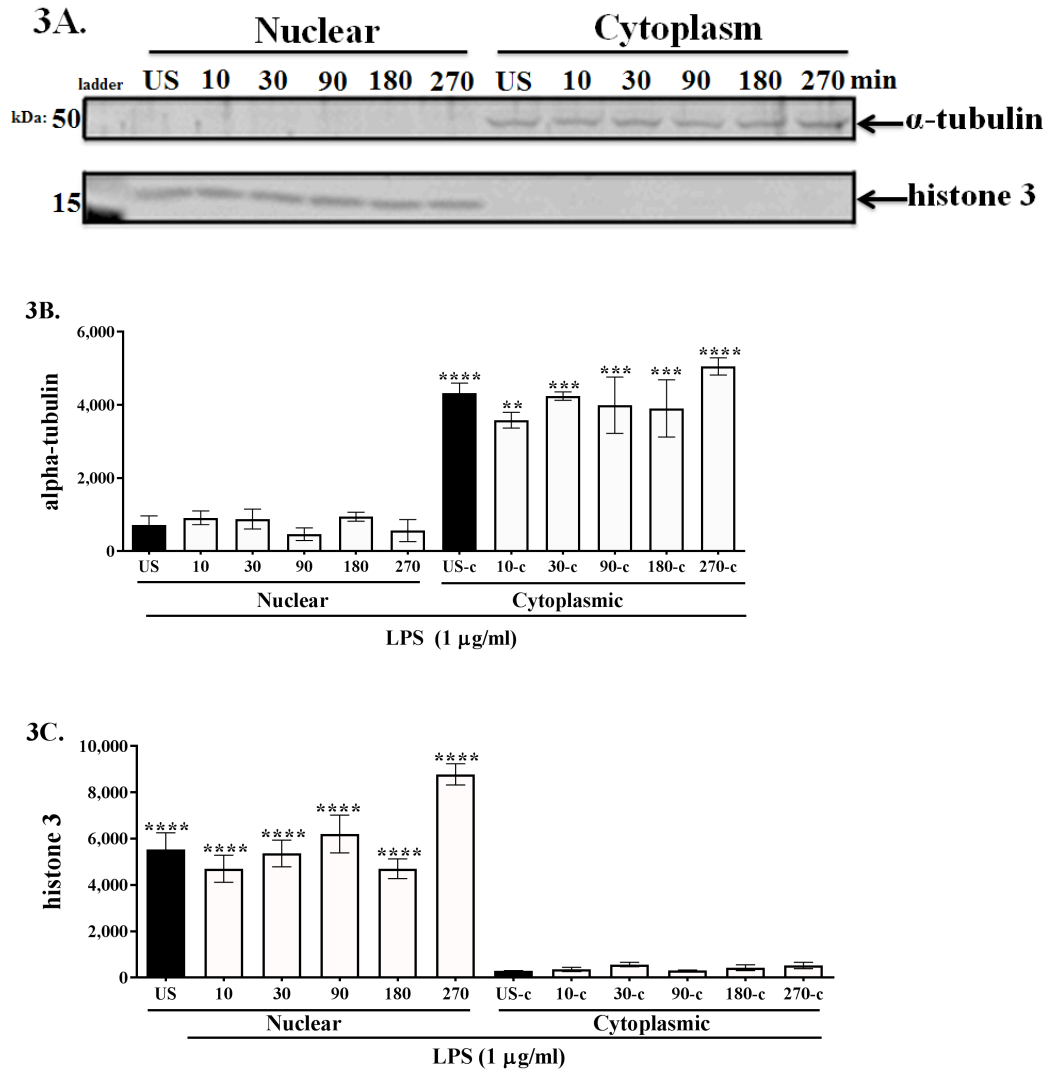


**Figure 3.  $\alpha$ -tubulin and histone 3-immunoreactivity in CHME-5 cellular fractions**

CHME-5 cells were stimulated with LPS and incubated at 37°C for a time course (0-270 min). **A.**

Cytoplasmic and nuclear extracts were subjected to SDS-PAGE and immunoblotted with  $\alpha$ -

tubulin (1:1000) or histone 3 (1:2000) antibodies. **B.** ANOVA and Tukey's multiple comparison

tests revealed significant increases in  $\alpha$ -tubulin-immunoreactivity in cytoplasmic fractions. **C.**

Similarly, histone 3-immunoreactivity was significantly increased in nuclear fractions. Images are

representative of four independent experiments (n=4) for each treatment group. Bars for all

experiments are presented as mean  $\pm$  SEM.

\*\*\*\* p<0.0001, \*\*\* p<0.001, \*\* p<0.01 vs. nuclear or cytoplasmic fractions

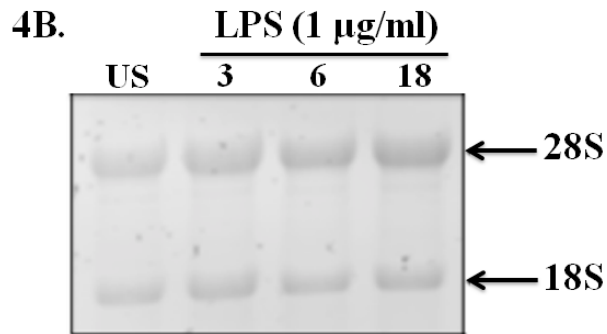
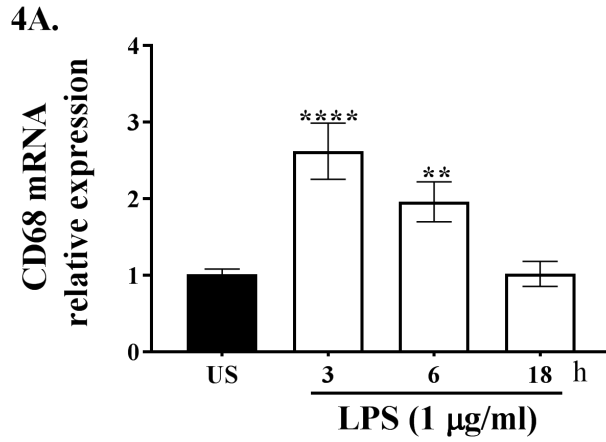


**Figure 4. LPS-induced *CD68* gene expression in CHME-5 cells**

CHME-5 cells were stimulated with LPS and incubated at 37°C for 3, 6, and 18 h. **A.** *CD68* mRNA expression was analyzed using RT-PCR. ANOVA and Dunnett's multiple comparison tests revealed significant increases at 3 and 6 h. Data were transformed using  $Y = \log(Y)$ . Image is representative of three independent experiments (n=3) for each treatment group. Data points are given as mean + SEM. **B.** RNA gels were used to verify the integrity of the 28S and 18S ribosomal RNAs (rRNAs). Image is representative of three independent experiments (n=3).

\*\*\*\*  $p < 0.0001$ , \*\*  $p < 0.01$  vs. unstimulated

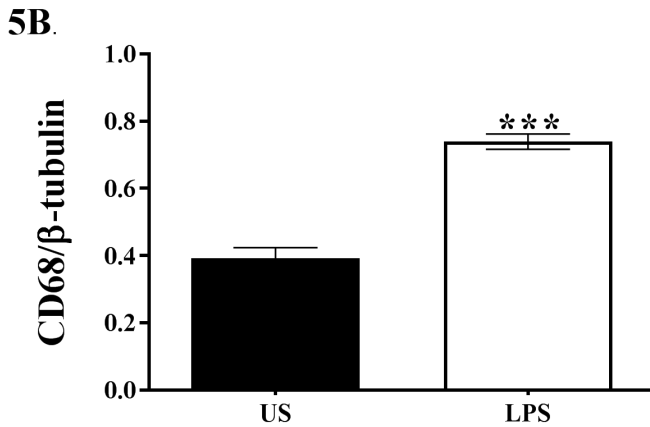
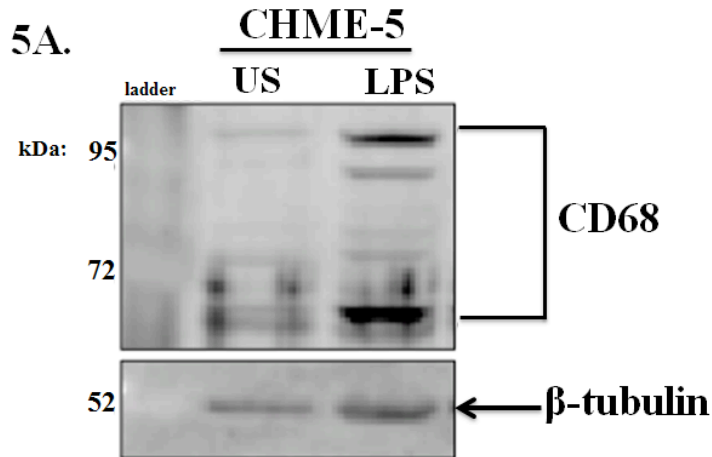


**Figure 5. LPS-induced CD68 protein expression in CHME-5 cells**

CHME-5 cells were stimulated with LPS and incubated at 37°C for 10 min. **A.** Whole cell lysates were subjected to SDS-page electrophoresis and immunoblotted with CD68 (1:500) and  $\beta$ -tubulin (1:1000) antibodies. **B.** Student's T-test revealed a significant increase in LPS-induced CD68 protein expression compared to unstimulated cells. Images are representative of four were independent experiments (n=4) for each group. Bars for all groups are presented as mean  $\pm$  SEM.

\*\*\* p<0.001 vs. unstimulated

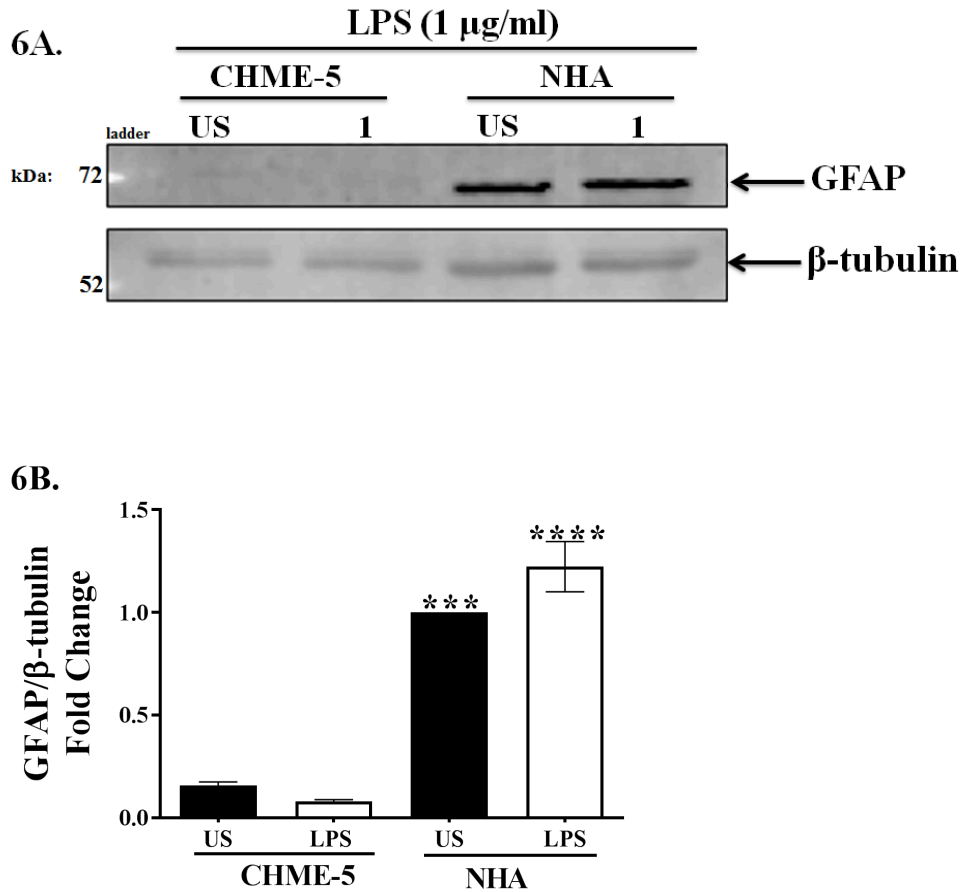
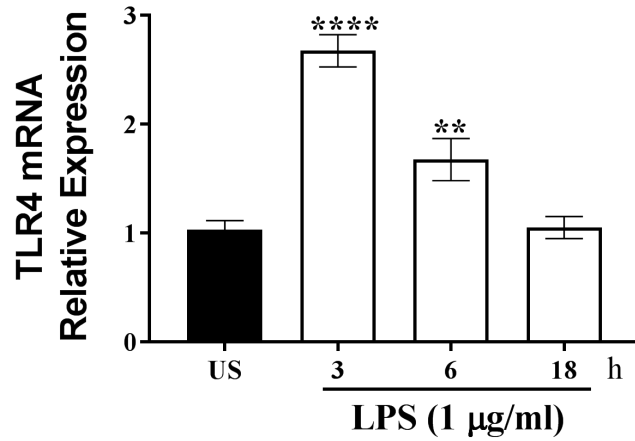


**Figure 6. CHME-5 cells are CD68-positive and GFAP-negative**

CHME-5 cells and normal human astrocytes (NHA) were stimulated with LPS and incubated at 37°C for 10 min. **A.** Whole cell lysates were subjected to SDS-page electrophoresis and immunoblotted with GFAP (1:2000) and  $\beta$ -tubulin (1:1000) antibodies. **B.** ANOVA and Tukey's multiple comparison tests revealed a significant fold change in GFAP-immunoreactivity in unstimulated and LPS-treated NHA compared to CHME-5 cells. Images are representative of three independent experiments (n=3) for each treatment group. Bars for all groups are presented as mean  $\pm$  SEM.

\*\*\*\* p<0.0001, \*\*\* p<0.001 vs. unstimulated

7A.



7B.

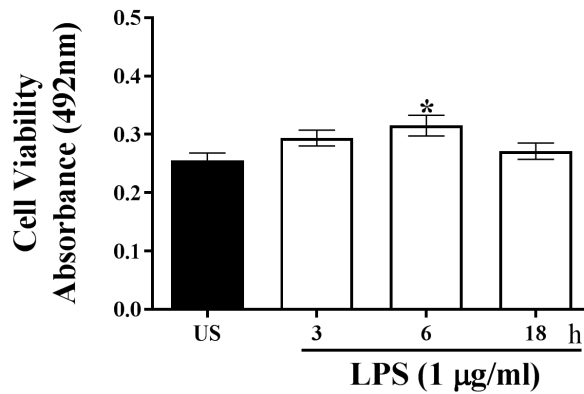


**Figure 7. LPS-induced *TLR4* gene expression in CHME-5 cells**

CHME-5 cells were stimulated with LPS and incubated at 37°C for 3, 6, and 18 h. **A.** *TLR4* mRNA expression was analyzed using RT-PCR. ANOVA and Dunnett's multiple comparison tests revealed significant increases at 3 and 6 h. Image is representative of three independent experiments (n=3) for each treatment group. **B.** Following stimulation, MTT cell viability assay was performed and absorbance was measured at 492 nm. ANOVA and Dunnett's multiple comparison tests revealed a minimal increase at 6 h. Three experiments were performed in duplicate with (n=3) for each treatment group. Bars for all groups are presented as mean  $\pm$  SEM.

\*\*\*\* p<0.0001, \*\*\* p<0.01, \* p<0.05 vs. unstimulated cells



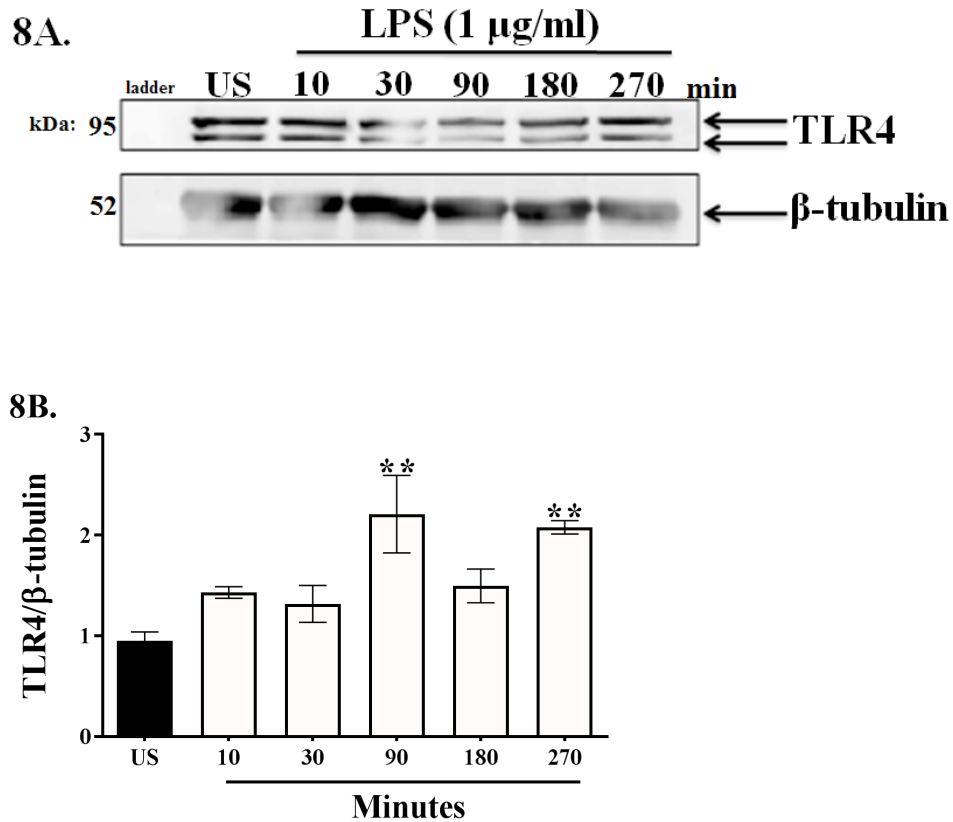


**Figure 8. LPS-induced TLR4 protein expression in CHME-5 cells**

CHME-5 cells were stimulated with LPS and incubated at 37°C for a time course (0-270 min). **A.** Whole cell lysates were subjected to SDS-page electrophoresis and immunoblotted with TLR4 (1:1000) and  $\beta$ -tubulin (1:1000) antibodies. **B.** ANOVA and Dunnett's multiple comparison tests revealed a significant increase in TLR4 protein expression at 90 and 270 min. Asterisks denote significant differences from unstimulated cells. Images are representative of five independent experiments (n=5) for each treatment group. Bars for all groups are presented as mean  $\pm$  SEM.

\*\* p<0.01 vs. unstimulated cells

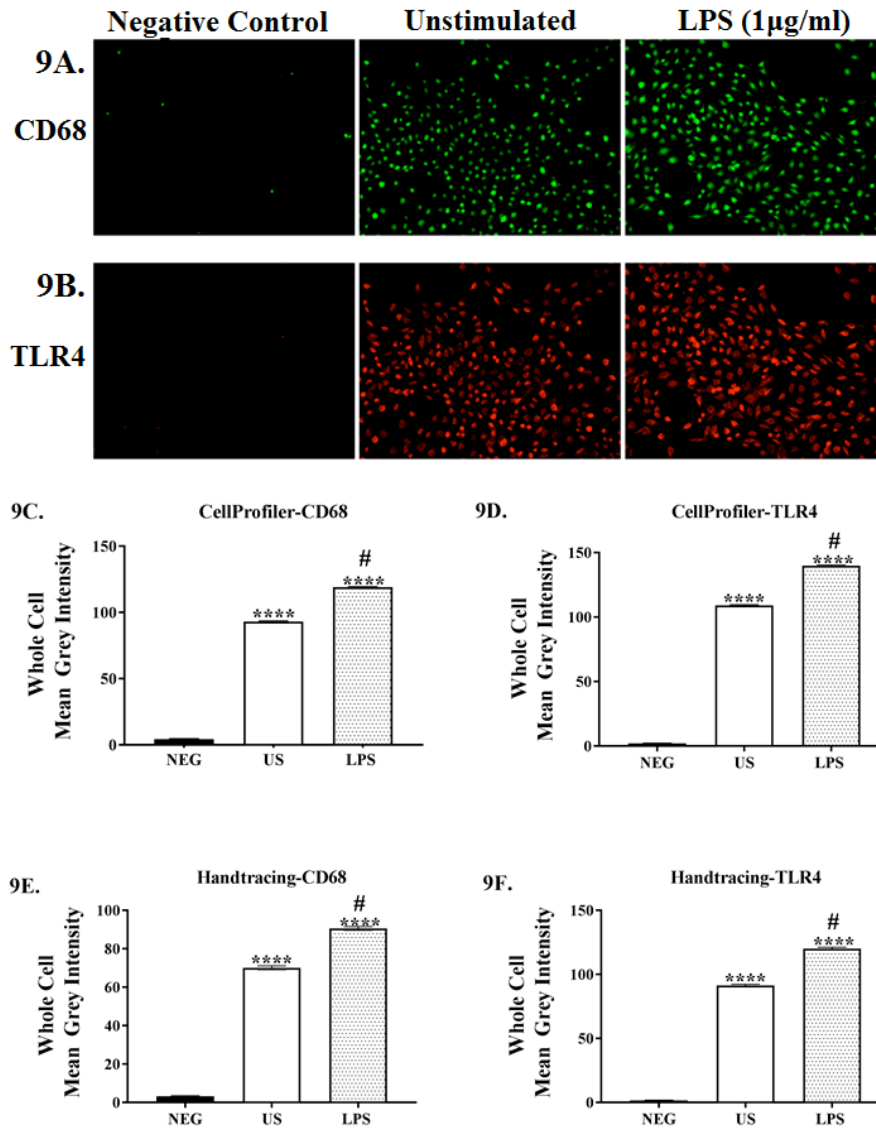


**Figure 9. Quantitative analysis of LPS-induced CD68- and TLR4-immunofluorescence with epifluorescence microscopy**

CHME-5 cells were stimulated with LPS and incubated at 37°C for 10 min. Cells were fixed and stained with **A.** CD68 (1:1000) and anti-rabbit-Alexa Fluor 647 (1:1000) or **B.** TLR4 (1:1000) and anti-mouse-Alexa Fluor 555 (1:1000). Negative control cells were not stained with primary antibody but stained with secondary antibody. Epifluorescence images were captured with the 40× objective using Texas Red-647 (CD68-green) and Cy5-555 (TLR4-red) fluorescent channels. **C.** Kruskal-Wallis and Dunn's multiple comparison tests revealed significant increases

in CD68-immunofluorescence and **D**. TLR4-immunofluorescence in LPS treated cells. **E and F**. CD68 and TLR4 immunofluorescence was also quantified with handtracing in Image J. Kruskal-Wallis and Dunn's multiple comparison tests revealed significant increases in CD68-immunofluorescence and **D**. TLR4-immunofluorescence in LPS treated cells. Asterisks denote significant differences from negative control and # denotes a significant difference from unstimulated cells. The contrast for CD68 and TLR4 (unstimulated and stimulated) images were adjusted to min, max= 29, 225. Bars for all experiments are presented as mean  $\pm$  SEM.

\*\*\*\*  $p < 0.0001$  vs. negative control, #  $p < 0.0001$  vs. unstimulated cells

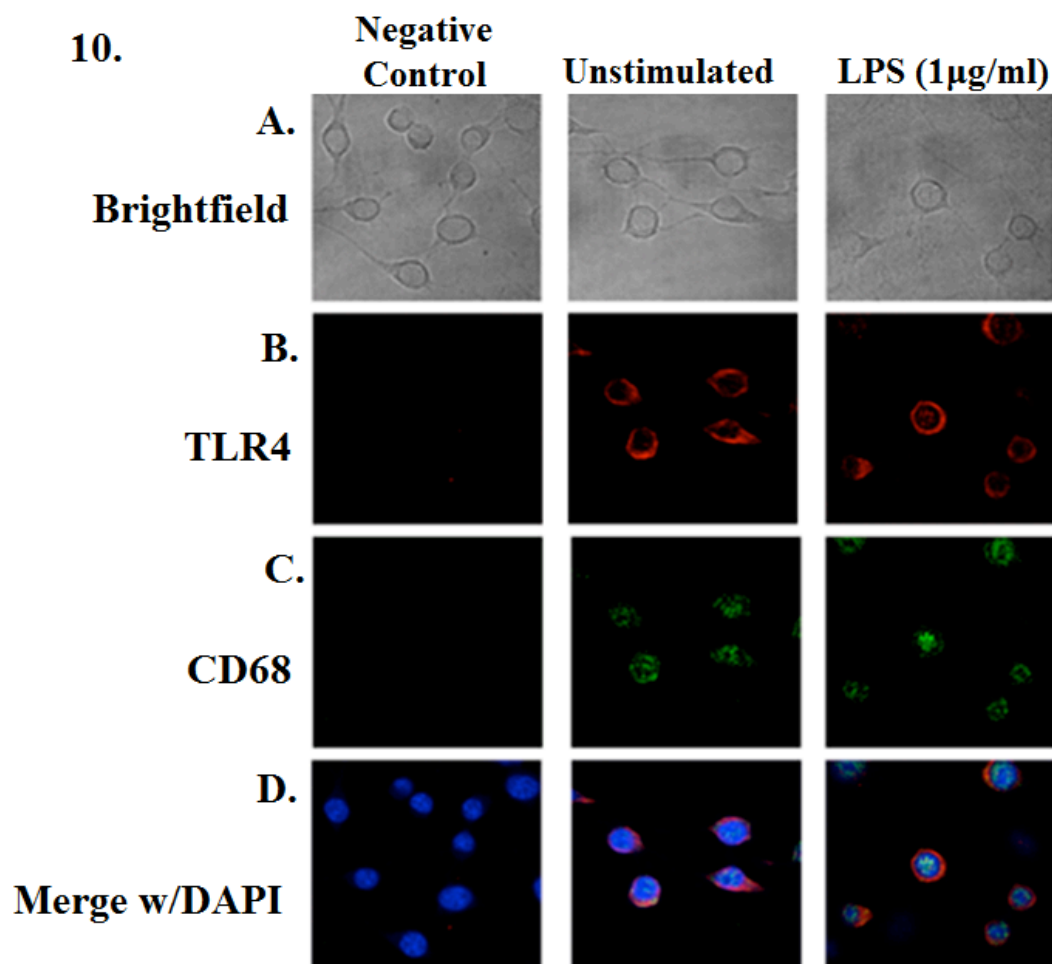


**Figure 10. Visualization of LPS-induced CD68- and TLR4-immunofluorescence with confocal microscopy**

CHME-5 cells were stimulated with LPS and incubated at 37°C for 10 min. **A.** Bright field images were captured with 100 $\times$  oil objective. Cells were fixed and stained with **B.** TLR4 (1:1000) and anti-mouse-Alexa Fluor 555 (1:1000), **C.** CD68 (1:1000) and anti-rabbit-Alexa Fluor 647 (1:1000), and **D.** DAPI (blue). Confocal images for CD68 and TLR4-immunofluorescence were captured with 100 $\times$  oil objective using Cy5-555 (TLR4-red), Texas Red-647 (CD68-green), and DAPI-388 (nucleus-blue) fluorescent channels. **D.** Images merged with DAPI



12A.

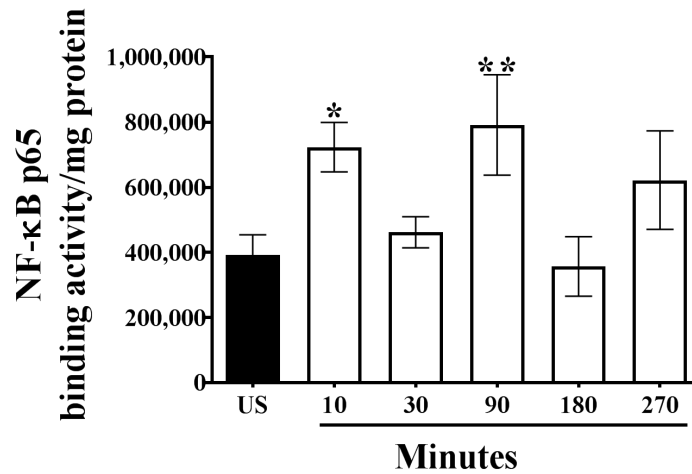


**Figure 12. LPS-induced NF-κB p65 activation in CHME-5 cells**

CHME-5 cells were stimulated with LPS and incubated at 37°C for a timecourse (10-270 min).

Nuclear extracts were analyzed for NF-κB p65 binding activity. ANOVA and uncorrected

Fisher's LSD revealed a significant increase in NF-κB p65 binding activity at 10 and 90 min.

Image is representative of five independent experiments (n=5) for each treatment group. Bars for all experiments are presented as mean ± SEM.

\*\*p<0.01, \* p<0.05 vs. unstimulated cells

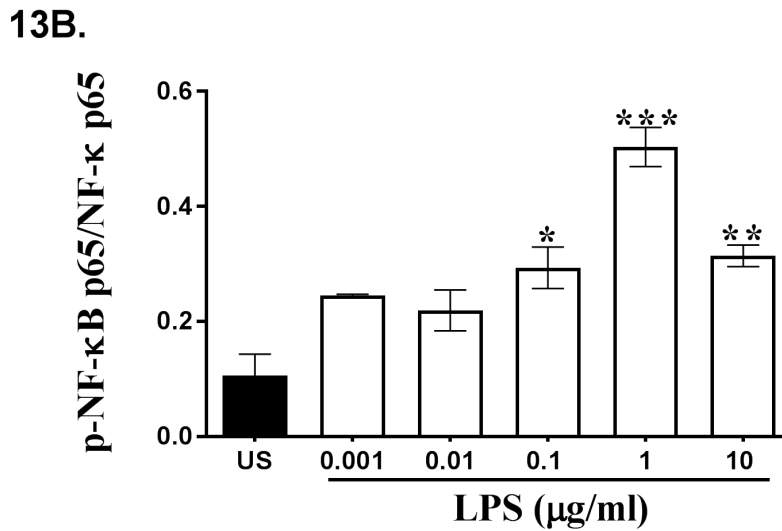
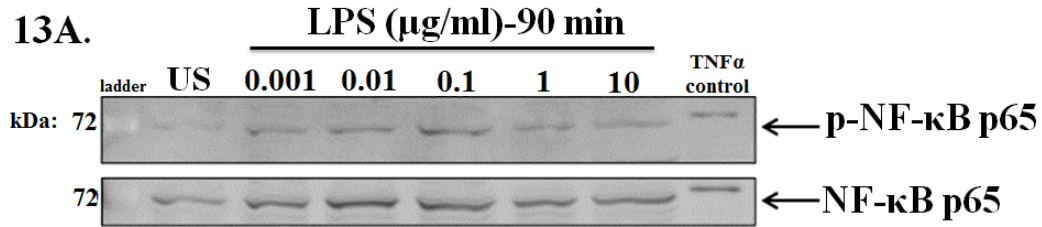


**Figure 13. LPS-induced NF-κB p65 activation at 90 minutes in CHME-5 cells**

CHME-5 cells were stimulated with LPS and incubated at 37°C for 90 min. **A.** Nuclear lysates were subjected to SDS-page electrophoresis and immunoblotted with phospho-NF-κB p65 (1:1000) and NF-κB p65 (1:1000) antibodies. **B.** ANOVA and Dunnett's multiple comparison tests revealed a significant increase in NF-κB p65 activation at 0.1, 1, and 10 μg/ml. Images are representative of three independent experiments (n=3) for each treatment group. Bars are presented as mean ± SEM.

\*\*\* p<0.001, \*\* p<0.01, \* p<0.05 vs. unstimulated cells

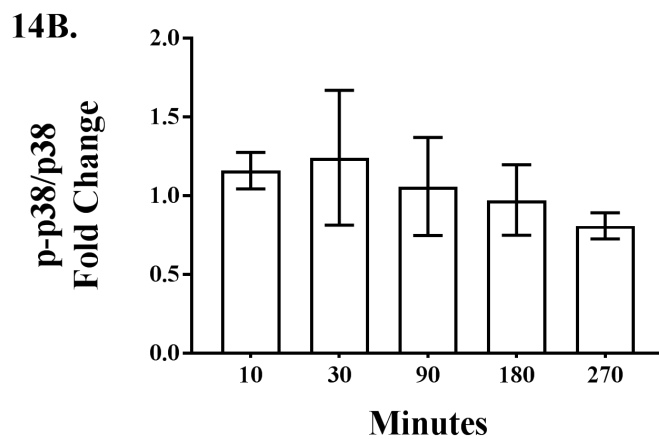
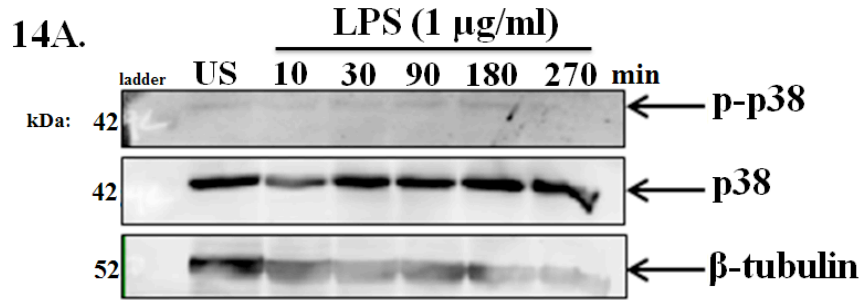


**Figure 14. LPS does not induce p38 activation in CHME-5 cells**

CHME-5 cells were stimulated with LPS and for 10-270 min. **A.** Cytoplasmic lysates were subjected to SDS-page electrophoresis and immunoblotted with phospho-p38 (1:1000) and p38 (1:1000) antibodies. **B.** ANOVA revealed no significant increase in p38 activation in LPS-treated cells as compared to unstimulated cells,  $p=0.80$ . Images are representative of three independent experiments ( $n=3$ ) for each treatment group. Bar are presented as mean  $\pm$  SEM.



15A.

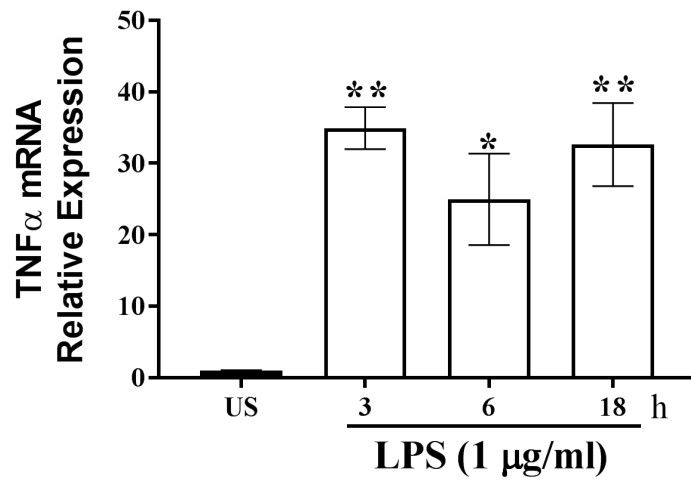


**Figure 15. LPS-induced TNF $\alpha$  gene expression in CHME-5 cells**

CHME-5 cells were treated with LPS for 3, 6, and 18 h. *TNF $\alpha$*  mRNA expression was analyzed with RT-PCR. Kruskal-Wallis and Dunn's multiple comparison tests revealed significant increase in LPS-induced *TNF $\alpha$*  gene expression at 3, 6, and 18 h. Images are representative of three individual with n=3 experiments. Bars for all experiments are presented as mean  $\pm$  SEM.

\*\* p<0.01, \* p<0.05 vs. unstimulated cells

## DISCUSSION

Microglia are considered the macrophages of the CNS, and are central to inflammation in the brain (Kettenmann et al., 2011). Microglia are of monocytic lineage and take residence in the CNS during the first and second trimesters of embryonic development (Kettenmann et al., 2011; Monier et al., 2007). Much of what is known about microglia is derived from *in vitro* studies using primary or transformed cell lines of mouse or rat origin. The establishment of a human microglial cell line, CHME-5, was an important advancement for investigating microglia. CHME-5 cells were immortalized and validated to have similar morphological and functional properties of primary microglia (Janabi et al., 1995; Peudenier et al., 1991). Here, we characterize TLR4 neuroinflammatory signaling in CHME-5 cells and demonstrate that CHME-5 cells are a reliable tool to study microglial-like inflammatory responses.

Presently, we illustrate morphological characteristics of “resting” vs. “activated” microglia using bright field imaging. Unstimulated and LPS-stimulated cells displayed morphological signatures of microglia, as seen in previous studies (Cheepsunthorn et al., 2001; Kettenmann et al., 2011; S. Lee et al., 2007; Sheng et al., 2011), which included smaller somas and elongated processes, or amoeboid-shaped and rounder cell bodies, respectively. This demonstrates that CHME-5 cells retain key characteristics of microglial cells.

We also wanted to ensure microglial phenotype through the expression of a microglial cell marker. Microglia are known to up-regulate several activation markers, such as CD68, in response to damage, disease, or loss of homeostatic conditions. CD68 is expressed in endolysosomes and in the plasma membrane of activated microglia (Pulford et al., 1990; Ramprasad et al., 1996; Saito et al., 1991). *CD68* gene and protein expression were increased after LPS treatment during early time points. This quick response indicates that microglia are the first responders in the CNS (Gehrmann et al., 1995; Kreutzberg, 1996), which aligns with their role of surveying and returning their environment to homeostasis (Hughes, 2012; Nimmerjahn et al., 2005). The expression of CD68 is confirmation that these cells still retain phenotypic properties of microglia, along with morphological attributes as seen with our immunocytochemistry studies.

It was important to ensure that cultures were not contaminated with astrocytes, considering astrocytes make up 40-50% cell type in the CNS (Bowman et al., 2003; Carpentier et al., 2005). GFAP-immunoreactivity was analyzed in both CHME-5 cells and normal human astrocytes (NHA). CHME-5 cells, unlike NHA, showed no GFAP-immunoreactivity, which confirmed CHME-5 cells are not astrocytes. These CHME-5 cells are indeed expressing CD68, and importantly are GFAP-negative, which eliminates our concern that CHME-5 may be astrocytes or that the culture is contaminated with astrocytes.

We also demonstrated that LPS induced inflammatory signaling without inducing cytotoxicity. This finding is consistent with other studies (Lindberg et al., 2005), and indicates that any observed decreases in gene/protein expression throughout these

experiments are not due to LPS toxicity, but rather to specific LPS-induced inflammatory responses.

To investigate LPS-induced TLR4 neuroinflammatory signaling, we used *Escherichia coli* LPS O55:B5 to model an inflammatory state in the CNS and studied several signaling proteins that are constitutively expressed and activated in the TLR4 pathway. Analysis of two crucial intracellular TLR4 signaling proteins, I $\kappa$ B $\alpha$  and NF- $\kappa$ B, were chosen to investigate neuroinflammatory signaling in CHME-5 cells. LPS-induced NF- $\kappa$ B p65 activation was consistent with other microglial cell lines (Cheepsunthorn et al., 2001; Horvath et al., 2008; S. C. Lee et al., 1993; Wu et al., 2007). Given that many studies investigating microglial responses used a similar dose of LPS (1  $\mu$ g/ml), we are confident that CHME-5 cells were adequately treated to observe inflammatory responses (Atanassov et al., 1995; Lindberg et al., 2005); unlike the use of a lower dose of LPS (1 ng/ml), which failed to activate and induce nitric oxide production in CHME-5 cells (Lisi et al., 2015).

The ability of p65 to be activated, translocate into the nucleus, and bind to NF- $\kappa$ B consensus sequences, is crucial in mediating effective inflammatory responses. Here, we demonstrate a second, more functional measure of NF- $\kappa$ B activation. LPS-induced NF- $\kappa$ B binding activity was exhibited in two waves, at 10 and 90 min. At first, this activity seemed to display a biphasic pattern but statistical analysis revealed it was not truly biphasic.

LPS-induced I $\kappa$ B $\alpha$  activation was observed with LPS within 10 minutes, which demonstrated that phosphorylation of I $\kappa$ B $\alpha$  is an early, transient event in CHME-5 cells. Since phosphorylation was assessed in cytoplasmic fractions, it is possible that after 10

minutes I $\kappa$ B $\alpha$  translocates into the nucleus via its nuclear localization sequence or that phosphorylation of I $\kappa$ B $\alpha$  leads to ubiquitinylation and proteasomal degradation through the ubiquitin-proteasome pathway (Arenzana-Seisdedos et al., 1997).

Toll-like receptor 4 (TLR4), a transmembrane glycoprotein, is part of the innate immune response, and is expressed in the CNS, primarily in microglia (Bsibsi et al., 2002; Laflamme & Rivest, 2001). Consequently, in addition to assessing LPS-induced signaling, we were interested in the effects of LPS on TLR4 expression. The increase observed in *TLR4* gene expression in CHME-5 cells following LPS treatment has been reported to occur through binding of the master regulator PU.1 to *TLR4* promoter regions, in response to endotoxin, which showed a significant increase in *TLR4* mRNA expression 2 h after LPS treatment (1  $\mu$ g/ml) in RAW 264.7 macrophages (Pedchenko et al., 2005). Another study demonstrated increases in TLR4 expression in whole blood cells and monocytes as early as 2 and 3 h, respectively (Armstrong et al., 2004; Bosisio et al., 2002). The expression of TLR4 as early as 3 h may be attributed to TLR4 being an early or middle phase gene that peaks at 1 h and 3 h (Tian et al., 2005). LPS-induced TLR4 protein expression increased compared to unstimulated cells as seen in both immunoblot analysis and immunocytochemistry. This pattern displayed in LPS-induced TLR4 expression may be due to regulatory control of the *TLR4* gene by miRNAs.

Several studies have shown the ability of miRNAs, mir-27a and mir-146b, to directly target TLR4 expression in primary rat microglial and HEK-293T cells, respectively, by binding to 3'-untranslated region of the TLR4 promoter (Curtale et al., 2013; Lv YN, 2016). Activation at 270 min may also be due to late-phase NF- $\kappa$ B activation, which is attributed to TRIF-dependent signaling (Akira & Takeda, 2004). On

the other hand, the lack of TLR4 protein expression at 180 min may be due to negative regulation. There are several negative regulators that control TLR4 inflammatory signaling at different stages in the signaling pathway, such as SARM, RP105, and ST2L, which can be induced as early as 10 min, as seen in the case of IRAK-M (Brint et al., 2004; Divanovic et al., 2005). Further investigation is needed to determine mechanisms for regulation of LPS-induced TLR4 signaling in CHME-5 cells.

In this aim I provide novel images of CHME-5 cells, showing TLR4 and CD68-immunofluorescence in the plasma membrane and cytoplasm. Epifluorescence imaging was employed to quantify CD68 and TLR4 expression in untreated and LPS-treated cells. CD68 and TLR4-immunofluorescence was observed at basal levels, but there was a significant increase in the expression of these proteins. Understandably, CD68 is expressed basally and increases with activation in response to LPS (Sasaki, 2016). Likewise, the increase in TLR4 expression after LPS treatment has been reported in previous studies, as TLR4 expression is under control of the PU.1 transcription factor, which binds to the TLR4 promoter in a time-dependent manner (Pedchenko et al., 2005).

Confocal imaging was used to visualize the expression and localization of TLR4 and CD68 in unstimulated and LPS-stimulated cells. In unstimulated cells, TLR4 expression was distributed to the plasma membrane, but subsequently internalized in response to LPS, which has been reported in detail (Husebye et al., 2006; Zanoni et al., 2011). CD68 was widely distributed in untreated cells, while activation of microglia cells triggered CD68 internalization, mainly to the cytoplasmic compartment, which is consistent with previous reports of CD68 trafficking to and from the plasma membrane at a high rate (Kurushima et al., 2000; Ramprasad et al., 1996). There was minimal

evidence of co-localization of CD68 and TLR4 at the plasma membrane and in the cytoplasm in unstimulated or LPS-stimulated cells.

In summary, studying microglial inflammatory responses is important due to their nature as the immune cell of the CNS. The ability to obtain human primary microglia is challenging, and therefore, the use of cultured cells or cell lines is essential to progress the field of neuroinflammation, in particular, inflammation-exacerbating neurodegenerative diseases. Relative to other cell types, availability of microglial cell lines is limited, thus, it is important to maximize our understanding of those tools that are available. Here, we provide novel insights into CHME-5 cells by characterizing TLR4 neuroinflammatory signaling as a rat microglial cell line, which aligned with responses seen in other microglial cell lines, such as BV-2 and HAPI, and in human primary cells. With this present research, it is our hope that CHME-5 will remain a useful tool and continue to be an asset for studying microglia

## CHAPTER TWO

# FENTANYL, AND TO A LESSER EXTENT MORPHINE, DISPLAY ANTI- INFLAMMATORY EFFECTS ON LPS-INDUCED TLR4 NEUROINFLAMMATORY SIGNALING



## LITERATURE REVIEW

### Opioid Receptors

Opioid receptors, located in the CNS and periphery, are GPCRs that consist of three extracellular N-terminus loops, responsible for selectivity of the receptor, a seven transmembrane domain, and an intracellular C-terminus with domains between the 5<sup>th</sup> and 6<sup>th</sup> segments, which interact with G proteins for signaling (Kieffer & Evans, 2009; Snyder & Pasternak, 2003). Opioid receptor activation can cause a myriad of pharmacological, physiological, and behavioral effects, which depend on the type of opioid receptor, receptor localization/distribution, and additional pharmacological receptor phenotypes. Opioid effects include analgesia, pupil constriction, constipation, euphoria, sedation, respiratory depression, bradycardia, hypothermia, insensitivity, tolerance, physical dependence, addiction, and even death (Jordan & Devi, 1998; Law & Loh, 2013).

The discovery of opioid receptors occurred through selective binding to endogenous opioid peptides present in the CNS that include enkephalin (met- and leu-), beta-endorphin, dynorphin (A and B) and nociceptin/orphanin FQ (N/OFQ), which are derived from precursor proteins pro-enkephalin, pro-opiomelanocortin, prodynorphin and pro-nociceptin, and endomorphin (-1 and -2) (Law et al., 2013; McDonald & Lambert, 2011; Waldhoer et al., 2004). The first opioid receptor genes, *mu*, *kappa* and *delta*, were cloned, and thereafter, a fourth receptor was discovered, opioid receptor-like 1 (ORL1), which shares 60% homology with the other three classical opioid receptors (Evans et al., 1992;

Law et al., 2013; Stevens, 2009; Waldhoer et al., 2004). Since the discovery of ORL1, the nomenclature for this fourth opioid-like receptor was changed to *nociceptin/orphanin* FQ peptide receptor or NOP (McDonald et al., 2011).

To determine opioid receptor localization, several studies were performed including auto-radiographic studies using selective radioactive ligands, in situ hybridization studies using cloned receptor mRNA, and histochemical and immunofluorescence studies using receptor-specific antibodies (Law et al., 2013). These studies revealed that opioid receptors are localized in several areas of the CNS including the caudate-putamen; periaqueductal gray; medial thalamus; limbic regions, such as amygdala and nucleus accumbens; locus coeruleus; substantia gelatinosa of the spinal cord and brainstem; and the vagal nuclei (Snyder et al., 2003).

### **Opioid Receptors in the Periphery**

In addition to distribution in the CNS, opioid receptors are also expressed in the periphery, such as the gastrointestinal tract, which is responsible for MOR and DOR-mediated constipation. Opioid receptors expressed in cardiac myocytes explains KOR-mediated bradycardia; and expression in immune cells, such as T cells, B cells, dendritic cells, macrophages, and neutrophils, may lead to crosstalk between other immune receptors such as TLRs (Law et al., 2013). Along with receptor type and tissue distribution, additional pharmacological phenotypes may trigger different opioid-induced effects, as a result of post-translational modifications, alternative mRNA splicing, homo-/hetero-dimerization, or scaffolding with additional proteins (Feng et al., 2012; Waldhoer et al., 2004). These are all factors that can influence pharmacological, physiological, and behavioral effects imparted by opioid receptors.

### ***Mu* ( $\mu$ ) Opioid Receptor (MOR)**

MORs are located in areas involved in sensory and motor functions, which include the cerebral cortex and amygdala; the caudate putamen; pre-synaptically on primary afferent neurons within the dorsal horn of the spinal cord; and in the periaqueductal gray (McDonald & Lambert, 2005). MORs are also located in different cellular and subcellular compartments of neurons, including the soma, dendrites and terminals, which implicates different functions based on spatial location (Williams et al., 2013). MORs are also highly expressed in areas of pain perception and respiration (Reisine, 1996).

### ***Delta* ( $\delta$ ) Opioid Receptor (DOR)**

The *delta* opioid receptor (DOR), the first opioid receptor to be cloned (1992), is most dense in the olfactory bulb; cerebral cortex; nucleus accumbens; caudate putamen; and pre-synaptically on afferent neurons; and to a lesser extent in the thalamus, hypothalamus and brainstem (McDonald et al., 2005; McDonald et al., 2011). Besides imparting analgesic/anti-nociceptive effects, recent evidence suggests that the DOR system may play a role in regulating mood and emotional states by promoting anti-anxiety and anti-depressant-like effects, while also having the potential to be used to treat PD (Feng et al., 2012; Hill et al., 2000; Jutkiewicz, 2006; McDonald et al., 2011). Conversely, DORs do not seem to have any regulation in acute pain but do reduce hyperalgesia in inflammatory and neuropathic pain (Kapitzke et al., 2005).

### ***Kappa* ( $\kappa$ ) Opioid Receptor (KOR)**

The *kappa* opioid receptor (KOR) is expressed in neocortical areas; the olfactory bulb; the amygdala and basal ganglia; the thalamus and hypothalamus; the ventral tegmental area; locus coeruleus; cerebral cortex; the pituitary gland; and in the cervical, dorsal and

lumbar levels of the spinal cord (Simonin et al., 1995). The KOR system exhibits a safer side-effect profile, namely the absence of respiratory depression, and has been implicated in a number of functions including nociception, neuroendocrine physiology, cognition, diuresis, and feeding (McDonald et al., 2011; Simonin et al., 1995). In addition, KOR activation may be beneficial for treatment of alcohol dependence and epilepsy, and, one study by Ikeda et al. 2009, showed amelioration of L-DOPA-induced dyskinesia symptoms in a rat model of Parkinson's disease (Feng et al., 2012; Ikeda et al., 2009; McDonald et al., 2011).

### ***Nociceptin/Orphanin* FQ Receptor Peptide (NOP)**

The *nociceptin/orphanin* FQ receptor peptide (NOP) is widely expressed in the CNS, in particular, in the thalamus; cortical areas; olfactory regions and limbic structures; throughout the brainstem in the central periaqueductal gray; substantia nigra; sensory and motor nuclei; and in both dorsal and ventral horns of the spinal cord (Mollereau & Mouldous, 2000). This receptor can also be found in the periphery in smooth muscle, peripheral ganglia and immune cells, such as human monocytes and peripheral blood lymphocytes (Mollereau et al., 2000; Peluso et al., 1998). Due to the wide distribution of NOP, this receptor is implicated in a range of central processes including learning and memory, attention and emotion, movement and motor processes, homeostasis, neuroendocrine secretion, sensory perceptions and immune-competence (Halford et al., 1995; Mollereau et al., 2000).

### **Opioid Peptides and Drugs**

Opioids can be classified as analgesics, which act primarily on the brain and spinal cord to inhibit the neurotransmission of pain, and non-analgesics, which act in peripheral

tissues to inhibit formation of pain-producing substances (Brenner & Stevens, 2010).

Opioids can be divided into four groups, which include naturally occurring endogenous opioid peptides, opium alkaloids, semi-synthetic opioids, and synthetic derivatives with structures unrelated to morphine, and can be classified as agonists, partial agonists and antagonists (McDonald et al., 2011).

Ligands that activate opioid receptors and produce maximal response are known as agonists, and include fentanyl and morphine (effects at MOR), DADLE and deltorphin I (effects at DOR) and  $\beta$ -funaltrexamine (effects at KOR). Some of these exogenous ligands also have the potential to be partial agonists, which impart submaximal responses, as in the case of morphine (partial effects at DOR) and buprenorphine (partial effects at MOR) (Law et al., 2013). On the other hand, ligands that inhibit receptor activation and signaling are known as antagonists, such as  $\beta$ -FNA (antagonist at MOR) and naloxone and naltrexone (non-selective, classical opioid receptor antagonists), which are often used to counteract adverse effects of overdose and treat drug dependence, respectively (Brenner et al., 2010; Law et al., 2013).

Apart from pain treatment, opioids have also been used to treat other conditions such as the use of codeine and hydrocodone for cough, loperamide for diarrhea, oxymorphone for anxiety due to shortness of breath, and methadone and buprenorphine for heroin detoxification and maintenance programs during heroin replacement therapy (Felder et al., 1999).

## **Opioid Agonists**

### **Morphine**

Opioid agonists are among the most effective analgesics for the treatment of pain (Fine & Portenoy, 2004; Leavitt, 2009). Morphine, which is considered the prototypical ligand for MOR, is used clinically for both acute and chronic pain management (Fine et al., 2004). Morphine has two biological metabolites, morphine-6-glucuronide, which binds to MOR and contributes to the effects of morphine, and morphine-3-glucuronide, which is pharmacologically inactive (Brenner et al., 2010; Fine et al., 2004). Oral administration of morphine has a duration of action of 4 h and undergoes first-pass metabolism in the liver (Brenner et al., 2010).

Investigations show that morphine modulates both the innate and adaptive immune systems, and the effects on innate immunity may have more severe consequences due to immune-depression of cellular functions (Ninkovic & Roy, 2013). During innate immune responses, morphine treatment has been shown to delay leukocyte migration, decrease proliferative capacity of macrophage progenitor cells, suppress macrophage phagocytosis, as well as inhibit oxidative burst activity and chemotaxis (Ninkovic et al., 2013; Perez-Castrillon et al., 1992; Roy et al., 2006). Morphine can modulate various B and T cell responses including *in vivo* suppression of primary antibody response in multiple strains of mice and reduction in cell viability, proliferation, and function in the CD4/CD8 population *in vivo* (Bussiere et al., 1992; Ninkovic et al., 2013).

### **Fentanyl**

Fentanyl, a synthetic opioid characterized by its high potency and lipid solubility, is considered to be about 100× more potent than morphine, clinically, with predominant activity at MOR and some affinity at DOR and KOR (Davis, 2011; Nelson & Schwaner,

2009; Stanley, 1992). Fentanyl is highly lipophilic, thus it rapidly crosses the BBB by diffusion, active transport and efflux by P-glycoprotein (Davis, 2011). Fentanyl is metabolized by the cytochrome P450 enzyme, CYP3A4, to norfentanyl, hydroxypropionyl fentanyl and hydroxypropionyl norfentanyl, which are metabolically inactive (Davis, 2011). Fentanyl can be administered through several routes for treatment of acute pain including intravenous, transmucosal, buccal, epidural, intrathecal or inhalational routes (Nelson et al., 2009).

### **Other Opioids**

Other opioid agents can be categorized into weak or strong opioid analgesics, and can be used to treat a variety of ailments besides pain. Codeine is a weak opioid analgesic with weak affinity for MOR, with a potency that is 50% of morphine, and its analgesic properties are presumed to come from its metabolism to morphine (Trescot et al., 2008). Dihydrocodeine is similar in structure to codeine and its analgesic properties are considered to be equipotent to codeine (S. C. Armstrong & Cozza, 2003; Trescot et al., 2008).

Along with codeine, meperidine is also a weak opioid agonist at MOR, which only has about 10% the effectiveness of morphine (Trescot et al., 2008). Meperidine is metabolized by glucuronidation to normeperidine, which has significant neurotoxic properties, such as mood effects, tremors, multi-focal myoclonus and seizures, which are not reversible by naloxone (Trescot et al., 2008). Another opioid analgesic, hydrocodone, is the most commonly used opioid and is indicated for moderate-to-moderately severe pain, as well as nonproductive cough (Trescot et al., 2008). Hydrocodone is also considered a prodrug, which displays weak binding capacity for MOR (Trescot et al.,

2008). Oxycodone is a phenanthrene class opioid that has activity at all three classical opioid receptors and is metabolized by glucuronidation to noroxycodone, which has less than 1% of the analgesic potency of its parent compound; as well as by CYP2D6 to oxymorphone, which is an active metabolite with high affinity for MOR (Poyhia et al., 1992; Trescot et al., 2008).

### **Opioid Antagonists**

Opioid antagonists are molecules that block opioid binding and activation of receptors and recent evidence suggests antagonists may provide potential benefits, such as monotherapy and adjuvants for enhancing analgesic effects of opioid agonists (Leavitt, 2009). Two such non-selective opioid antagonists, naloxone and naltrexone, are chemical analogs of morphine that were first synthesized in the 1960s and are currently used as antidotes for opioid overdose, and treatments for opioid addiction and alcoholism, respectively (Brenner et al., 2010; Leavitt, 2009). These antagonists interact with the classical opioid receptors, *mu*, *delta*, and *kappa* but have greater affinity for MOR (Reisine, 1996).

The first account of an antagonist-like molecule was in 1915, when N-allylnorcodeine was observed to block respiratory depression mediated by morphine and heroin. Soon after, the opioid antagonist, nalorphine was synthesized, which was also a partial agonist that produced dysphoria as a side effect (Gonzalez & Brogden, 1988; Leavitt, 2009). Due to adverse effects of nalorphine, treatment was discouraged and instead naloxone and naltrexone are favored. Naloxone is more potent and less toxic than nalorphine, but has a short duration of action (1-4 h) and limited oral bioavailability (2%) due to its high first-pass metabolism, and, therefore, is fifteen times more potent by



intravenous/intramuscular injection (Leavitt, 2009). Additionally, naltrexone, is 2× as potent as naloxone, has a longer duration of action (up to 24+ h) and 40% oral bioavailability (Gonzalez et al., 1988; Reisine, 1996).

Treatment with low dose antagonists leads to up-regulation of MOR in areas of the brain responsible for pain responses, which leads to an increase in the number of receptors available for binding to pain-relieving opioids, whether endogenous or exogenous (Leavitt, 2009; Mannelli et al., 2006). Opioid receptor blockage by antagonists also increases endogenous levels of natural endorphins, but this also depends on the extent and length of exposure (Leavitt, 2009; Smith et al., 2007).

The analgesic effects of naloxone occur at low-doses (up to 2 mg), but not at higher doses (7.5-10 mg) (Sloan & Hamann, 2006). Several studies have indicated analgesic therapeutic use of naloxone, or in conjunction with other opioid agents. For example, significant analgesic effects were produced with naloxone (0.4 or 1.0 mg) compared with placebo for postoperative dental pain in a trial of 90 patients. Additionally, naloxone plus pentazocine (60 mg, mixed agonist-antagonist opioid) produced greater dental pain relief than monotherapy with pentazocine (Levine et al., 1988). Another proposed application for naloxone is the prevention or relief of opioid-induced constipation, which can be a side effect of long-term opioid use (Leavitt, 2009).

Like naloxone, low-dose naltrexone can enhance opioid analgesia with opioid drug reduction, and even increase responses to morphine (Crain & Shen, 2001; Gonzalez et al., 1988; Leavitt, 2009). In addition to treatment for opioid tolerance and alcoholism, clinical trials have been successful with treatment of low-dose naltrexone for Crohn's disease (89% achieved favorable response, 67% achieved remission), irritable bowel

syndrome (76% showed symptom relief), and fibromyalgia (greater than 30% reduction of symptoms over placebo) (Kariv et al., 2006; Leavitt, 2009; Smith et al., 2007). Studies have also shown the benefits of combination therapy with low-dose naltrexone including treatment of oxycodone plus naltrexone (Oxytrex) in patients with chronic, painful osteoarthritis and chronic back pain and naltrexone combined with intrathecal morphine infusions in patients with chronic, refractory nonmalignant pain (Chindalore et al., 2005; Hamann & Sloan, 2007; Webster et al., 2006). Additionally, research as early as 1997, showed that opioid combination therapy with low-dose naltrexone led to suppression of opioid-induced tolerance and dependence in MOR signaling in mice, attenuation of chronic morphine-induced gliosis in rats, and suppression of rewarding and adverse effects of opioids in rats (Mattioli et al., 2010; Olmstead & Burns, 2005; Shen & Crain, 1997; Wang et al., 2005).

Another well-characterized opioid antagonist is  $\beta$ -FNA, which is highly selective for MOR. X-ray crystal structures of alpha-funaltrexamine ( $\alpha$ -FNA) and  $\beta$ -FNA revealed that these two enantiomers have almost identical conformations in the fused ring moiety except for ring C, where  $\alpha$ -FNA is observed in a twist boat confirmation, while  $\beta$ -FNA exist in the chair conformation (Griffin et al., 1986). Both of these isoforms have interactions between the receptor and positively charged nitrogen, the phenolic ring, and hydroxyl group (Griffin et al., 1986).  $\beta$ -FNA, on the other hand, goes through a second recognition step, where the nucleophilic residue in the receptor is positioned to attack the fumarate group in  $\beta$ -FNA (Griffin et al., 1986). Thus, unlike  $\alpha$ -FNA,  $\beta$ -FNA binds MOR in an irreversible manner (Griffin et al., 1986).

$\beta$ -FNA, a fumarate methyl ester derivative of naltrexone, is not used clinically but is widely employed as a tool to investigate opioid receptor mechanisms due to its high selectivity at MOR and the ability to bind to *delta* and *kappa* (acts as agonist) receptors as well (Takemori et al., 1981; Takemori & Portoghesi, 1985; Ward et al., 1982).

### **Opioid Receptor Signaling**

Opioid receptors activate signaling via conformational change in the cytoplasmic domain and interaction with G proteins (Kieffer et al., 2009). These intracellular domains interact with inhibitory G proteins ( $G_o/G_i$ ), which then dissociate and initiate signal transduction that can lead to inhibition of neuronal activity or modification of gene expression; the exact pathway depends on the specific ligand (Kieffer et al., 2009).

Opioid receptor activation in neurons typically results in inhibition of neurotransmitter release, although some neurotransmitters are differentially modulated based on the receptor-agonist interaction. For instance, *mu* and *delta* agonists increase dopamine (DA) release by inhibiting the GABAergic interneurons that inhibit DA release, while *kappa* agonists inhibit DA release by acting directly at the presynaptic dopaminergic terminals (Corbett et al., 2006; Law et al., 2013). These opioid receptor effects, and many others, are mediated by receptor-ligand binding and association with G-proteins, which lead to signaling, mediated by pertussis toxin (PTX)-sensitive  $G_{ai}$  and  $G_{ao}$ , and possibly, cholera toxin-sensitive  $G_{as}$  (Connor & Christie, 1999; Jordan et al., 1998).

Receptor signaling is controlled by the ability of G proteins to bind and hydrolyze guanosine triphosphate (GTP) to guanine diphosphate (GDP) (Snyder et al., 2003). During basal conditions, the heterotrimeric G-protein complex  $\alpha\beta\gamma$  associates with GDP.

Ligand binding to the receptor induces a conformational change, which allows GDP dissociation from and GTP binding to the alpha subunit leading to dissociation of the  $\beta\gamma$  subunit (McDonald et al., 2011; Y. Wang et al., 2013). This cascade of events allows both the  $\alpha$  and  $\beta\gamma$  subunits to associate with intracellular effector molecules thereby affecting change in downstream signaling pathways. In the case of opioid  $G_{ai}/G_{ao}$  signaling, these effects include closing of N/P-type voltage-sensitive  $Ca^{2+}$  channels, opening of inwardly rectifying  $K^{+}$  channels and inhibition of cyclic adenosine monophosphate (cAMP) production through inhibition of adenylyl cyclase (McDonald et al., 2011; Y. Wang et al., 2013).

### **Opioid Receptor Signaling Regulation: Internalization and Down-regulation**

Opioid receptor signaling is regulated through receptor desensitization, internalization, and degradation. Regulatory steps include G protein-coupled receptor kinase (GRK)-mediated receptor phosphorylation,  $\beta$ -arrestin recruitment, and receptor signaling disruption via G-protein coupled effectors (Kovoor et al., 1998; Nagi & Pineyro, 2011; Qiu et al., 2007; X. Zhang et al., 2005b). The propensity for opioid receptor desensitization, which is the progressive loss of receptor function under continued exposure to an agonist, and internalization, results from activation by specific agonists (Hong et al., 2009; Liu & Anand, 2001).

*Mu* and *delta* activated receptors at the plasma membrane are phosphorylated by GPCR kinases (GRKs), and other protein kinases such as protein kinases A and C (PKA & PKC), mitogen-associated protein kinases (MAPKs) and  $Ca^{2+}$ /calmodulin-dependent protein kinase II (CaMKII), which facilitate arrestin binding and prevent receptor coupling to G proteins (Bailey & Connor, 2005; Liu et al., 2001). Receptor-arrestin

complexes are engulfed in clathrin-coated pits and undergo dynamin-mediated internalization into early endosomes (Corbett et al., 2006). One factor responsible for receptor sorting to lysosomes is receptor ubiquitination, which both MOR and DOR undergo (Marchese et al., 2008; Nagi et al., 2011). In addition, trafficking to late endosomes/lysosomes is dependent upon association with sorting proteins of the G protein-coupled receptor-associated sorting protein (GASP) family, which bind with high affinity to *delta* but not *mu* opioid receptors, which may explain the low (20%) frequency of MOR lysosomal degradation (Heydorn et al., 2004; Nagi et al., 2011; Whistler et al., 2002). Due to high affinity association with GASP family members, *delta* receptors are trafficked to lysosomes for receptor degradation and about 80% of *mu* opioid receptors translocate to early endosomes for dephosphorylation and recycling back to the plasma membrane (resensitization); *Kappa* opioid receptors do not undergo agonist-mediated internalization (Bailey et al., 2005; Corbett et al., 2006).

### **Opioid Tolerance, Dependence, and Addiction**

The mesolimbic reward system is activated by opioids. Once opioids bind to MOR in the brain, cells located in the ventral tegmental area (VTA) release DA that is then recognized in the nucleus accumbens and produces a sensitization of pleasure (Kosten & George, 2002). For this reason, it is important to be cautious when using opioids because they may lead to tolerance and addiction (Compton, 2008; DuPen et al., 2007; C. Stein et al., 2003). Morphine-induced receptor activation does not lead to receptor internalization, which may be related to the increased potential for producing opioid tolerance (Liu et al., 2001). The inability of opioid receptors to uncouple from G proteins during long-exposure of morphine treatment may be another explanation for clinical manifestations of

opioid tolerance and dependence (Liu et al., 2001). Phosphorylation of opioid receptors is mediated by different kinases depending on whether treatment is chronic or acute. PKA-mediated phosphorylation causes uncoupling of opioid receptors from G proteins during chronic therapy, while PKC-mediated phosphorylation occurs during acute opioid treatment (Liu et al., 2001).

In addition to receptor phosphorylation by protein kinases, changes in signal transduction mechanisms also are implicated in clinical manifestations of opioid tolerance and dependence. Up-regulation or super-sensitization of the cAMP signal transduction system, including adenylate cyclase (AC), PKA, CaMKII, and MAPK cascades in opioid-sensitive neurons contribute to clinical manifestations of opioid tolerance and dependence (Feng et al., 2012; Liu et al., 2001; Suresh & Anand, 1998).

Opioid abuse leads to addiction, which affects brain function and homeostasis (Feng et al., 2012). Addiction often results in several neurological impairments and behavioral patterns including deficits in cognition, motivation, emotional instability, depression, impulsiveness, movement disorders, compulsive drug-seeking, persistent abuse of substances regardless of emotional detachment from loved ones, or deterioration of physical health and high probability of relapse even after prolonged drug-free periods (Cunha-Oliveira et al., 2008; Feng et al., 2012; Ivanov et al., 2006). Chronic morphine exposure *in vivo* up-regulates cAMP formation and PKA activity in specific brain regions that mediate drug addiction, for example, intracerebro-ventricular or LC administration of a selective and non-selective PKA inhibitor attenuated the behavioral signs of opioid withdrawal (Liu et al., 2001; Maldonado et al., 1995; Self & Nestler, 1995). Drugs of

abuse also directly or indirectly affect neurotransmitters, particularly dopaminergic and glutaminergic neurons (Cunha-Oliveira et al., 2008; Feng et al., 2012).

### **Opioid Receptors and Immune Function**

Opioid receptor activation has been shown to modulate immune responses and functions by suppressing humoral and cell-mediated responses including inhibition of antimicrobial resistance, antibody production, cytokine expression, natural killer activity, monocyte-mediated phagocytosis and neutrophil and monocyte chemotaxis (Feng et al., 2012; Ordaz-Sanchez et al., 2003). Additionally, acute and chronic administration of opioids has been associated with increased susceptibility of animals to bacterial and viral infections with decreased survival in tumor-bearing animals (Vallejo et al., 2004). Immune suppression by opioids may also predispose individuals to opportunistic infections, such as bacterial pneumonia, tuberculosis, hepatitis, CNS infections, abscesses, endocarditis and AIDS (Feng et al., 2012; Quaglio et al., 2003).

The effects by which central opioid receptors modulate immune function can be attributed to central and peripheral mechanisms, involving both the hypothalamic-pituitary-adrenal (HPA) axis and the autonomic nervous system (Vallejo et al., 2004). Acute administration of opioids alters immune function through the sympathetic nervous system, while chronic administration largely affects the HPA axis (Vallejo et al., 2004). Alternatively, immune cells expressed in the periphery, under the influence of cytokines, can also secrete endogenous opioids and modulate analgesia and inflammation at the site of injury (Vallejo et al., 2004).

Several studies have demonstrated opioid-mediated immune suppression including morphine-induced down-regulation of MCP-1 and MIP-1 $\beta$ , and increased

expression of specific receptors, CCR2b, CCR3 and CCR5 in normal human astrocytes, which was reversed by naloxone, and DOR agonist-mediated monocyte adhesion (Feng et al., 2012; Mahajan et al., 2005; Pello et al., 2006). On the other hand, it has been suggested that KOR-mediated activation promotes anti-inflammatory responses, such as down-regulation of cytokine, chemokine and chemokine receptor expression (Feng et al., 2012; Finley et al., 2008).

The presence of opioid receptors on immune cells may contribute to crosstalk with other immune receptors. Opioid modulation of immune function is mediated through direct interaction with opioid receptors expressed in immune cells, as in studies showing TNF $\alpha$  inhibition in naltrexone-treated MOR knockout mice and differential morphine-modulation in LPS-induced IL-6 and TNF $\alpha$  expression in macrophages (Feng et al., 2012; Greeneltch et al., 2004; Roy et al., 1998; Roy et al., 2006).

Opioids can modulate immune function, whether anti-inflammatory or pro-inflammatory, in cells of the CNS, such as microglia, neurons and astrocytes, through opioid interaction at non-opioid sites. Studies from the Hutchinson/Watkins group demonstrated that opioid agonists, in particular morphine, induced neuroinflammation via an extracellular TLR4 event, and not via the classic opioid receptors (Hutchinson et al., 2010). For example, co-immunoprecipitation studies revealed that morphine binds to the accessory molecule, MD2, thereby inducing TLR4 oligomerization in HekBlue-hTLR4 and Ba/F3 cells (X. Wang et al., 2012b). Morphine also induced *IL-1 $\beta$* , *TLR4* and *MD2* mRNA expression in CNS endothelial cells, and an increase in IL-1 $\beta$  in BV-2 murine microglial cells; this induction was reduced with administration of a TLR4 or MD2 small molecule inhibitor (X. Wang et al., 2012b). These studies suggest that morphine and



possibly other opioid agonists have the potential to cause neuroinflammation through a TLR4-dependent mechanism. In contrast, other studies have demonstrated the anti-inflammatory potential that opioid agonists produce in immune-competent cells of the CNS. Morphine ( $IC_{50}$ = 1 fM) and DAMGO ( $IC_{50}$ =1 nM) potently inhibited directed migration of human fetal microglial cells to complement factor 5a, suggesting an anti-inflammatory role of hMOR within the brain (Chao et al., 1997). In addition, morphine exerted potent anti-inflammatory and neuroprotective effects through inhibition of LPS- and 1-methyl-4-phenylpyridinium ( $MPP^+$ )-induced microglial activation in rat primary mesencephalic neuron-glia cultures (Qian et al., 2007). Others demonstrated morphine-mediated suppression of LPS-induced IL-6, TNF $\alpha$  and NF- $\kappa$ B, which was not reversible with naloxone, suggesting the involvement of a non-classical opioid receptor (Ninkovic et al., 2013; Roy et al., 1998).

More recently, studies in the Davis/Stevens lab using NHA and HekBlue-hTLR4 cells have shown that IFN- $\gamma$  + HIV-1 Tat-induced CXCL10 expression was inhibited by  $\beta$ -FNA, and, LPS-induced NF- $\kappa$ B activation was inhibited by opioid agonists, morphine and fentanyl, but these inhibitory effects were not reversed by opioid antagonists, naltrexone and  $\beta$ -FNA, respectively (R. L. Davis et al., 2013; Stevens et al., 2013). LPS-induced TLR4 activity was decreased in response to increasing doses of morphine and fentanyl (Stevens et al., 2013). Taken together, these studies indicate the potential for opioid agents, both agonists and antagonists, to impart anti-inflammatory properties through down-regulation of immune functions.

### **Expression of MOR in microglia**

Opioids can cross the BBB, and in doing so are construed as foreign to immune receptors in the brain mainly expressed on microglia (Batchell et al. 2015). Because opioids can induce immune-modulatory effects, it is almost certain that opioid receptors are expressed across many cell types, including those in the CNS. Research shows that MOR is expressed in many cell types, but substantive evidence showing the expression of MOR in microglial cells is controversial. In this next section we look at the literature to provide *in vivo*, *ex vivo*, and *in vitro* evidence regarding MOR expression in microglia. One such study prepared microglial cells from 16-22 week old human fetal brain tissue and found constitutive MOR gene and protein expression in untreated cells using RT-PCR, sequence analysis, and immunocytochemical staining (Chao et al., 1997). Several other studies have validated MOR gene and protein expression in primary microglia from Balb/c mice and Sprague Dawley rats, utilizing flow cytometry, immunofluorescence, and siRNA knockdown analyses (El-Hage et al., 2013; Gessi et al., 2016; Horvath et al., 2008).

## **PURPOSE**

The effect of opioids on inflammation and neuroinflammation still remains debatable. With these controversial implications at the forefront, we chose to investigate the opioid-mediated effects on LPS-induced TLR4 neuroinflammatory signaling using an immortalized microglial cell line, CHME-5. Studies have indicated that opioid agents mediate immunomodulatory effects, specifically, on TLR4 inflammatory signaling in the CNS. Fentanyl, a potent MOR agonist, is used to treat acute and chronic pain associated with cancer and other neurodegenerative diseases. There is evidence that microglia, along with other cells of the CNS, differentially express TLRs and opioid receptors, but the

precise mechanisms on how fentanyl and morphine modulate TLR signaling is not well understood. CHME-5 cells were treated with *Escherichia coli* LPS to simulate a neuroinflammatory environment through the activation of TLR4, and fentanyl citrate, morphine sulfate, and naltrexone hydrochloride were used as pharmacological agents to study immune modulation of the TLR4 MyD88-dependent signal transduction pathway. Defining the effects of fentanyl and morphine on TLR4 signaling mechanisms in microglial cells has the potential to advance therapeutic strategies for neuroinflammatory processes involved in injury, chronic diseases (AD, PD and MS) or cancer-associated pain.

## **AIM II**

This aim was to determine the effects of fentanyl (fentanyl citrate) and morphine (morphine sulfate) on LPS-induced TLR4 inflammatory signaling and determine the extent to which MOR is involved, using the opioid antagonist, naltrexone hydrochloride.

## **HYPOTHESIS (H<sub>1</sub>)**

Previous studies from the Davis/Stevens laboratory demonstrated the anti-inflammatory properties of both fentanyl and morphine in several *in vitro* models. Therefore, I hypothesized that fentanyl and morphine down-regulate LPS-induced TLR4 neuroinflammatory signaling in CHME-5 microglial cells.

## **NULL (H<sub>0</sub>) HYPOTHESIS**

Opioid agonists fentanyl and morphine have no effect on LPS-induced TLR4 neuroinflammatory signaling in CHME-5 microglial cells.

## **METHODOLOGY**

### **CHME-5**

CHME-5 GM consisted of DMEM with 4.5 g/L glucose and sodium pyruvate without L-glutamine, FBS, 200 mM L-glutamine, penicillin-streptomycin (100 U/ml potassium penicillin, 100 µg/ml streptomycin sulfate, and 250 µg/ml amphotericin B. CHME-5 cells were maintained in GM at 37°C, with 5% CO<sub>2</sub>. Growth media was replaced every 48 h and for experimental assays, GM was replaced with serum free media (SFM), for no less than 16 hours at 37°C.

### **LPS Treatment**

Lipopolysaccharide from *Escherichia coli* O55:B5 (L2880) was purified by phenol extraction (Sigma-Aldrich, Saint Louis, MO). The lyophilized powder was reconstituted in HyPure cell culture grade water and sterile filtered to a stock concentration of 1.2 mg/ml.

### **Opioid Compounds**

Fentanyl citrate salt (Sigma, #F-3886), morphine sulfate (Sigma, #M8777), and naltrexone HCl (NIH-National Institute on Drug Abuse) were reconstituted in nuclease-free water and sterile filtered to a stock concentration of 10 mM. Fentanyl citrate and morphine sulfate were used at a final concentration range (1-100 µM) and naltrexone HCl at final concentrations of 10, 30 and 100 µM. CHME-5 cells were stimulated with LPS (1

µg/ml) and fentanyl citrate (1-100 µM) or morphine sulfate (1-100 µM) and incubated at 37°C for 10min-18h. For naltrexone studies, naltrexone (10, 30, and 100 µM) was added to CHME-5 cells after LPS and opioid agonists and stimulated for 10 min at 37°C.

### **RNA Extraction with Trizol**

Following cell stimulation, cells were washed three times with ice-cold PBS, incubated in Trizol (1 ml/100 mm dish) at 25°C for 5 min, and then lysates were collected in nuclease-free tubes. Chloroform (0.2 ml) was added to lysates followed by manual shaking of tubes for 15 sec. Lysates were then incubated at 25°C for 3 min, centrifuged at  $12,000 \times g$  for 15 min (4°C) and then the upper aqueous phase was collected. Isopropanol (0.5 ml) was added to the aqueous phase, followed by incubation at 25°C for 10 min, and centrifuged at  $12,000 \times g$  for 10 min (4°C). Next, the supernatant was removed and RNA pellets washed with ethanol, and centrifuged at  $7,500 \times g$  for 2 min (4°C). This ethanol wash step was repeated twice. RNA pellets were dried at 25°C for 15 min, followed by addition of 35 µl nuclease-free water. RNA samples were incubated in a 65°C water bath for 10 min and then stored at -80°C. To obtain RNA concentrations, RNA was thawed on ice and ng/ml determined with a Nanodrop Spectrophotometer 1000 (ThermoScientific), and validated with the 260/280 and 260/230 ratios greater than 1.80.

### **RNA Integrity with NorthernMax-Gly Kit**

RNA gels were prepared with NorthernMax-Gly Reagents to assess RNA integrity. A 1% agarose gel was prepared with NorthernMax-Gly buffer. To prepare samples, 3 µl RNA, 3 µl nuclease-free water and 6 µl glyoxal sample loading dye (equal parts) were

incubated at 50°C for 30 min. Samples were loaded and electrophoresed at 100 V for 45 min. RNA gels were stained with SYBR Safe (3 µl/50 ml in NorthernMax-Gly buffer) and rocked on a Multimixer for 30 min. To visualize the 28S and 18S bands, RNA gels were imaged on Typhoon Scanner 9410 at 450 V.

### **Reverse Transcription**

First 10× ezDNase buffer and ezDNase enzyme were added to 2 µg RNA, and nuclease-free water was added up to 10 µl total volume. Samples were mixed gently and incubated at 37°C for 2 min. Samples were placed on ice and Superscript master mix (4 µl) or “no RT” control (4 µl) was added to each sample and water added up to 20 µl total volume. Samples were gently mixed and incubated at 25°C for 10 min, 50°C for 10 min, and 85°C for 5 min. Samples were diluted with nuclease-free water up to 100 µl volume, for a final concentration of 20 ng/ml.

### **Reverse Transcription-Polymerase Chain Reaction**

cDNA (100 ng/ml) was used to perform reverse-transcription polymerase chain reaction (RT-PCR) for genes of interests. The primer for MOR was designed using rat MOR mRNA from the NIH NCBI website and ordered from IDT Technologies. RT-PCR mix included 2× PowerUp SYBR Green, 0.5 µM forward primer, 0.5 µM reverse primer, and nuclease-free water up to 15 µl. Thermocycler settings were as follows: 50°C-2 min, 95°C-2 min, (95°C-15 sec, 60°C-1 min for 40 cycles), 95°C-15 sec, 60°C-1 min, 95°C-15 sec. Primer sequences were as follows: *MOR*-Forward: 5'-CTC AGT TAC AGC CTA CCT AGT CCG C -3', 60.2°C; Reverse: 5'-CCA TCA ACG TGG GAC AAG TTG AGC

-3', 60.4°C and *β-actin*-Forward: 5'-GAA GGA TTC CTA TGT GGG CGA CGA-3', 60.5°C; Reverse: 5'-GAG CCA CAC GCA GCT CAT TGT AG-3', 60.3°C.

### **Protein extraction**

For WCLs, cells were washed with ice-cold PBS and then 400 µl of CBL was added to each 100-mm dish. Following a 5 min incubation at 4°C, lysates were collected and centrifuged at  $14,000 \times g$  (4°C) for 10 min. The supernatant was collected and stored at -20°C. For cytoplasmic and nuclear extracts, cells were washed with and collected in 1 ml ice-cold PBS. Cells were centrifuged at  $129 \times g$  (4°C) for 5 min. The supernatant was aspirated and combined with 400 µl LB1 and vortexed vigorously for 10 sec, followed by incubation on ice for 15 min. Next, 100 µl 5.4% Igepal was added, samples were vortexed for 10 sec, then centrifuged at  $14,000 \times g$  (4°C) for 5 min. The supernatant was collected and stored at -20°C; then 100 µl LB2 was added to the remaining pellet. The samples were vortexed for 15 min at 4°C and then centrifuged at  $14,000 \times g$  (4°C) for 22 min. The supernatant was collected and stored at -20°C.

### **Protein assay**

The BCA protein assay was used to determine protein concentrations for WCL, and, cytoplasmic and nuclear extracts. WCLs and cytoplasmic/nuclear extracts were measured using BCA. First, a standard curve was prepared from lysis buffer, 1 mg/ml BSA, and water to reflect the following concentrations: 0, 2, 4, 6, 8, 10, 12 µg/ml. Standards and samples (10 µl), in duplicate, were pipetted into a 96-well plate. The working solution

containing Reagent A + Reagent B (200  $\mu$ l) was added to each well, incubated at 37°C for 1 h, and absorbance read at 570 nm.

### **Immunoblot analysis**

**Antibodies:** Several antibodies were obtained from Santa Cruz including phospho-I $\kappa$ B $\alpha$ -Ser32/36 (sc-847), total I $\kappa$ B $\alpha$  (sc-101713), TLR4 (sc-293072), and  $\beta$ -tubulin (sc-9104). Antibodies purchased from Cell Signaling included phospho-p38, p38, MyD88 (4283S), anti-rabbit IgG (7054S), and anti-mouse IgG (7056S). Protein lysates were subjected to SDS-page electrophoresis and immunoblot analysis. Acrylamide gels (10-well) were made ranging from 7-13% (depending on the protein being measured) and placed in 4°C, overnight. Protein extracts (50  $\mu$ g) were prepared using loading dye, 0.05% bromophenol blue, and 50  $\mu$ l/ml  $\beta$ -mercaptoethanol). Samples were boiled for 10 min and brought to a standing temperature of 37°C. Samples were loaded into gels with running buffer and electrophoresed at 100 V for 15 min, and then increased to 125 V for 145 min for an overall running time of 2 h. Proteins were transferred onto PVDF membranes in transfer buffer and electrophoresed at 100 V for 90 min. After transfer, PVDF membranes were rinsed and blocked in 5% BSA-TBST for 2 h at 25°C with rocking. Primary antibodies (1:500-1:2000) diluted in 5% BSA-TBST, were added to membranes and rocked overnight at 4°C. The following day, membranes were washed three times with TBST for 5 min. AP-linked secondary antibodies (1:1000-1:5000) diluted in 5% BSA-TBST were added to membranes, which were rocked for 2 h at 25°C and then washed three times with TBST for 20 min. ECF fluorescent substrate was used to image blots using the



Typhoon Scanner 9410. Image J software was used to obtain the mean grey intensity for the bands of interest. Protein expression was normalized to  $\beta$ -tubulin.

### **MTT assay**

MTT assays were performed to determine reagent cytotoxicity. CHME-5 cells were plated in 12-well plates at a density of 40,000 cells/well. Cells were incubated overnight with SFM. After corresponding treatments, fresh SFM (1 ml) was added to each well followed by addition of 111  $\mu$ l MTT. Cultures were then incubated at 37°C for 45 min. Media was aspirated from each well and 1.5 ml DMSO added for 30 min, rocking at 25°C. Absorbance was read at 492 nm with the Synergy 2 plate reader.

### **NF- $\kappa$ B p65 binding assay**

CHME-5 nuclear extracts were used to analyze NF- $\kappa$ B p65 binding activity using the NF- $\kappa$ B p65 transcription factor kit. Initially, binding buffer (50  $\mu$ l) was added to each well, which contained the NF- $\kappa$ B consensus sequence. Then, 10  $\mu$ l of nuclear extracts or positive control, TNF $\alpha$ -activated HeLa cells, were added to duplicate wells. Extracts were incubated for 1 h with mild agitation. Wells were washed three times with 200  $\mu$ l of wash buffer; 100  $\mu$ l of primary antibody (1:1000) was then added to each well, and incubated for 1 h at 25°C, without agitation. Wells were washed three times with 200  $\mu$ l of wash buffer, 100  $\mu$ l of secondary antibody (1:10,000) was then added, and incubated for 1 h at 25°C, without agitation. Wells were washed four times with 200  $\mu$ l of wash buffer, and 100  $\mu$ l of chemiluminescence substrate added to each well.

Chemiluminescence was read immediately with a Synergy 2 plate reader. Binding

activity was quantified relative to protein concentrations obtained with BCA protein assay.

### **Statistical Analysis**

Image J Software was used to obtain the mean grey intensity of all immunoblots and the mean was calculated for each time point. GraphPad Prism 7.0 was used for transformation, quantification, and graphing of all data. For statistical analysis of mRNA and protein expression, binding activity, cell viability, and immunofluorescence, an ANOVA with Dunnett's multiple comparison tests compared to LPS-treated cells were used, unless otherwise stated in the results section. Kruskal-Wallis and Dunn's multiple comparison's non-parametric tests were used for data that failed the Bartlett's test and two  $Y=\text{Log}(Y)$  transformations. Significance was determined at  $p<0.05$ .

## RESULTS

### **LPS-induced *mu* opioid receptor (MOR) gene expression in CHME-5 cells.**

*MOR* gene expression was examined in CHME-5 cells. Stimulation with LPS significantly increased *MOR* gene expression at 3 ( $p<0.01$ ) and 6 ( $p<0.05$ ) h compared to unstimulated cells, as indicated by Kruskal-Wallis and Dunn's multiple comparison tests (**Figure 1A**). As an internal control, RNA integrity was verified by visualizing the 28S and 18S ribosomal RNA (rRNA) bands (**Figure 1B**).

### **Fentanyl-mediated effect on LPS-induced TLR4 expression**

TLR4 protein expression was analyzed in whole cell lysates after LPS and fentanyl treatment for 3, 10, and 30 min (**Figure 2A, 2C, 2E**). TLR4 expression remained at basal levels at 3 ( $p=0.81$ ), 10 ( $p=0.54$ ), and 30 ( $p=0.14$ ) min, as indicated by ANOVA (**Figure 2B, 2D, 2F**).

### **Fentanyl-mediated effect on LPS-induced MyD88 expression**

MyD88 protein expression was analyzed in whole cell lysates after LPS and fentanyl treatment for 3, 10, and 30 min (**Figure 3A, 3C, 3E**). MyD88 expression remained at basal levels at 3 ( $p=0.40$ ), 10 ( $p=0.30$ ), and 30 ( $p=0.21$ ) minutes, as indicated by ANOVA (**Figure 3B, 3D, 3F**).

### **Fentanyl-mediated effect on LPS-induced I $\kappa$ B $\alpha$ activation**

Phosphorylation of I $\kappa$ B $\alpha$  was used as a measure of I $\kappa$ B $\alpha$  activation in cytoplasmic lysates (**Figure 4A**). ANOVA and Dunnett's multiple comparison tests revealed that fentanyl significantly decreased LPS-induced I $\kappa$ B $\alpha$  activation at 100  $\mu$ M,  $p < 0.001$ , as compared to cells treated with LPS alone (**Figure 4B**).

### **Fentanyl-mediated effect on LPS-induced NF- $\kappa$ B p65 binding activity**

The fentanyl-mediated effect on NF- $\kappa$ B p65 binding activity was assessed at 10 min using CHME-5 nuclear lysates. ANOVA and Dunnett's multiple comparison tests revealed significant down-regulation of LPS-induced NF- $\kappa$ B p65 binding activity at 10 ( $p < 0.05$ ) and 100  $\mu$ M ( $p < 0.05$ ) (**Figure 5A**). MTT assay was performed to ensure the viability of cells after co-treatment with LPS and fentanyl citrate. ANOVA revealed no significant differences between control and LPS/fentanyl co-treated cells,  $p = 0.54$  (**Figure 5B**).

### **Effect of naltrexone on fentanyl-mediated down-regulation of LPS-induced NF- $\kappa$ B p65 binding activity**

Nuclear NF- $\kappa$ B p65 binding activity was analyzed after treatment with LPS, fentanyl, and naltrexone. ANOVA and Tukey's multiple comparison tests revealed a 1.0-fold decrease in response to LPS and fentanyl co-treatment compared to cells treated with LPS alone ( $p < 0.01$ ), and no difference with naltrexone treatment compared to cells co-treated with LPS and fentanyl (10  $\mu$ M:  $p = 1.0$ ; 30  $\mu$ M:  $p = 0.90$ ; 100  $\mu$ M:  $p = 0.30$ ) (**Figure 6A**). MTT assay was performed to ensure the viability of cells after co-treatment with

LPS, fentanyl, and naltrexone. ANOVA revealed no significant difference between control and LPS/fentanyl/naltrexone co-treated cells,  $p=0.94$  (**Figure 6B**).

#### **Morphine-mediated effect on LPS-induced TLR4 expression**

TLR4 protein expression was analyzed in whole cell lysates after LPS and morphine treatment for 3, 10, and 30 min (**Figure 7A, 7C, 7E**). There was no change in TLR4 expression at 3 ( $p=0.32$ ), 10 ( $p=0.50$ ) or 30 ( $p=0.60$ ) min as compared to cells treated with LPS alone (**Figure 7B, 7D, 7F**).

#### **Morphine-mediated effect on LPS-induced MyD88 expression**

MyD88 protein expression was analyzed in whole cell lysates after LPS and morphine treatment for 3, 10, and 30 min (**Figure 8A, 8C, 8E**). Kruskal-Wallis revealed no change in MyD88 expression at 3 ( $p=1.0$ ), 10 ( $p=0.53$ ), and 30 ( $p=1.0$ ) min, as compared to cells treated with LPS alone (**Figure 8B, 8D, 8F**).

#### **Morphine-mediated effect on LPS-induced I $\kappa$ B $\alpha$ activation**

Phosphorylation of I $\kappa$ B $\alpha$  was used as a measure of I $\kappa$ B $\alpha$  activation in cytoplasmic lysates (**Figure 9A**). ANOVA and Dunnett's multiple comparison tests revealed morphine significantly decreased LPS-induced I $\kappa$ B $\alpha$  activation at 1  $\mu$ M ( $p<0.01$ ), 3  $\mu$ M ( $p<0.01$ ), 10  $\mu$ M ( $p<0.01$ ), 30  $\mu$ M ( $p<0.001$ ), 100  $\mu$ M ( $p<0.01$ ), as compared to cells treated with LPS alone (**Figure 9B**).

#### **Morphine-mediated effect on LPS-induced NF- $\kappa$ B p65 binding activity**

The morphine-mediated effect on NF- $\kappa$ B p65 binding activity was assessed at 10 min using CHME-5 nuclear lysates. ANOVA revealed no difference in LPS-induced NF- $\kappa$ B p65 binding activity in response to morphine treatment,  $p=0.10$  (**Figure 10A**). MTT assay was performed to ensure the viability of cells after co-treatment with LPS and morphine. ANOVA revealed no significant difference between treatment groups and untreated cells,  $p=0.70$  (**Figure 10B**).

## FIGURES

1A.

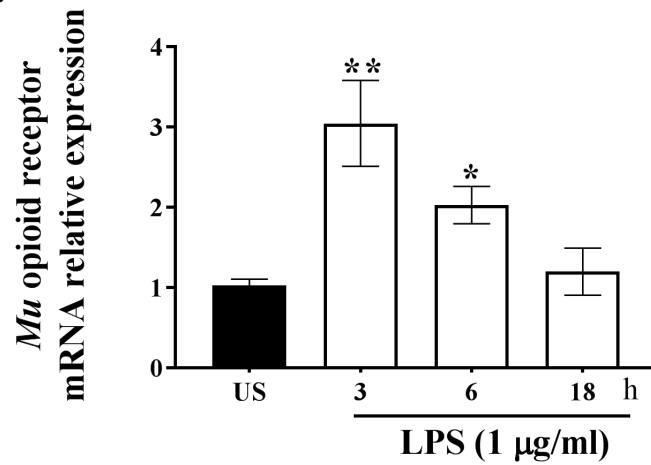
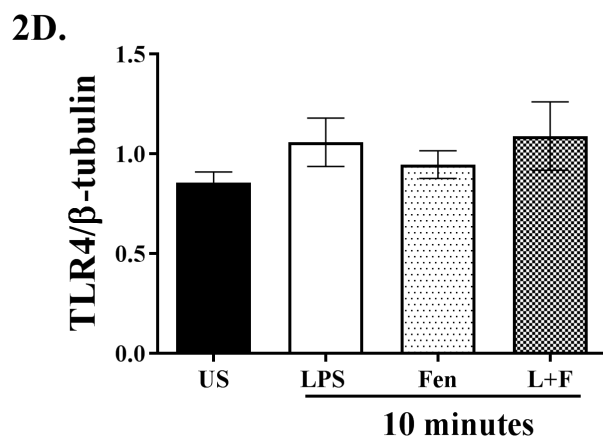
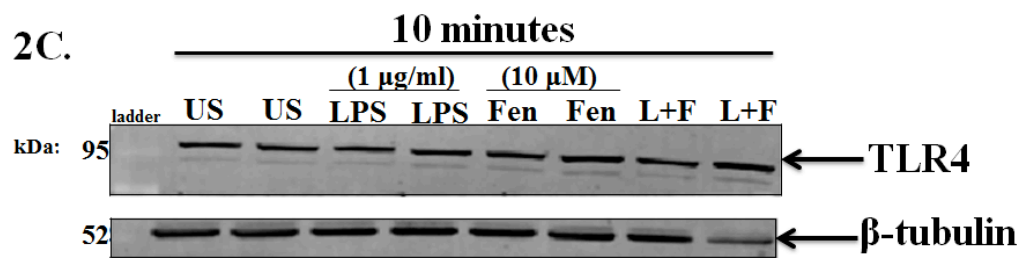
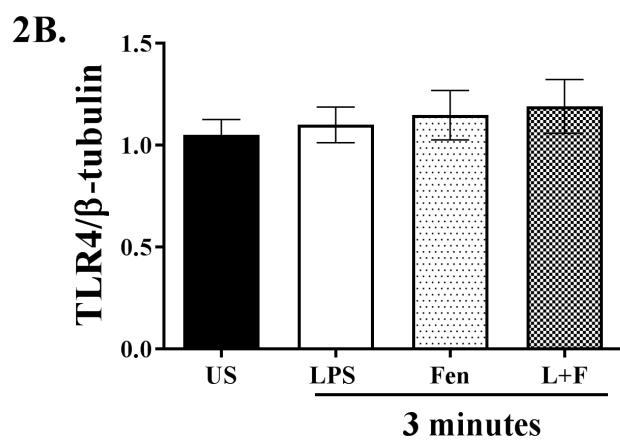
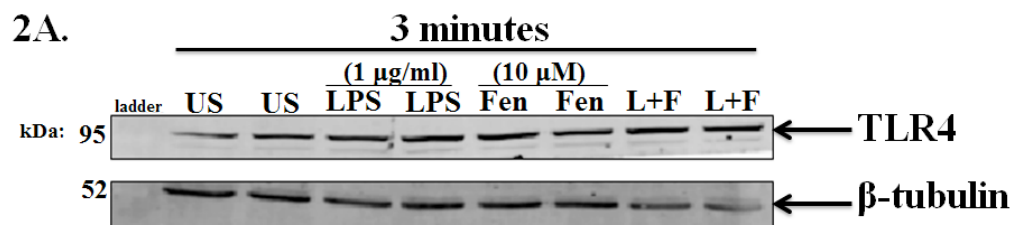


**Figure 1. LPS-induced mu opioid receptor expression in CHME-5 cells.**

CHME-5 cells were stimulated with (1 µg/ml) and incubated at 37°C for 3, 6, and 18 h. **A.** MOR mRNA expression was analyzed using RT-PCR. Kruskal-Wallis and Dunn's multiple comparison tests revealed a significant increase at 3 and 6 h compared to unstimulated cells. Image is representative of three independent experiments (n=3) for each treatment group. Bars for all experiments are presented as mean ± SEM.

\*\* p<0.01, \* p<0.05 vs. unstimulated cells









[illegible]

**3C.**

**10 minutes**

		(1 µg/ml)		(10 µM)						
	ladder	US	US	LPS	LPS	Fen	Fen	L+F	L+F	
kDa: 34										← MyD88
52										← β-tubulin



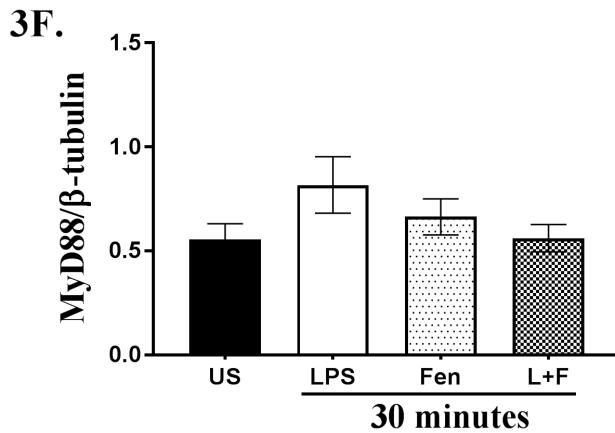
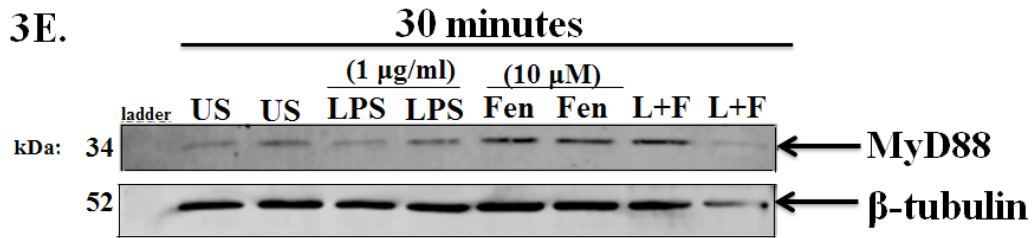


**Figure 3. Fentanyl does not affect LPS-induced MyD88 expression in CHME-5 cells**

CHME-5 cells were stimulated with or without LPS and/or fentanyl for 3, 10, and 30 min. Whole cell lysates were subjected to SDS-PAGE and immunoblotted with MyD88 (1:1000) and β-tubulin (1:1000) antibodies (**A**, **C**, **E**). ANOVA revealed no difference in MyD88 expression at **B**, 3 (p=0.40), **D**, 10 (p=0.30), or **F**, 30 (p=0.21) min. Three independent experiments were performed in duplicate; n=3 for each treatment group. Bars for all experiments are presented as mean ± SEM.

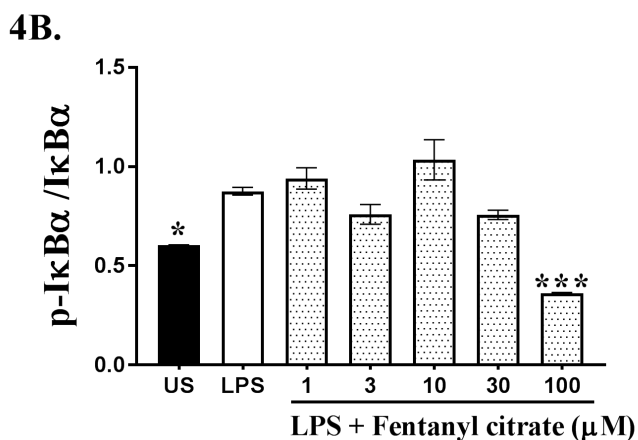
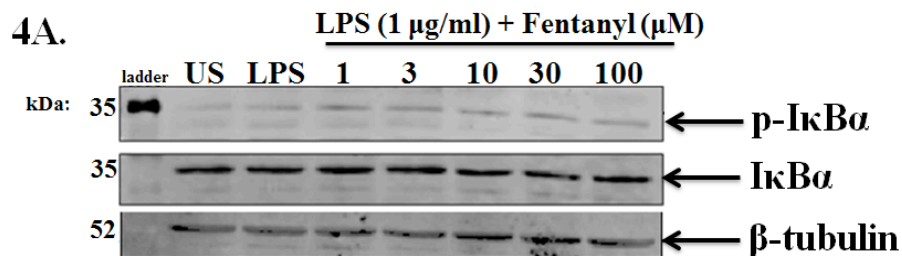
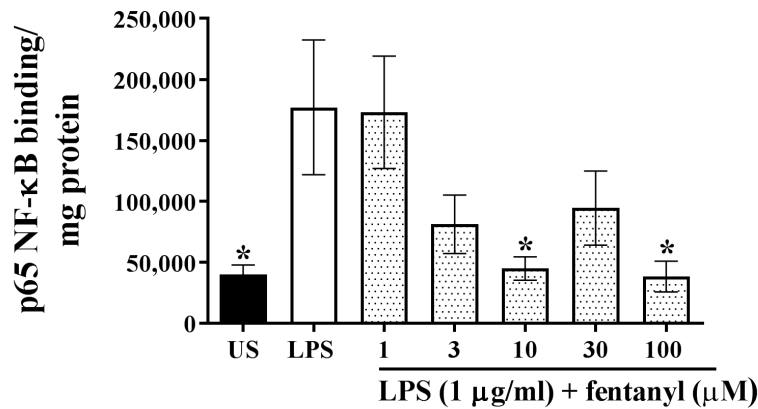


**Figure 4. Fentanyl down-regulates LPS-induced I $\kappa$ B $\alpha$  activation in CHME-5 cells**

CHME-5 cells were stimulated with LPS and fentanyl for 10 min. **A.** Cytoplasmic lysates were subjected to SDS-PAGE and immunoblotted with p-I $\kappa$ B $\alpha$  (1:1000), I $\kappa$ B $\alpha$  (1:1000), and  $\beta$ -tubulin (1:1000) antibodies. **B.** phospho-I $\kappa$ B $\alpha$  was quantified with I $\kappa$ B $\alpha$  and ANOVA and Dunnett's multiple comparison tests revealed a significant decrease with fentanyl at 100  $\mu$ M ( $p < 0.001$ ). Images are representative of three independent experiments ( $n=3$ ) for each treatment group. Bars for all experiments are presented as mean  $\pm$  SEM.

\*\*\*  $p < 0.001$ , \*  $p < 0.05$  vs. cells treated with LPS alone

**5A.**



**5B.**

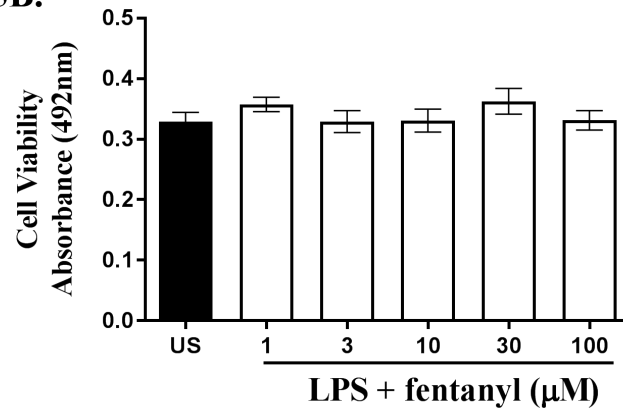
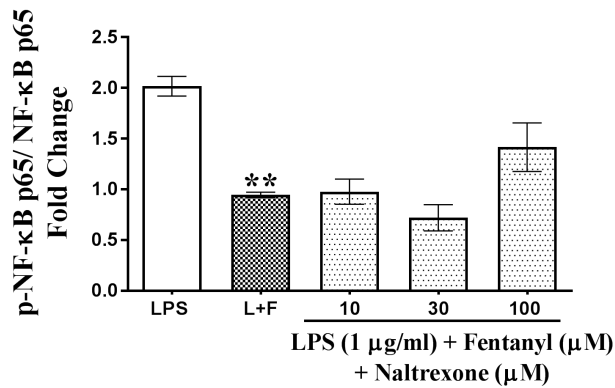


**Figure 5. Fentanyl down-regulates LPS-induced NF-κB activity in CHME-5 cells**

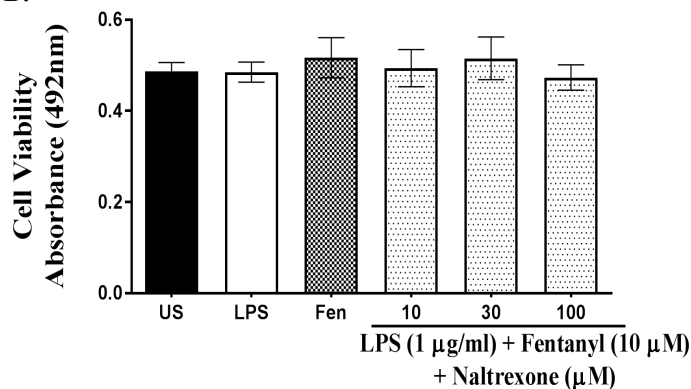
CHME-5 cells were stimulated with LPS and fentanyl for 10min. **A.** Nuclear extracts were analyzed for NF-κB p65 binding activity. ANOVA and Dunnett's multiple comparison tests revealed significant decreases in NF-κB p65 binding activity with fentanyl at 10 and 100 μM, as compared to cells treated with LPS alone. Image is representative of six independent experiments (n=6) for each treatment group. **B.** Following cell stimulation, MTT cell viability was performed and absorbance measured at 492 nm. ANOVA revealed no significant difference between control and LPS/fentanyl co-treated cells, p=0.54. Three experiments were performed in duplicate; n=3 for each treatment group. Bars for all experiments are presented as mean ± SEM.

\*p<0.05 vs. cells treated with LPS alone

6A.



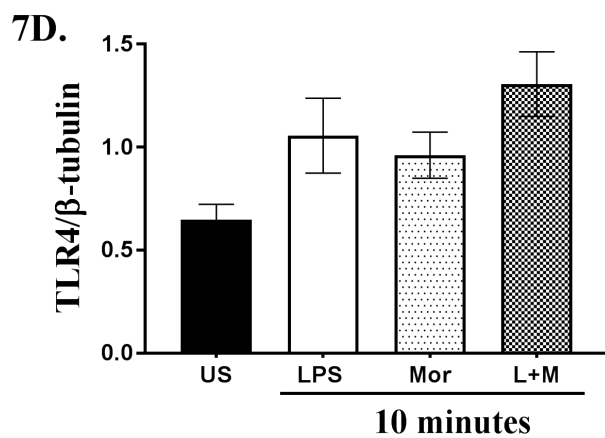
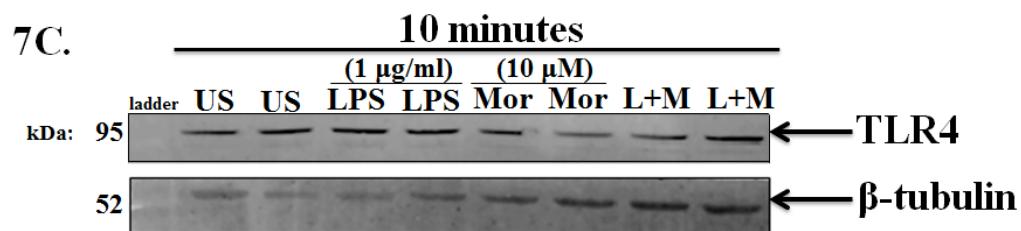
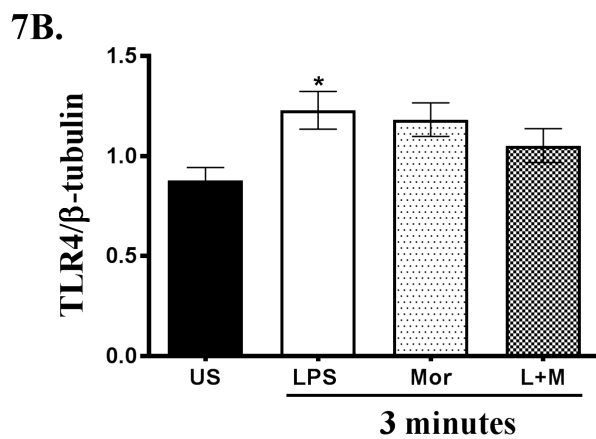
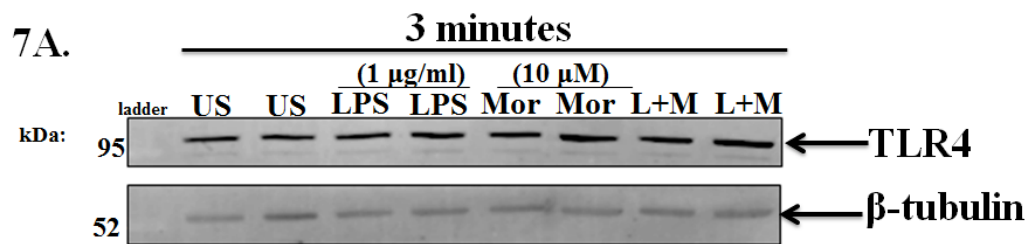
6B.



**Figure 6. Naltrexone has no effect on fentanyl-mediated effect in CHME-5 cells**

CHME-5 cells were stimulated with LPS, fentanyl, and naltrexone for 10min. **A.** Nuclear extracts were analyzed for NF-κB p65 binding activity. ANOVA with Tukey's multiple comparison tests revealed a 1-fold decrease in LPS/fentanyl co-treated cells and no difference in cells co-treated with naltrexone, as compared to LPS/fentanyl co-treated cells. Image is representative of four independent experiments (n=4) for each treatment group. **B.** MTT cell viability absorbance was measured at 492 nm. ANOVA revealed no significant difference between control and LPS/fentanyl/naltrexone co-treated cells, p=0.94. Three experiments were performed in duplicate (n=3) for each treatment group. Bars for all experiments are presented as mean ± SEM.

\*\* p<0.01 vs. cells treated with LPS alone



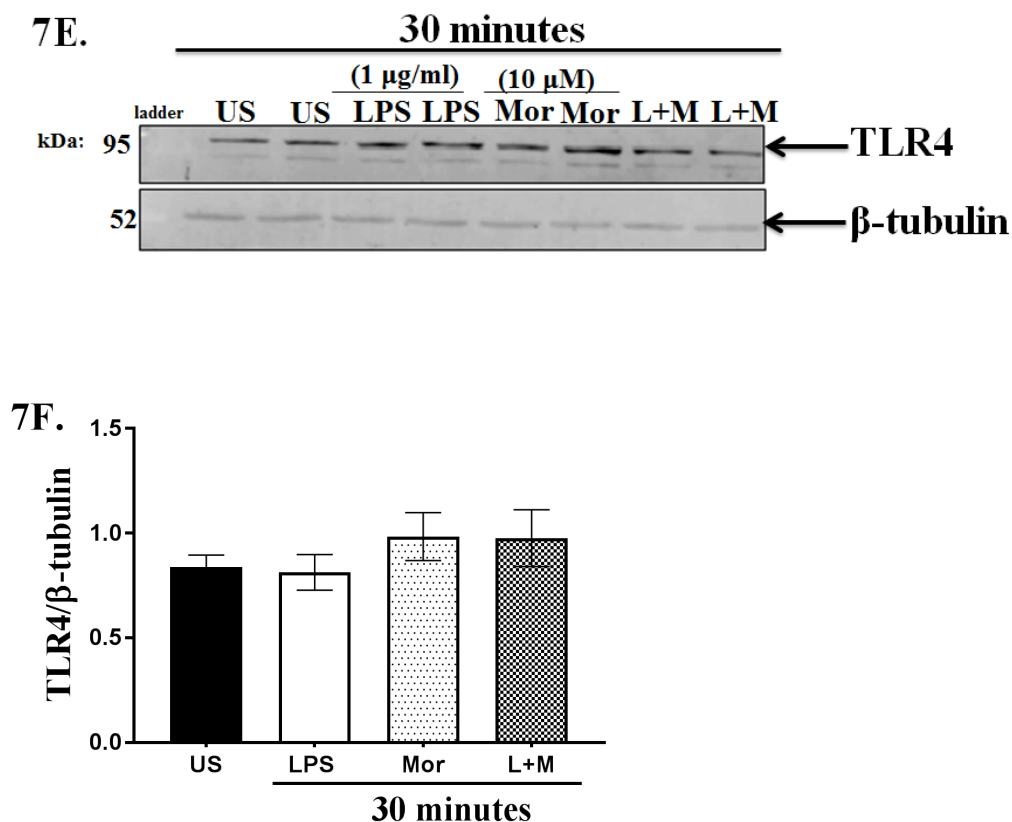
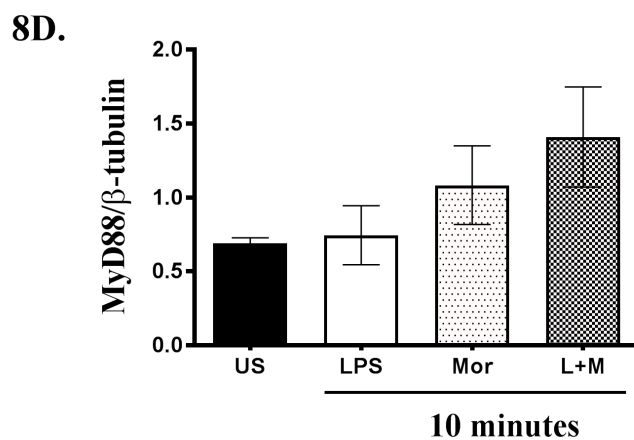
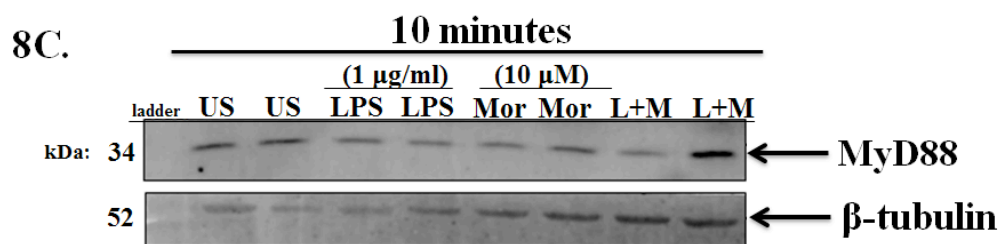
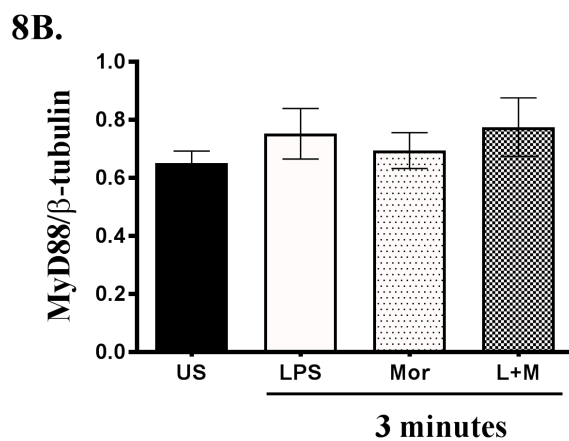
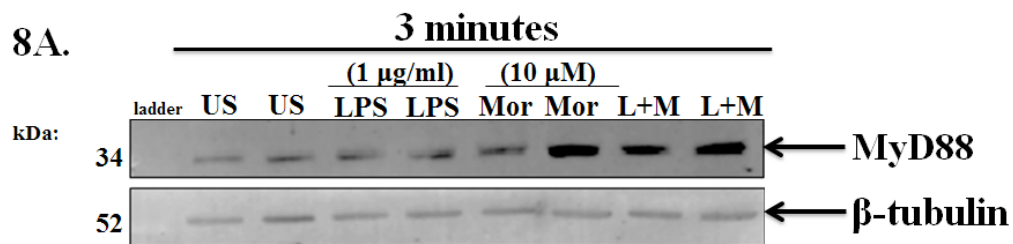


**Figure 7. Morphine does not affect LPS-induced TLR4 expression in CHME-5 cells**

CHME-5 cells were stimulated with or without LPS and/or morphine for 3, 10, and 30 min.

Whole cell lysates were subjected to SDS-PAGE and immunoblotted with TLR4 (1:1000) and β-tubulin (1:1000) antibodies (**A**, **C**, **E**). ANOVA revealed no difference in TLR4 expression with LPS/morphine co-treatment at **B**. 3 (p=0.32), **D**. 10 (p=0.50), nor **F**. 30 (p=0.60) min, as to cell treated with LPS alone. Three independent experiments were performed in duplicate; n=3 for each treatment group. Bars for all experiments are presented as mean ± SEM.





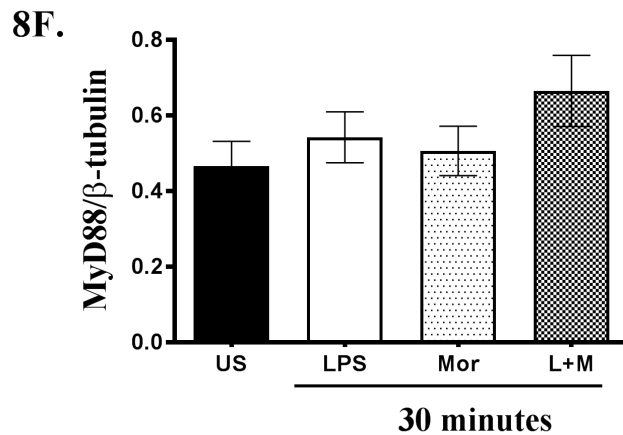
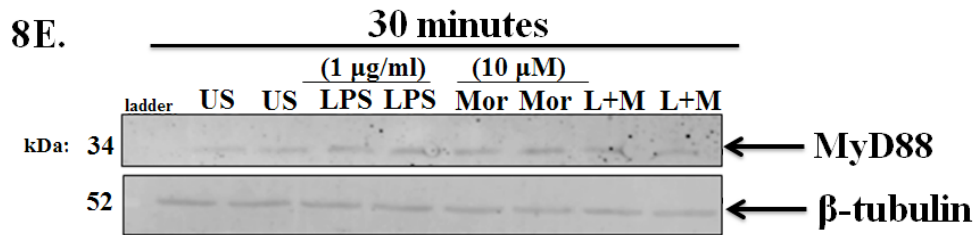


**Figure 8. Morphine does not affect LPS-induced MyD88 expression in CHME-5 cells**

CHME-5 cells were stimulated with or without LPS and morphine for 3, 10, and 30 min. Whole cell lysates were subjected to SDS-PAGE and immunoblotted with MyD88 (1:1000) and β-tubulin (1:1000) antibodies (A, C, E). A. Kruskal-Wallis revealed no difference in MyD88 expression at B. 3 (p=0.80), D. 10 min (p=0.50), nor F. 30 min (p=0.35). Three independent experiments were performed in duplicate; n=3 for each treatment group. Bars for all experiments are presented as mean ± SEM.

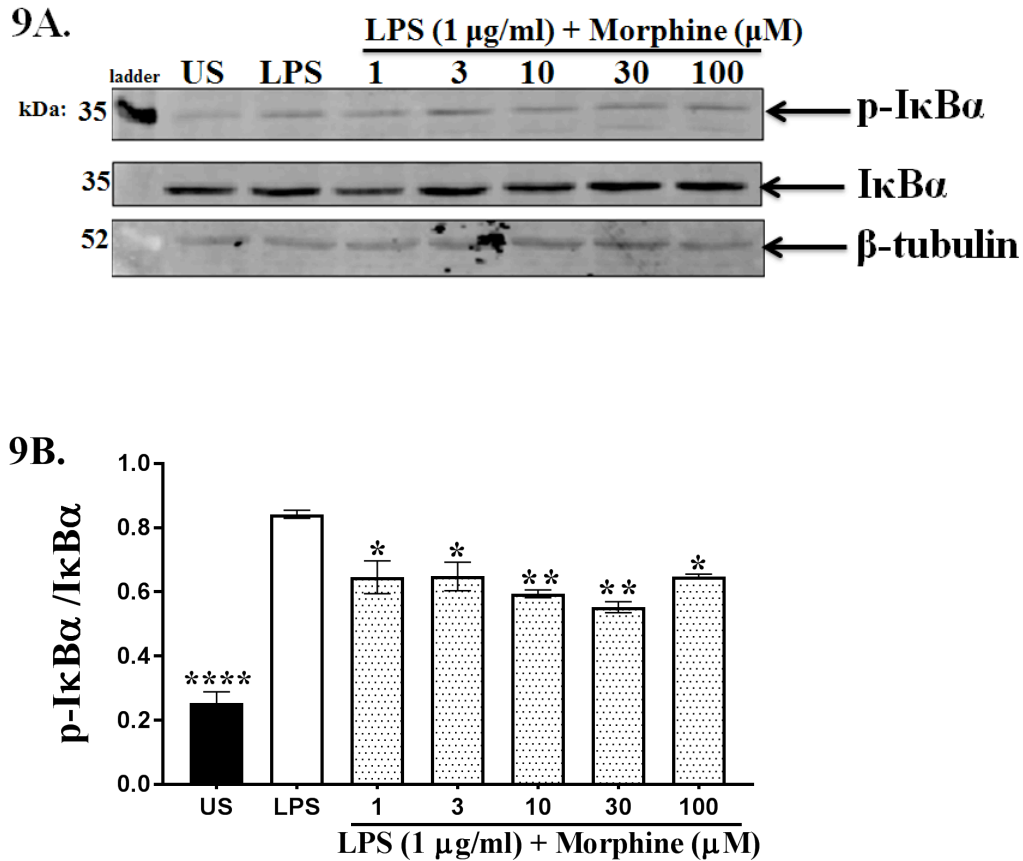
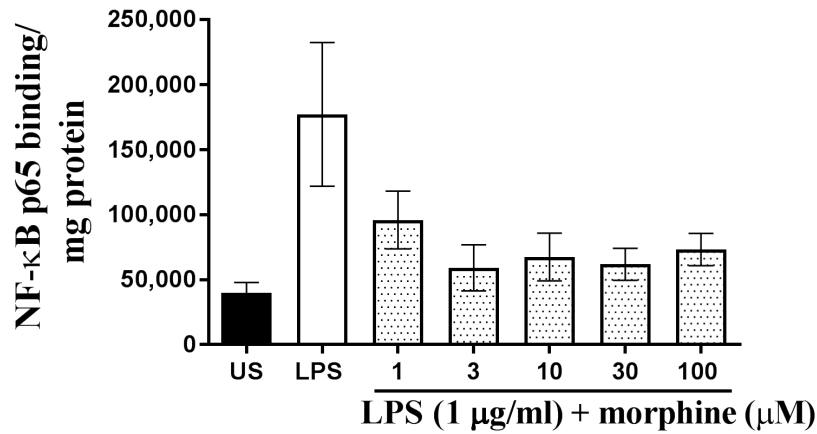


**Figure 9. Morphine decreases LPS-induced I $\kappa$ B $\alpha$  activation in CHME-5 cells**

CHME-5 cells were stimulated with or without LPS and morphine for 10 min. **A.** Cytoplasmic lysates were subjected to SDS-PAGE and immunoblotted with p-I $\kappa$ B $\alpha$  (1:1000), I $\kappa$ B $\alpha$  (1:1000), and  $\beta$ -tubulin (1:1000) antibodies. **B.** phospho-I $\kappa$ B $\alpha$  was quantified with I $\kappa$ B $\alpha$  and ANOVA and Dunnett's multiple comparison tests revealed a significant decrease in LPS-induced I $\kappa$ B $\alpha$  activation with morphine at 1-100  $\mu$ M. Images are representative of four independent experiments (n=4) for each treatment group. Bars for all experiments are presented as mean  $\pm$  SEM.

\*\*\*\* p<0.0001, \*\* p<0.01, \* p<0.05 vs. cells treated with LPS alone

**10A.**



**10B.**

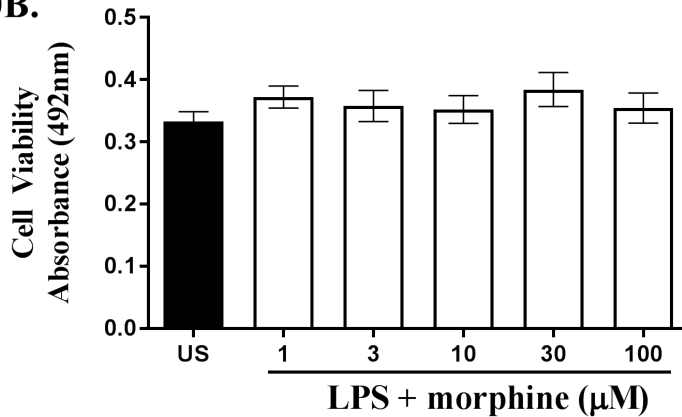


**Figure 10. Morphine does not affect LPS-induced NF-κB p65 activation in CHME-5 cells**

CHME-5 cells were stimulated with LPS and morphine for 10 min. **A.** Nuclear extracts were used to analyze NF-κB p65 binding activity. ANOVA revealed no difference in NF-κB p65 binding activity ( $p=1.00$ ). Image is representative of six independent experiments ( $n=6$ ) for each treatment group. **B.** Following stimulation, MTT cell viability was performed and absorbance was measured at 492 nm. ANOVA revealed no difference between control and LPS/morphine co-treated cells,  $p=0.70$ . Three independent experiments were performed in duplicate;  $n=3$  for each treatment group. Bars for all experiments are presented as mean  $\pm$  SEM.

## DISCUSSION

Opioids remain the gold standard for analgesia of postoperative and chronic pain, including pain associated with cancer. More research indicates the use of opioids to treat pain during neurodegeneration including MS, AD and PD, which display inflammatory components (Broen et al., 2012; de Tommaso et al., 2016). It is important therefore to understand the exact mechanisms occurring during treatment with opioid agonists and antagonists to determine the impact of opioids on inflammation. In the present study, we show the anti-inflammatory potential of fentanyl, and to a lesser extent morphine, on LPS-induced TLR4 neuroinflammatory signaling in microglia.

Microglia are the “macrophages” of the CNS and, therefore, are responsible for a majority of inflammation potentiated during injury or infection. Microglia have been shown to express TLRs 1-9, and thus, LPS was used to induce an inflammatory response through activation of TLR4 in a microglial cell line, CHME-5. Determination of MOR expression in the CHME-5 microglial cell line was important because of the use of fentanyl and morphine, which are agonists for the MOR. To our knowledge this is the first time *MOR* gene expression is shown in CHME-5 cells, which was up-regulated in response to LPS. As previously discussed, MOR gene and protein expression in microglia has been detailed using *in vivo*, *ex vivo*, and *in vitro* analysis, including in human, mice, and rat microglia, so it was not surprising that MOR expression was up-regulated in CHME-5 cells (Chao et al., 1997; El-Hage et al., 2013; Gessi et al., 2016; Horvath et al.,

2008). Other reports have also shown a 2-fold increase in MOR mRNA expression in response to LPS (10 µg/ml) in rat peritoneal macrophages, and a 1.5-fold difference with LPS (5 µg/ml) at 24 h in TPA-HL-60 macrophage-like human cells (Byrne et al., 2012; Chang et al., 2007; Langsdorf et al., 2011). It would be interesting to investigate whether up-regulation of LPS-induced MOR gene expression is correlated with protein expression, even though expression of these two biological molecules are not always equivalent, as in the case of TLR4 (Bachtell et al., 2015).

Along with changes in LPS-induced MOR expression, we examined TLR4 and MyD88, which are two crucial proteins in the TLR4-MyD88-dependent pathway that are necessary for LPS recognition and signaling, respectively, leading to production of inflammatory mediators. Thus, I examined whether fentanyl or morphine could modulate LPS-induced TLR4 and MyD88 protein expression in CHME-5 cells. There were no significant changes in LPS-induced TLR4 expression, as opposed to what was observed previously in chapter one, which revealed increases in response to LPS no earlier than 90 minutes. The fact that expression was examined at earlier time points (3, 10, and 30 min) may be the reason we did not see this increase. A previous study in our lab, Stevens et al. 2013, showed significant increases in TLR4 signaling, which differs from TLR4 expression, because TLR4 signaling was measured as a response of NF-κB activation in HEK-Blue-hTLR4 cells (Stevens et al., 2013). In contrast, other studies have detected increases in LPS-induced TLR4 expression in mouse and rat microglial cells, BV2 and N9, respectively, which could be due to longer incubation periods (24 h) and higher doses of LPS (up to 30 µg/ml) (Dai et al., 2015; P. Wang et al., 2014; Yoon et al., 2013). LPS-induced MyD88 expression did not change in response to LPS treatment in CHME-5

microglial cells. Similarly, one such study using human pericytes detected no change in MyD88 expression at 4 h in response to LPS (1  $\mu$ g/ml) (Guijarro-Munoz et al., 2014). Conversely, the studies mentioned above also showed increases in LPS-induced MyD88 expression in BV2 and N9 microglial cells at 24 h with LPS doses as high as 30  $\mu$ g/ml (Dai et al., 2015; P. Wang et al., 2014; Yoon et al., 2013). Thus, modulation of these two proteins in response to LPS may differ based on cell type, LPS concentration, and duration of LPS exposure. With regard to opioid co-treatment, neither fentanyl nor morphine had any effect on TLR4 and MyD88 expression. A survey of the literature revealed no studies on fentanyl or morphine-mediated effects on TLR4 and MyD88 expression with LPS co-treatment. Once again, Stevens et al. 2013, showed that fentanyl and morphine-mediated down-regulation of LPS-induced TLR4 signaling in HEK-Blue-hTLR4 cells at 24 h. These data suggest that fentanyl and morphine do not affect earlier events in the TLR4/MyD88 pathway in CHME-5 microglial cells. Further investigation is needed to determine whether stimulation for 24 h leads to a difference in TLR4 and MyD88 expression in response LPS and fentanyl or morphine co-treatment.

Upon LPS-induced TLR4 activation, there are several downstream signaling events that occur, including activation of I $\kappa$ B $\alpha$  and NF- $\kappa$ B nuclear translocation. I $\kappa$ B $\alpha$  activation was increased in response to LPS, as determined by protein phosphorylation, and subsequently decreased with fentanyl or morphine co-treatment. LPS-induced NF- $\kappa$ B p65 binding activity was also down-regulated with fentanyl co-treatment. In contrast, others observed an increase in p-I $\kappa$ B $\alpha$  immunoreactivity and NF- $\kappa$ B p65 activation in cytoplasmic and nuclear extracts, respectively, in primary murine microglial cells following LPS and morphine (10  $\mu$ M) co-treatment for 15 minutes in primary murine

microglial cells (Gessi et al., 2016). Previous research in our lab revealed that opioids reduced cytokine-induced NF- $\kappa$ B activation in astrocytes. For instance, IL-1 $\beta$  induced p65 activity, which was inhibited by  $\beta$ -FNA; and TNF $\alpha$ -induced NF- $\kappa$ B nuclear translocation was inhibited by fentanyl, morphine, and  $\beta$ -FNA (R. L. Davis et al., 2007; R. L. Davis et al., 2013). In the present study, unlike fentanyl, morphine did not significantly affect LPS-induced NF- $\kappa$ B p65 binding activity, which may have been due to the high degree of variability in the response. Alternatively, the differential effects between fentanyl and morphine may be attributed to their potency as MOR agonists; fentanyl is 80-100 $\times$  more potent than morphine. These responses indicate that fentanyl, and to a lesser extent morphine, can modulate TLR4-mediated downstream signaling events.

I investigated whether fentanyl-mediated down-regulation of LPS-induced NF- $\kappa$ B p65 binding activity was occurring through MOR or through another non-classical opioid site. Co-treatment with naltrexone did not reverse the fentanyl-mediated effect seen during co-treatment with LPS and fentanyl, which is consistent with data from our lab showing that naltrexone did not reverse the fentanyl or morphine-mediated effects of LPS-induced TLR4 signaling (Stevens et al., 2013). Together, these findings suggest that the fentanyl-mediated effect on LPS-induced NF- $\kappa$ B p65 binding activity is MOR-independent.

Data published by the Hutchinson and Watkins labs suggest that opioid agonists and antagonists mediate their effects by interacting with the MD2 binding pocket (Hutchinson et al., 2012; Hutchinson et al., 2010; Wang et al., 2012a). Several studies showed that morphine interacts with the MD2 binding pocket, induces TLR4



oligomerization, and mediates MD2 conformational changes, thereby stabilizing the TLR4/morphine heterotetrameric complex, all of which are similar characteristics of LPS binding (Wang et al., 2012a). Naltrexone may not have reversed the fentanyl-mediated effect due to lower affinity for the TLR4/MD2 pocket than LPS (Wang et al. unpublished data) or naltrexone may not have had sufficient incubation time to mediate an effect. Additionally, naltrexone was added after LPS/fentanyl co-treatment, therefore naltrexone may not have had the opportunity to bind the MD2 docking site before LPS and fentanyl; this may be important because computer modeling showed that pre-docking of naltrexone disrupted the preferred binding sites of morphine, which led to displacement of opioids outside LPS binding pocket (Bachtell et al., 2015).

We also demonstrated that co-treatment with LPS and fentanyl or morphine, along with addition of naltrexone was not cytotoxic to the CHME-5 microglial cells, which is consistent with data from other cell viability assays in our laboratory showing that increasing doses of opioid agonists and antagonists are not cytotoxic (R. L. Davis et al., 2007). This data suggests that down-regulation in response to opioid co-treatments was not due to cytotoxicity of the compound(s).

And finally, I guess I should address the elephant in the room: what about the opioid-induced addiction epidemic? Opioid dependence and addiction results from biological abnormalities that occur as a result of chronic opioid use (Kosten et al., 2002). Brain centers in the VTA are stimulated upon opioid-receptor activation, which leads to release of DA thereby producing a feeling of pleasure, and ultimately dependence and addiction. How can it be suggested that opioids be given to patients therapeutically to treat neurodegeneration or inflammatory conditions when there is an opioid epidemic

around the world? Data from this study, along with others cited throughout this dissertation, suggests that during inflammatory conditions, opioids have anti-inflammatory effects, which are not mediated through MOR. But even though the anti-inflammatory effects are MOR-independent, the opioids are still binding MOR. Therefore, the potential for using opioids to treat neuroinflammatory conditions is still a work in progress, given the risk of tolerance and addiction.

Additionally, since the literature shows that neurons and astrocytes express TLRs, including TLR4, it will be necessary to determine if similar fentanyl and morphine-mediated effects, along with effects of opioid antagonists, are present in the other cells within the CNS. This would give us a sense as to whether the non-classical opioid site theory translates across all cell types in the CNS.

## CONCLUSION

This dissertation focused on two main points: LPS-induced neuroinflammatory signaling and the opioid-mediated effects in microglia. CHME-5 immortalized microglial cells were expected to impart similar responses as have been defined in peripheral immune cells, due to their nature as the immune cell of the CNS. Neuroinflammatory signaling was achieved through activation of TLR4 in response to Gram-negative bacterial LPS, which allowed us to assess signaling mechanisms occurring in the MyD88-dependent pathway.

Due to the unforeseen event that occurred at the latter end of my research, namely discovering that CHME-5 were not of human origin, we needed to redirect our purpose for this project. Nevertheless, the literature shows homology (>60%) in the human *TLR4* gene compared to its rat counterpart, as well as conservation of biological function and downstream signaling, which was demonstrated in similarities seen from data collected throughout this dissertation as compared to human microglial studies. Ultimately, these data confirmed that CHME-5 cells remain a useful tool as evidenced by the retention of morphological, phenotypical, and functional characteristics of microglia.

The effects of the two opioid agonists, fentanyl and morphine, on LPS-induced TLR4 neuroinflammatory signaling were also assessed. Fentanyl, and to a lesser extent morphine, displayed anti-inflammatory actions on several crucial signaling molecules in the TLR4 MyD88-dependent pathway. Fentanyl and morphine are prototypical ligands

for the MOR and were expected to mediate their effects through this classical opioid receptor. What we discovered was that treatment with the opioid antagonist, naltrexone, failed to reverse the opioid-mediated effects on LPS-induced neuroinflammatory signaling.

Therefore, these data lead us to several conclusions: 1) CHME-5 cells are rat microglial cells that retain microglial attributes, 2) CHME-5 cells remain a beneficial tool for studying neuroinflammatory responses in microglia, 3) fentanyl and morphine have anti-inflammatory potential, and 4) opioid-mediated effects on inflammatory signaling in CHME-5 cells are not occurring through the MOR, but through a non-classical opioid site.

## REFERENCES

- Akira, S., & Takeda, K. (2004). Toll-like receptor signalling. *Nat Rev Immunol*, 4(7), 499-511.
- Akiyama, H., Barger, S., Barnum, S., Bradt, B., Bauer, J., Cole, G. M., et al. (2000). Inflammation and Alzheimer's disease. *Neurobiol Aging*, 21(3), 383-421.
- Alexopoulou, L., Holt, A. C., Medzhitov, R., & Flavell, R. A. (2001). Recognition of double-stranded RNA and activation of NF-kappaB by Toll-like receptor 3. *Nature*, 413(6857), 732-738.
- Arenzana-Seisdedos, F., Turpin, P., Rodriguez, M., Thomas, D., Hay, R. T., Virelizier, J. L., et al. (1997). Nuclear localization of I kappa B alpha promotes active transport of NF-kappa B from the nucleus to the cytoplasm. *J Cell Sci*, 110 ( Pt 3), 369-378.
- Armstrong, Medford, A. R., Hunter, K. J., Uppington, K. M., & Millar, A. B. (2004). Differential expression of Toll-like receptor (TLR)-2 and TLR-4 on monocytes in human sepsis. *Clin Exp Immunol*, 136(2), 312-319.
- Armstrong, S. C., & Cozza, K. L. (2003). Pharmacokinetic drug interactions of morphine, codeine, and their derivatives: theory and clinical reality, part I. *Psychosomatics*, 44(2), 167-171.
- Atanassov, C. L., Muller, C. D., Dumont, S., Rebel, G., Poindron, P., & Seiler, N. (1995). Effect of ammonia on endocytosis and cytokine production by immortalized human microglia and astroglia cells. *Neurochem Int*, 27(4-5), 417-424.
- Bachtell, R., Hutchinson, M. R., Wang, X., Rice, K. C., Maier, S. F., & Watkins, L. R. (2015). Targeting the Toll of Drug Abuse: The Translational Potential of Toll-Like Receptor 4. *CNS Neurol Disord Drug Targets*, 14(6), 692-699.

- Bailey, C. P., & Connor, M. (2005). Opioids: cellular mechanisms of tolerance and physical dependence. *Curr Opin Pharmacol*, 5(1), 60-68.
- Barton, G. M., & Kagan, J. C. (2009). A cell biological view of Toll-like receptor function: regulation through compartmentalization. *Nat Rev Immunol*, 9(8), 535-542. doi: 510.1038/nri2587.
- Bell, J. K., Mullen, G. E., Leifer, C. A., Mazzoni, A., Davies, D. R., & Segal, D. M. (2003). Leucine-rich repeats and pathogen recognition in Toll-like receptors. *Trends Immunol*, 24(10), 528-533.
- Blasi, E., Barluzzi, R., Bocchini, V., Mazzolla, R., & Bistoni, F. (1990). Immortalization of murine microglial cells by a v-raf/v-myc carrying retrovirus. *J Neuroimmunol*, 27(2-3), 229-237.
- Bosisio, D., Polentarutti, N., Sironi, M., Bernasconi, S., Miyake, K., Webb, G. R., et al. (2002). Stimulation of toll-like receptor 4 expression in human mononuclear phagocytes by interferon-gamma: a molecular basis for priming and synergism with bacterial lipopolysaccharide. *Blood*, 99(9), 3427-3431.
- Bowman, C. C., Rasley, A., Tranguch, S. L., & Marriott, I. (2003). Cultured astrocytes express toll-like receptors for bacterial products. *Glia*, 43(3), 281-291.
- Brenner, G. M., & Stevens, C. W. (2010). *Pharmacology* (3rd ed.). Philadelphia, PA: Saunders Elsevier.
- Brint, E. K., Xu, D., Liu, H., Dunne, A., McKenzie, A. N., O'Neill, L. A., et al. (2004). ST2 is an inhibitor of interleukin 1 receptor and Toll-like receptor 4 signaling and maintains endotoxin tolerance. *Nat Immunol*, 5(4), 373-379.
- Broen, M. P., Braaksma, M. M., Patijn, J., & Weber, W. E. (2012). Prevalence of pain in Parkinson's disease: a systematic review using the modified QUADAS tool. *Mov Disord*, 27(4), 480-484. doi: 410.1002/mds.24054.
- Bruttger, J., Karram, K., Wortge, S., Regen, T., Marini, F., Hoppmann, N., et al. (2015). Genetic Cell Ablation Reveals Clusters of Local Self-Renewing Microglia in the Mammalian Central Nervous System. *Immunity*, 43(1), 92-106. doi: 110.1016/j.immuni.2015.1006.1012.

Bsibsi, M., Ravid, R., Gveric, D., & van Noort, J. M. (2002). Broad expression of Toll-like receptors in the human central nervous system. *J Neuropathol Exp Neurol*, 61(11), 1013-1021.

Bussiere, J. L., Adler, M. W., Rogers, T. J., & Eisenstein, T. K. (1992). Differential effects of morphine and naltrexone on the antibody response in various mouse strains. *Immunopharmacol Immunotoxicol*, 14(3), 657-673.

Byrne, L. S., Peng, J., Sarkar, S., & Chang, S. L. (2012). Interleukin-1 beta-induced up-regulation of opioid receptors in the untreated and morphine-desensitized U87 MG human astrocytoma cells. *J Neuroinflammation*, 9:252.(doi), 10.1186/1742-2094-1189-1252.

Cao, Z., Xiong, J., Takeuchi, M., Kurama, T., & Goeddel, D. V. (1996). TRAF6 is a signal transducer for interleukin-1. *Nature*, 383(6599), 443-446.

Carpenter, A. E., Jones, T. R., Lamprecht, M. R., Clarke, C., Kang, I. H., Friman, O., et al. (2006). CellProfiler: image analysis software for identifying and quantifying cell phenotypes. *Genome Biol*, 7(10), R100.

Carpentier, P. A., Begolka, W. S., Olson, J. K., Elhofy, A., Karpus, W. J., & Miller, S. D. (2005). Differential activation of astrocytes by innate and adaptive immune stimuli. *Glia*, 49(3), 360-374.

Cartier, L., Hartley, O., Dubois-Dauphin, M., & Krause, K. H. (2005). Chemokine receptors in the central nervous system: role in brain inflammation and neurodegenerative diseases. *Brain Res Rev*, 48(1), 16-42.

Chang, S. L., Beltran, J. A., & Swarup, S. (2007). Expression of the mu opioid receptor in the human immunodeficiency virus type 1 transgenic rat model. *J Virol*, 81(16), 8406-8411. Epub 2007 Jun 8406.

Chao, C. C., Hu, S., Shark, K. B., Sheng, W. S., Gekker, G., & Peterson, P. K. (1997). Activation of mu opioid receptors inhibits microglial cell chemotaxis. *J Pharmacol Exp Ther*, 281(2), 998-1004.

Cheepsunthorn, P., Radov, L., Menzies, S., Reid, J., & Connor, J. R. (2001). Characterization of a novel brain-derived microglial cell line isolated from neonatal rat brain. *Glia*, 35(1), 53-62.

Chindalore, V. L., Craven, R. A., Yu, K. P., Butera, P. G., Burns, L. H., & Friedmann, N. (2005). Adding ultralow-dose naltrexone to oxycodone enhances and prolongs analgesia: a randomized, controlled trial of Oxytrex. *J Pain*, 6(6), 392-399.

Compton, P. (2008). Should opioid abusers be discharged from opioid-analgesic therapy? *Pain Med*, 9(4), 383-390.

Connor, M., & Christie, M. D. (1999). Opioid receptor signalling mechanisms. *Clin Exp Pharmacol Physiol*, 26(7), 493-499.

Conrad, A. T., & Dittel, B. N. (2011). Taming of macrophage and microglial cell activation by microRNA-124. *Cell Res*, 21(2), 213-216. doi: 210.1038/cr.2011.1039. Epub 2011 Jan 1011.

Corbett, A. D., Henderson, G., McKnight, A. T., & Paterson, S. J. (2006). 75 years of opioid research: the exciting but vain quest for the Holy Grail. *Br J Pharmacol*, 147 Suppl 1, S153-162.

Crain, S. M., & Shen, K. F. (2001). Acute thermal hyperalgesia elicited by low-dose morphine in normal mice is blocked by ultra-low-dose naltrexone, unmasking potent opioid analgesia. *Brain Res*, 888(1), 75-82.

Cunha-Oliveira, T., Rego, A. C., & Oliveira, C. R. (2008). Cellular and molecular mechanisms involved in the neurotoxicity of opioid and psychostimulant drugs. *Brain Res Rev*, 58(1), 192-208.

Curtale, G., Mirolo, M., Renzi, T. A., Rossato, M., Bazzoni, F., & Locati, M. (2013). Negative regulation of Toll-like receptor 4 signaling by IL-10-dependent microRNA-146b. *Proc Natl Acad Sci U S A*, 110(28), 11499-11504. doi: 11410.11073/pnas.1219852110.

Dai, X. J., Li, N., Yu, L., Chen, Z. Y., Hua, R., Qin, X., et al. (2015). Activation of BV2 microglia by lipopolysaccharide triggers an inflammatory reaction in PC12 cell apoptosis through a toll-like receptor 4-dependent pathway. *Cell Stress Chaperones*, 20(2), 321-331. doi: 310.1007/s12192-12014-10552-12191.

Davis, M. P. (2011). Fentanyl for breakthrough pain: a systematic review. *Expert Rev Neurother*, 11(8), 1197-1216.



Davis, R. L., Buck, D. J., Saffarian, N., & Stevens, C. W. (2007). The opioid antagonist, beta-funaltrexamine, inhibits chemokine expression in human astroglial cells. *J Neuroimmunol*, 186(1-2), 141-149.

Davis, R. L., Das, S., Buck, D. J., & Stevens, C. W. (2013). Beta-funaltrexamine inhibits chemokine (CXCL10) expression in normal human astrocytes. *Neurochem Int*, 62(4), 478-485.

de Tommaso, M., Arendt-Nielsen, L., Defrin, R., Kunz, M., Pickering, G., & Valeriani, M. (2016). Pain in Neurodegenerative Disease: Current Knowledge and Future Perspectives. *Behav Neurol*, 2016:7576292.(doi), 10.1155/2016/7576292.

Diebold, S. S., Kaisho, T., Hemmi, H., Akira, S., & Reis e Sousa, C. (2004). Innate antiviral responses by means of TLR7-mediated recognition of single-stranded RNA. *Science*, 303(5663), 1529-1531.

Divanovic, S., Trompette, A., Atabani, S. F., Madan, R., Golenbock, D. T., Visintin, A., et al. (2005). Negative regulation of Toll-like receptor 4 signaling by the Toll-like receptor homolog RP105. *Nat Immunol*, 6(6), 571-578.

DuPen, A., Shen, D., & Ersek, M. (2007). Mechanisms of opioid-induced tolerance and hyperalgesia. *Pain Manag Nurs*, 8(3), 113-121.

Durafourt, B. A., Moore, C. S., Zammit, D. A., Johnson, T. A., Zaguia, F., Guiot, M. C., et al. (2012). Comparison of polarization properties of human adult microglia and blood-derived macrophages. *Glia*, 60(5), 717-727. doi: 10.1002/glia.22298.

Dziarski, R., & Gupta, D. (2000). Role of MD-2 in TLR2- and TLR4-mediated recognition of Gram-negative and Gram-positive bacteria and activation of chemokine genes. *J Endotoxin Res*, 6(5), 401-405.

El-Hage, N., Dever, S. M., Podhaizer, E. M., Arnatt, C. K., Zhang, Y., & Hauser, K. F. (2013). A novel bivalent HIV-1 entry inhibitor reveals fundamental differences in CCR5-mu-opioid receptor interactions between human astroglia and microglia. *AIDS*, 27(14), 2181-2190. doi: 10.1097/QAD.2180b2013e3283639804.

Evans, C. J., Keith, D. E., Jr., Morrison, H., Magendzo, K., & Edwards, R. H. (1992). Cloning of a delta opioid receptor by functional expression. *Science*, 258(5090), 1952-1955.

Felder, C., Uehlinger, C., Baumann, P., Powell, K., & Eap, C. B. (1999). Oral and intravenous methadone use: some clinical and pharmacokinetic aspects. *Drug Alcohol Depend*, 55(1-2), 137-143.

Feng, Y., He, X., Yang, Y., Chao, D., Lazarus, L. H., & Xia, Y. (2012). Current research on opioid receptor function. *Curr Drug Targets*, 13(2), 230-246.

Fine, P., & Portenoy, R. K. (2004). *Opioid Drugs: Overview of Clinical Pharmacology*. New York: McGraw Hill.

Finley, M. J., Happel, C. M., Kaminsky, D. E., & Rogers, T. J. (2008). Opioid and nociceptin receptors regulate cytokine and cytokine receptor expression. *Cell Immunol*, 252(1-2), 146-154.

Garcia-Mesa, Y., Jay, T. R., Checkley, M. A., Luttge, B., Dobrowolski, C., Valadkhan, S., et al. (2017). Immortalization of primary microglia: a new platform to study HIV regulation in the central nervous system. *J Neurovirol*, 23(1), 47-66.

Gehrmann, J., Matsumoto, Y., & Kreutzberg, G. W. (1995). Microglia: intrinsic immune effector cell of the brain. *Brain Res Rev*, 20(3), 269-287.

Gessi, S., Borea, P. A., Bencivenni, S., Fazzi, D., Varani, K., & Merighi, S. (2016). The activation of mu-opioid receptor potentiates LPS-induced NF- $\kappa$ B promoting an inflammatory phenotype in microglia. *FEBS Lett.*, 590(17), 2813-2826. doi: 2810.1002/1873-3468.12313.

Giulian, D. (1987). Ameboid microglia as effectors of inflammation in the central nervous system. *J Neurosci Res*, 1987;18(1), 155-171.

Giulian, D., & Ingeman, J. E. (1988). Colony-stimulating factors as promoters of ameboid microglia. *J Neurosci*, 8(12), 4707-4717.

Glass, C. K., Saijo, K., Winner, B., Marchetto, M. C., & Gage, F. H. (2010). Mechanisms underlying inflammation in neurodegeneration. *Cell*, 140(6), 918-934.

Godfroy, J. I., 3rd, Roostan, M., Moroz, Y. S., Korendovych, I. V., & Yin, H. (2012). Isolated Toll-like receptor transmembrane domains are capable of oligomerization. *PLoS One*, 7(11), e48875. doi: 48810.41371/journal.pone.0048875.

Gonzalez, J. P., & Brogden, R. N. (1988). Naltrexone. A review of its pharmacodynamic and pharmacokinetic properties and therapeutic efficacy in the management of opioid dependence. *Drugs*, 35(3), 192-213.

Gordon, S., & Taylor, P. R. (2005). Monocyte and macrophage heterogeneity. *Nat Rev Immunol*, 5(12), 953-964.

Govindaraj, R. G., Manavalan, B., Lee, G., & Choi, S. (2010). Molecular modeling-based evaluation of hTLR10 and identification of potential ligands in Toll-like receptor signaling. *PLoS One*, 5(9), e12713. doi: 12710.11371/journal.pone.0012713.

Graeber, M. B., & Streit, W. J. (2010). Microglia: biology and pathology. *Acta Neuropathol*, 119(1), 89-105.

Greeneltch, K. M., Haudenschild, C. C., Keegan, A. D., & Shi, Y. (2004). The opioid antagonist naltrexone blocks acute endotoxic shock by inhibiting tumor necrosis factor- $\alpha$  production. *Brain Behav Immun*, 18(5), 476-484.

Griffin, J. F., Larson, D. L., & Portoghese, P. S. (1986). Crystal structures of alpha- and beta-funaltrexamine: conformational requirement of the fumaramate moiety in the irreversible blockage of mu opioid receptors. *J Med Chem*, 29(5), 778-783.

Guan, Y., Ranao, D. R., Jiang, S., Mutha, S. K., Li, X., Baudry, J., et al. (2010). Human TLRs 10 and 1 share common mechanisms of innate immune sensing but not signaling. *J Immunol*, 184(9), 5094-5103. doi: 5010.4049/jimmunol.0901888.

Guijarro-Munoz, I., Compte, M., Alvarez-Cienfuegos, A., Alvarez-Vallina, L., & Sanz, L. (2014). Lipopolysaccharide activates Toll-like receptor 4 (TLR4)-mediated NF-kappaB signaling pathway and proinflammatory response in human pericytes. *J Biol Chem*, 289(4), 2457-2468. doi: 2410.1074/jbc.M2113.521161.

Halford, W. P., Gebhardt, B. M., & Carr, D. J. (1995). Functional role and sequence analysis of a lymphocyte orphan opioid receptor. *J Neuroimmunol*, 59(1-2), 91-101.

Hamann, S., & Sloan, P. (2007). Oral naltrexone to enhance analgesia in patients receiving continuous intrathecal morphine for chronic pain: a randomized, double-blind, prospective pilot study. *J Opioid Manag*, 3(3), 137-144.

Hanisch, U. K., Johnson, T. V., & Kipnis, J. (2008). Toll-like receptors: roles in neuroprotection? *Trends Neurosci*, 31(4), 176-182. doi: 110.1016/j.tins.2008.1001.1005.

Hanisch, U. K., & Kettenmann, H. (2007). Microglia: active sensor and versatile effector cells in the normal and pathologic brain. *Nat Neurosci*, 10(11), 1387-1394.

Hanke, M. L., & Kielian, T. (2011). Toll-like receptors in health and disease in the brain: mechanisms and therapeutic potential. *Clin Sci (Lond)*, 121(9), 367-387.

Hasan, U., Chaffois, C., Gaillard, C., Saulnier, V., Merck, E., Tancredi, S., et al. (2005). Human TLR10 is a functional receptor, expressed by B cells and plasmacytoid dendritic cells, which activates gene transcription through MyD88. *J Immunol*, 174(5), 2942-2950.

Hayashi, F., Smith, K. D., Ozinsky, A., Hawn, T. R., Yi, E. C., Goodlett, D. R., et al. (2001). The innate immune response to bacterial flagellin is mediated by Toll-like receptor 5. *Nature*, 410(6832), 1099-1103.

Heil, F., Hemmi, H., Hochrein, H., Ampenberger, F., Kirschning, C., Akira, S., et al. (2004). Species-specific recognition of single-stranded RNA via toll-like receptor 7 and 8. *Science*, 303(5663), 1526-1529.

Henn, A., Lund, S., Hedtjarn, M., Schrattenholz, A., Porzgen, P., & Leist, M. (2009). The suitability of BV2 cells as alternative model system for primary microglia cultures or for animal experiments examining brain inflammation. *ALTEX*, 26(2), 83-94.

Heydorn, A., Sondergaard, B. P., Ersboll, B., Holst, B., Nielsen, F. C., Haft, C. R., et al. (2004). A library of 7TM receptor C-terminal tails. Interactions with the proposed post-endocytic sorting proteins ERM-binding phosphoprotein 50 (EBP50), N-ethylmaleimide-sensitive factor (NSF), sorting nexin 1 (SNX1), and G protein-coupled receptor-associated sorting protein (GASP). *J Biol Chem*, 279(52), 54291-54303.

Hill, M. P., Hille, C. J., & Brotchie, J. M. (2000). Delta-opioid receptor agonists as a therapeutic approach in Parkinson's disease. *Drug News Perspect*, 13(5), 261-268.

Hirsch, E. C., & Hunot, S. (2009). Neuroinflammation in Parkinson's disease: a target for neuroprotection? *Lancet Neurol*, 8(4), 382-397.

Hoebe, K., Janssen, E. M., Kim, S. O., Alexopoulou, L., Flavell, R. A., Han, J., et al. (2003). Upregulation of costimulatory molecules induced by lipopolysaccharide and

double-stranded RNA occurs by Trif-dependent and Trif-independent pathways. *Nat Immunol*, 4(12), 1223-1229.

Hoek, R. M., Ruuls, S. R., Murphy, C. A., Wright, G. J., Goddard, R., Zurawski, S. M., et al. (2000). Down-regulation of the macrophage lineage through interaction with OX2 (CD200). *Science*, 290(5497), 1768-1771.

Hong, M. H., Xu, C., Wang, Y. J., Ji, J. L., Tao, Y. M., Xu, X. J., et al. (2009). Role of Src in ligand-specific regulation of delta-opioid receptor desensitization and internalization. *J Neurochem*, 108(1), 102-114.

Horvath, R. J., Natile-McMenemy, N., Alkaitis, M. S., & Deleo, J. A. (2008). Differential migration, LPS-induced cytokine, chemokine, and NO expression in immortalized BV-2 and HAPI cell lines and primary microglial cultures. *J Neurochem*, 107(2), 557-569.

Hughes, V. (2012). Microglia: The constant gardeners. *Nature*, 485(7400), 570-572.

Husebye, H., Halaas, O., Stenmark, H., Tunheim, G., Sandanger, O., Bogen, B., et al. (2006). Endocytic pathways regulate Toll-like receptor 4 signaling and link innate and adaptive immunity. *EMBO J*, 25(4), 683-692.

Hutchinson, M. R., Northcutt, A. L., Hiranita, T., Wang, X., Lewis, S. S., Thomas, J., et al. (2012). Opioid activation of toll-like receptor 4 contributes to drug reinforcement. *J Neurosci*, 32(33), 11187-11200.

Hutchinson, M. R., Zhang, Y., Shridhar, M., Evans, J. H., Buchanan, M. M., Zhao, T. X., et al. (2010). Evidence that opioids may have toll-like receptor 4 and MD-2 effects. *Brain Behav Immun*, 24(1), 83-95. doi: 10.1016/j.bbi.2009.1008.1004.

Ikeda, K., Yoshikawa, S., Kurokawa, T., Yuzawa, N., Nakao, K., & Mochizuki, H. (2009). TRK-820, a selective kappa opioid receptor agonist, could effectively ameliorate L-DOPA-induced dyskinesia symptoms in a rat model of Parkinson's disease. *Eur J Pharmacol*, 620(1-3), 42-48.

Irie, T., Muta, T., & Takeshige, K. (2000). TAK1 mediates an activation signal from toll-like receptor(s) to nuclear factor-kappaB in lipopolysaccharide-stimulated macrophages. *FEBS Lett*, 467(2-3), 160-164.

- Ivanov, I. S., Schulz, K. P., Palmero, R. C., & Newcorn, J. H. (2006). Neurobiology and evidence-based biological treatments for substance abuse disorders. *CNS Spectr*, 11(11), 864-877.
- Jack, C. S., Arbour, N., Manusow, J., Montgrain, V., Blain, M., McCrea, E., et al. (2005). TLR signaling tailors innate immune responses in human microglia and astrocytes. *J Immunol*, 175(7), 4320-4330.
- Janabi, N., Peudener, S., Heron, B., Ng, K. H., & Tardieu, M. (1995). Establishment of human microglial cell lines after transfection of primary cultures of embryonic microglial cells with the SV40 large T antigen. *Neurosci Lett*, 195(2), 105-108.
- Jin, M. S., Kim, S. E., Heo, J. Y., Lee, M. E., Kim, H. M., Paik, S. G., et al. (2007). Crystal structure of the TLR1-TLR2 heterodimer induced by binding of a tri-acylated lipopeptide. *Cell*, 130(6), 1071-1082.
- Jordan, B., & Devi, L. A. (1998). Molecular mechanisms of opioid receptor signal transduction. *Br J Anaesth*, 81(1), 12-19.
- Jutkiewicz, E. M. (2006). The antidepressant-like effects of delta-opioid receptor agonists. *Mol Interv*, 6(3), 162-169.
- Kagan, J. C., Su, T., Horng, T., Chow, A., Akira, S., & Medzhitov, R. (2008). TRAM couples endocytosis of Toll-like receptor 4 to the induction of interferon-beta. *Nat Immunol*, 9(4), 361-368. doi: 310.1038/ni1569.
- Kang, J. Y., Nan, X., Jin, M. S., Youn, S. J., Ryu, Y. H., Mah, S., et al. (2009). Recognition of lipopeptide patterns by Toll-like receptor 2-Toll-like receptor 6 heterodimer. *Immunity*, 31(6), 873-884. doi: 810.1016/j.immuni.2009.1009.1018.
- Kapitzke, D., Vetter, I., & Cabot, P. J. (2005). Endogenous opioid analgesia in peripheral tissues and the clinical implications for pain control. *Ther Clin Risk Manag*, 1(4), 279-297.
- Karin, M. (1999). How NF-kappaB is activated: the role of the IkappaB kinase (IKK) complex. *Oncogene*, 18(49), 6867-6874.

Kariv, R., Tiomny, E., Greshpon, R., Dekel, R., Waisman, G., Ringel, Y., et al. (2006). Low-dose naltrexone for the treatment of irritable bowel syndrome: a pilot study. *Dig Dis Sci*, 51(12), 2128-2133.

Kawai, T., & Akira, S. (2007). Signaling to NF-kappaB by Toll-like receptors. *Trends Mol Med*, 13(11), 460-469.

Kawai, T., & Akira, S. (2010). The role of pattern-recognition receptors in innate immunity: update on Toll-like receptors. *Nat Immunol*, 11(5), 373-384. doi: 310.1038/ni.1863.

Kawai, T., & Akira, S. (2011). Toll-like receptors and their crosstalk with other innate receptors in infection and immunity. *Immunity*, 34(5), 637-650.

Kettenmann, H., Hanisch, U. K., Noda, M., & Verkhratsky, A. (2011). Physiology of microglia. *Physiol Rev*, 91(2), 461-553.

Khandaker, M. H., Xu, L., Rahimpour, R., Mitchell, G., DeVries, M. E., Pickering, J. G., et al. (1998). CXCR1 and CXCR2 are rapidly down-modulated by bacterial endotoxin through a unique agonist-independent, tyrosine kinase-dependent mechanism. *J Immunol*, 161(4), 1930-1938.

Khandelwal, P. J., Herman, A. M., & Moussa, C. E. (2011). Inflammation in the early stages of neurodegenerative pathology. *J Neuroimmunol*, 238(1-2), 1-11.

Kieffer, B. L., & Evans, C. J. (2009). Opioid receptors: from binding sites to visible molecules in vivo. *Neuropharmacology*, 56(Suppl 1), 205-212. doi: 210.1016/j.neuropharm.2008.1007.1033.

Kielian, T. (2009). Overview of toll-like receptors in the CNS. *Curr Top Microbiol Immunol*, 336:1-14.(doi), 10.1007/1978-1003-1642-00549-00547-00541.

Korzhevskii, D. E., & Kirik, O. V. (2015). Brain Microglia and Microglial Markers. *Neuroscience and Behavioral Physiology*, 46(3), 284-290.

Kosten, T. R., & George, T. P. (2002). The neurobiology of opioid dependence: implications for treatment. *Sci Pract Perspect*, 1(1), 13-20.

Kovoor, A., Celver, J. P., Wu, A., & Chavkin, C. (1998). Agonist induced homologous desensitization of mu-opioid receptors mediated by G protein-coupled receptor kinases is dependent on agonist efficacy. *Mol Pharmacol*, 54(4), 704-711.

Kreutzberg, G. W. (1996). Microglia: a sensor for pathological events in the CNS. *Trends Neurosci*, 19(8), 312-318.

Kurt-Jones, E. A., Chan, M., Zhou, S., Wang, J., Reed, G., Bronson, R., et al. (2004). Herpes simplex virus 1 interaction with Toll-like receptor 2 contributes to lethal encephalitis. *Proc Natl Acad Sci U S A*, 101(5), 1315-1320.

Kurushima, H., Ramprasad, M., Kondratenko, N., Foster, D. M., Quehenberger, O., & Steinberg, D. (2000). Surface expression and rapid internalization of macrosialin (mouse CD68) on elicited mouse peritoneal macrophages. *J Leukoc Biol*, 67(1), 104-108.

Laflamme, N., & Rivest, S. (2001). Toll-like receptor 4: the missing link of the cerebral innate immune response triggered by circulating gram-negative bacterial cell wall components. *FASEB J*, 15(1), 155-163.

Lampron, A., Elali, A., & Rivest, S. (2013). Innate immunity in the CNS: redefining the relationship between the CNS and Its environment. *Neuron*, 78(2), 214-232.

Langsdorf, E. F., Mao, X., & Chang, S. L. (2011). A role for reactive oxygen species in endotoxin-induced elevation of MOR expression in the nervous and immune systems. *J Neuroimmunol*, 236(1-2), 57-64. doi: 10.1016/j.jneuroim.2011.1005.1009.

Lauw, F. N., Caffrey, D. R., & Golenbock, D. T. (2005). Of mice and man: TLR11 (finally) finds profilin. *Trends Immunol*, 26(10), 509-511.

Law, P. Y., & Loh, H. H. (2013). Opioid Receptors. *Signaling*, 354-358.

Lawson, L. J., Perry, V. H., & Gordon, S. (1992). Turnover of resident microglia in the normal adult mouse brain. *Neuroscience*, 48(2), 405-415.

Leavitt, S. B. (2009). Opioid Antagonists, Naloxone & Naltrexone- Aids for Pain Management: An Overview of Clinical Evidence. *Pain Innovations*, 1-16.



Lee, S., Lee, J., Kim, S., Park, J. Y., Lee, W. H., Mori, K., et al. (2007). A dual role of lipocalin 2 in the apoptosis and deramification of activated microglia. *J Immunol*, 179(5), 3231-3241.

Lee, S. C., Liu, W., Dickson, D. W., Brosnan, C. F., & Berman, J. W. (1993). Cytokine production by human fetal microglia and astrocytes. Differential induction by lipopolysaccharide and IL-1 beta. *J Immunol*, 150(7), 2659-2667.

Lee, Y. B., Nagai, A., & Kim, S. U. (2002). Cytokines, chemokines, and cytokine receptors in human microglia. *J Neurosci Res*, 69(1), 94-103.

Leong, S. K., & Ling, E. A. (1992). Amoeboid and ramified microglia: their interrelationship and response to brain injury. *Glia*, 6(1), 39-47.

Levine, J. D., Gordon, N. C., Taiwo, Y. O., & Coderre, T. J. (1988). Potentiation of pentazocine analgesia by low-dose naloxone. *J Clin Invest*, 82(5), 1574-1577.

Libby, P. (2007). Inflammatory mechanisms: the molecular basis of inflammation and disease. *Nutr Rev*, 65(12 Pt 2), S140-146.

Lin, S. C., Lo, Y. C., & Wu, H. (2010). Helical assembly in the MyD88-IRAK4-IRAK2 complex in TLR/IL-1R signalling. *Nature*, 465(7300), 885-890. doi: 810.1038/nature09121.

Lindberg, C., Crisby, M., Winblad, B., & Schultzberg, M. (2005). Effects of statins on microglia. *J Neurosci Res*, 82(1), 10-19.

Ling, E. A. (1979). Transformation of monocytes into amoeboid microglia in the corpus callosum of postnatal rats, as shown by labelling monocytes by carbon particles. *J Anat*, 128(Pt 4), 847-858.

Ling, E. A., & Wong, W. C. (1993). The origin and nature of ramified and amoeboid microglia: a historical review and current concepts. *Glia*, 7(1), 9-18.

Lisi, L., Laudati, E., Miscioscia, T. F., Dello Russo, C., Topai, A., & Navarra, P. (2015). Antiretrovirals inhibit arginase in human microglia. *J Neurochem*, 136(2), 363-72.

Liu, J. G., & Anand, K. J. (2001). Protein kinases modulate the cellular adaptations associated with opioid tolerance and dependence. *Brain Res Rev*, 38(1-2), 1-19.

Lu, Y. C., Yeh, W. C., & Ohashi, P. S. (2008). LPS/TLR4 signal transduction pathway. *Cytokine*, 42(2), 145-151. doi: 110.1016/j.cyto.2008.1001.1006.

Luo, X. G., & Chen, S. D. (2012). The changing phenotype of microglia from homeostasis to disease. *Transl Neurodegener*, 1(1), 9. doi: 10.1186/2047-9158-1181-1189.

Lv YN, O.-Y. A., Fu LS. (2016). MicroRNA-27a Negatively Modulates the Inflammatory Response in Lipopolysaccharide-Stimulated Microglia by Targeting TLR4 and IRAK4. *Cell Mol Neurobiol*, 37(2), 195-210. doi: 110.1007/s10571-10016-10361-10574.

Lynn, W. A., & Golenbock, D. T. (1992). Lipopolysaccharide antagonists. *Immunol Today*, 13(7), 271-276.

Mahajan, S. D., Schwartz, S. A., Aalinkeel, R., Chawda, R. P., Sykes, D. E., & Nair, M. P. (2005). Morphine modulates chemokine gene regulation in normal human astrocytes. *Clin Immunol*, 115(3), 323-332.

Maldonado, R., Valverde, O., Garbay, C., & Roques, B. P. (1995). Protein kinases in the locus coeruleus and periaqueductal gray matter are involved in the expression of opiate withdrawal. *Naunyn Schmiedebergs Arch Pharmacol*, 352(5), 565-575.

Mandrekar, S., Jiang, Q., Lee, C. Y., Koenigsknecht-Talboo, J., Holtzman, D. M., & Landreth, G. E. (2009). Microglia mediate the clearance of soluble Abeta through fluid phase macropinocytosis. *J Neurosci*, 29(13), 4252-4262.

Mannelli, P., Gottheil, E., & Van Bockstaele, E. J. (2006). Antagonist treatment of opioid withdrawal translational low dose approach. *J Addict Dis*, 25(2), 1-8.

Marchese, A., Paing, M. M., Temple, B. R., & Trejo, J. (2008). G protein-coupled receptor sorting to endosomes and lysosomes. *Annu Rev Pharmacol Toxicol*, 48, 601-629.

Mattioli, T. A., Milne, B., & Cahill, C. M. (2010). Ultra-low dose naltrexone attenuates chronic morphine-induced gliosis in rats. *Mol Pain*, 6:22.(doi), 10.1186/1744-8069-1186-1122.

- Matyszak, M. K. (1998). Inflammation in the CNS: balance between immunological privilege and immune responses. *Prog Neurobiol*, 56(1), 19-35.
- McDonald, J., & Lambert, D. G. (2005). Opioid receptors. *Continuing Education in Anaesthesia, Critical Care & Pain*, 5(1), 22-25.
- McDonald, J., & Lambert, D. G. (2011). Opioid mechanisms and opioid drugs. *Anaesthesia & Intensive Care Medicine*, 12(1), 31-35.
- Melief, J., Sneeboer, M. A., Litjens, M., Ormel, P. R., Palmen, S. J., Huitinga, I., et al. (2016). Characterizing primary human microglia: A comparative study with myeloid subsets and culture models. *Glia*, 64(11), 1857-1868. doi: 1810.1002/glia.23023.
- Mitrasinovic, O. M., Vincent, V. A., Simsek, D., & Murphy, G. M., Jr. (2003). Macrophage colony stimulating factor promotes phagocytosis by murine microglia. *Neurosci Lett*, 344(3), 185-188.
- Mollereau, C., & Mouledous, L. (2000). Tissue distribution of the opioid receptor-like (ORL1) receptor. *Peptides*, 21(7), 907-917.
- Monier, A., Adle-Biasette, H., Delezoide, A. L., Evrard, P., Gressens, P., & Verney, C. (2007). Entry and distribution of microglial cells in human embryonic and fetal cerebral cortex. *J Neuropathol Exp Neurol*, 66(5), 372-382.
- Monier, A., Evrard, P., Gressens, P., & Verney, C. (2006). Distribution and differentiation of microglia in the human encephalon during the first two trimesters of gestation. *J Comp Neurol*, 499(4), 565-582.
- Nagai, A., Mishima, S., Ishida, Y., Ishikura, H., Harada, T., Kobayashi, S., et al. (2005). Immortalized human microglial cell line: phenotypic expression. *J Neurosci Res*, 81(3), 342-348.
- Nagai, A., Nakagawa, E., Hatori, K., Choi, H. B., McLarnon, J. G., Lee, M. A., et al. (2001). Generation and characterization of immortalized human microglial cell lines: expression of cytokines and chemokines. *Neurobiol Dis*, 8(6), 1057-1068.
- Nagi, K., & Pineyro, G. (2011). Regulation of opioid receptor signalling: implications for the development of analgesic tolerance. *Mol Brain*, 4, 25.

- Napoli, I., & Neumann, H. (2010). Protective effects of microglia in multiple sclerosis. *Exp Neurol*, 225(1), 24-28. doi: 10.1016/j.expneurol.2009.1004.1024.
- Nelson, L., & Schwaner, R. (2009). Transdermal fentanyl: pharmacology and toxicology. *J Med Toxicol*, 5(4), 230-241.
- Neumann, H. (2001). Control of glial immune function by neurons. *Glia*, 36(2), 191-199.
- Neumann, H., Kotter, M. R., & Franklin, R. J. (2009). Debris clearance by microglia: an essential link between degeneration and regeneration. *Brain*, 132(Pt 2), 288-295. doi: 210.1093/brain/awn1109.
- Nimmerjahn, A., Kirchhoff, F., & Helmchen, F. (2005). Resting microglial cells are highly dynamic surveillants of brain parenchyma in vivo. *Science*, 308(5726), 1314-1318.
- Ninkovic, J., & Roy, S. (2013). Role of the mu-opioid receptor in opioid modulation of immune function. *Amino Acids*, 45(1), 9-24.
- O'Neill, L. A. (2006). How Toll-like receptors signal: what we know and what we don't know. *Curr Opin Immunol*, 18(1), 3-9.
- O'Neill, L. A., & Bowie, A. G. (2007). The family of five: TIR-domain-containing adaptors in Toll-like receptor signalling. *Nat Rev Immunol*, 7(5), 353-364.
- Okun, E., Griffioen, K. J., & Mattson, M. P. (2011). Toll-like receptor signaling in neural plasticity and disease. *Trends Neurosci*, 34(5), 269-281.
- Olmstead, M. C., & Burns, L. H. (2005). Ultra-low-dose naltrexone suppresses rewarding effects of opiates and aversive effects of opiate withdrawal in rats. *Psychopharmacology (Berl.)*, 181(3), 576-581.
- Ordaz-Sanchez, I., Weber, R. J., Rice, K. C., Zhang, X., Rodriguez-Padilla, C., Tamez-Guerra, R., et al. (2003). Chemotaxis of human and rat leukocytes by the delta-selective non-peptidic opioid SNC 80. *Rev Latinoam Microbiol*, 45(1-2), 16-23.
- Orihuela, R., McPherson, C. A., & Harry, G. J. (2016). Microglial M1/M2 polarization and metabolic states. *Br J Pharmacol*, 173(4), 649-665. doi: 610.1111/bph.13139.

- Palsson-McDermott, E. M., & O'Neill, L. A. (2004). Signal transduction by the lipopolysaccharide receptor, Toll-like receptor-4. *Immunology*, 113(2), 153-162.
- Park, B. S., Song, D. H., Kim, H. M., Choi, B. S., Lee, H., & Lee, J. O. (2009). The structural basis of lipopolysaccharide recognition by the TLR4-MD-2 complex. *Nature*, 458(7242), 1191-1195. doi: 1110.1038/nature07830.
- Pasare, C., & Medzhitov, R. (2004). Toll-like receptors: linking innate and adaptive immunity. *Microbes Infect*, 6(15), 1382-1387.
- Pedchenko, T. V., Park, G. Y., Joo, M., Blackwell, T. S., & Christman, J. W. (2005). Inducible binding of PU.1 and interacting proteins to the Toll-like receptor 4 promoter during endotoxemia. *Am J Physiol Lung Cell Mol Physiol*, 289(3), L429-437.
- Pedras-Vasconcelos, J., Puig, M., & Verthelyi, D. (2009). TLRs as therapeutic targets in CNS inflammation and infection. *Front Biosci (Elite Ed)*, 1, 476-487.
- Pello, O. M., Duthey, B., Garcia-Bernal, D., Rodriguez-Frade, J. M., Stein, J. V., Teixeira, J., et al. (2006). Opioids trigger alpha 5 beta 1 integrin-mediated monocyte adhesion. *J Immunol*, 176(3), 1675-1685.
- Peluso, J., LaForge, K. S., Matthes, H. W., Kreek, M. J., Kieffer, B. L., & Gaveriaux-Ruff, C. (1998). Distribution of nociceptin/orphanin FQ receptor transcript in human central nervous system and immune cells. *J Neuroimmunol*, 81(1-2), 184-192.
- Perez-Castrillon, J. L., Perez-Arellano, J. L., Garcia-Palomo, J. D., Jimenez-Lopez, A., & De Castro, S. (1992). Opioids depress in vitro human monocyte chemotaxis. *Immunopharmacology*, 23(1), 57-61.
- Perry, V. H., & Teeling, J. (2013). Microglia and macrophages of the central nervous system: the contribution of microglia priming and systemic inflammation to chronic neurodegeneration. *Semin Immunopathol*, 35(5), 601-612. doi: 10.1007/s00281-00013-00382-00288.
- Peterson, A. A., & McGroarty, E. J. (1985). High-molecular-weight components in lipopolysaccharides of *Salmonella typhimurium*, *Salmonella minnesota*, and *Escherichia coli*. *J Bacteriol*, 162(2), 738-745.

Peudener, S., Hery, C., Montagnier, L., & Tardieu, M. (1991). Human microglial cells: characterization in cerebral tissue and in primary culture, and study of their susceptibility to HIV-1 infection. *Ann Neurol*, 29(2), 152-161.

Ponomarev, E. D., Shriver, L. P., & Dittel, B. N. (2006). CD40 expression by microglial cells is required for their completion of a two-step activation process during central nervous system autoimmune inflammation. *J Immunol*, 176(3), 1402-1410.

Poyhia, R., Seppala, T., Olkkola, K. T., & Kalso, E. (1992). The pharmacokinetics and metabolism of oxycodone after intramuscular and oral administration to healthy subjects. *Br J Clin Pharmacol*, 33(6), 617-621.

Pulford, K. A., Sipos, A., Cordell, J. L., Stross, W. P., & Mason, D. Y. (1990). Distribution of the CD68 macrophage/myeloid associated antigen. *Int Immunol*, 2(10), 973-980.

Qian, L., Tan, K. S., Wei, S. J., Wu, H. M., Xu, Z., Wilson, B., et al. (2007). Microglia-mediated neurotoxicity is inhibited by morphine through an opioid receptor-independent reduction of NADPH oxidase activity. *J Immunol*, 179(2), 1198-1209.

Qiu, Y., Loh, H. H., & Law, P. Y. (2007). Phosphorylation of the delta-opioid receptor regulates its beta-arrestins selectivity and subsequent receptor internalization and adenylyl cyclase desensitization. *J Biol Chem*, 282(31), 22315-22323.

Quaglio, G. L., Lugoboni, F., Pajusco, B., Sarti, M., Talamini, G., Mezzelani, P., et al. (2003). Hepatitis C virus infection: prevalence, predictor variables and prevention opportunities among drug users in Italy. *J Viral Hepat*, 10(5), 394-400.

Ramprasad, M. P., Terpstra, V., Kondratenko, N., Quehenberger, O., & Steinberg, D. (1996). Cell surface expression of mouse macrosialin and human CD68 and their role as macrophage receptors for oxidized low density lipoprotein. *Proc Natl Acad Sci U S A*, 93(25), 14833-14838.

Reisine, T. (1996). Opioid analgesics and antagonists. *Goodman & Gilman's the pharmacological basis of therapeutics*.

Rietschel, E. T., Brade, H., Brade, L., Brandenburg, K., Schade, U., Seydel, U., et al. (1987). Lipid A, the endotoxic center of bacterial lipopolysaccharides: relation of chemical structure to biological activity. *Prog Clin Biol Res*, 231, 25-53.

- Rietschel, E. T., Kirikae, T., Schade, F. U., Mamat, U., Schmidt, G., Loppnow, H., et al. (1994). Bacterial endotoxin: molecular relationships of structure to activity and function. *FASEB J*, 8(2), 217-225.
- Righi, M., Mori, L., De Libero, G., Sironi, M., Biondi, A., Mantovani, A., et al. (1989). Monokine production by microglial cell clones. *Eur J Immunol*, 19(8), 1443-1448.
- Rivest, S. (2009). Regulation of innate immune responses in the brain. *Nat Rev Immunol*, 9(6), 429-439.
- Rock, R. B., Gekker, G., Hu, S., Sheng, W. S., Cheeran, M., Lokensgard, J. R., et al. (2004). Role of microglia in central nervous system infections. *Clin Microbiol Rev*, 17(4), 942-964, table of contents.
- Roodveldt, C., Christodoulou, J., & Dobson, C. M. (2008). Immunological features of alpha-synuclein in Parkinson's disease. *J Cell Mol Med*, 12(5B), 1820-1829.
- Roy, S., Cain, K. J., Chapin, R. B., Charboneau, R. G., & Barke, R. A. (1998). Morphine modulates NF kappa B activation in macrophages. *Biochem Biophys Res Commun*, 245(2), 392-396.
- Roy, S., Wang, J., Kelschenbach, J., Koodie, L., & Martin, J. (2006). Modulation of immune function by morphine: implications for susceptibility to infection. *J Neuroimmune Pharmacol*, 1(1), 77-89.
- Saito, N., Pulford, K. A., Breton-Gorius, J., Masse, J. M., Mason, D. Y., & Cramer, E. M. (1991). Ultrastructural localization of the CD68 macrophage-associated antigen in human blood neutrophils and monocytes. *Am J Pathol*, 139(5), 1053-1059.
- Sasaki, A. (2016). Microglia and brain macrophages: An update. *Neuropathology*, 12354.
- Sato, S., Sanjo, H., Takeda, K., Ninomiya-Tsuji, J., Yamamoto, M., Kawai, T., et al. (2005). Essential function for the kinase TAK1 in innate and adaptive immune responses. *Nat Immunol*, 6(11), 1087-1095. Epub 2005 Sep 1025.
- Schilling, T., Nitsch, R., Heinemann, U., Haas, D., & Eder, C. (2001). Astrocyte-released cytokines induce ramification and outward K<sup>+</sup> channel expression in microglia via distinct signalling pathways. *Eur J Neurosci*, 14(3), 463-473.

Schumann, R. R., Leong, S. R., Flaggs, G. W., Gray, P. W., Wright, S. D., Mathison, J. C., et al. (1990). Structure and function of lipopolysaccharide binding protein. *Science*, 249(4975), 1429-1431.

Sebire, G., Emilie, D., Wallon, C., Hery, C., Devergne, O., Delfraissy, J. F., et al. (1993). In vitro production of IL-6, IL-1 beta, and tumor necrosis factor-alpha by human embryonic microglial and neural cells. *J Immunol*, 150(4), 1517-1523.

Sedgwick, J. D., Schwender, S., Imrich, H., Dorries, R., Butcher, G. W., & ter Meulen, V. (1991). Isolation and direct characterization of resident microglial cells from the normal and inflamed central nervous system. *Proc Natl Acad Sci U S A*, 88(16), 7438-7442.

Self, D. W., & Nestler, E. J. (1995). Molecular mechanisms of drug reinforcement and addiction. *Annu Rev Neurosci*, 18, 463-495.

Shen, K. F., & Crain, S. M. (1997). Ultra-low doses of naltrexone or etorphine increase morphine's antinociceptive potency and attenuate tolerance/dependence in mice. *Brain Res*, 757(2), 176-190.

Sheng, W., Zong, Y., Mohammad, A., Ajit, D., Cui, J., Han, D., et al. (2011). Pro-inflammatory cytokines and lipopolysaccharide induce changes in cell morphology, and upregulation of ERK1/2, iNOS and sPLA(2)-IIA expression in astrocytes and microglia. *J Neuroinflammation*, 8, 121.

Shimazu, R., Akashi, S., Ogata, H., Nagai, Y., Fukudome, K., Miyake, K., et al. (1999). MD-2, a molecule that confers lipopolysaccharide responsiveness on Toll-like receptor 4. *J Exp Med*, 189(11), 1777-1782.

Simonin, F., Gaveriaux-Ruff, C., Befort, K., Matthes, H., Lannes, B., Micheletti, G., et al. (1995). kappa-Opioid receptor in humans: cDNA and genomic cloning, chromosomal assignment, functional expression, pharmacology, and expression pattern in the central nervous system. *Proc Natl Acad Sci U S A*, 92(15), 7006-7010.

Sloan, P., & Hamann, S. (2006). Ultra-low-dose opioid antagonists to enhance opioid analgesia. *J Opioid Manag*, 2(5), 295-304.

Smith, J. P., Stock, H., Bingaman, S., Mauger, D., Rogosnitzky, M., & Zagon, I. S. (2007). Low-dose naltrexone therapy improves active Crohn's disease. *Am J Gastroenterol*, 102(4), 820-828.



Snyder, S. H., & Pasternak, G. W. (2003). Historical review: Opioid receptors. *Trends Pharmacol Sci*, 24(4), 198-205.

Stanley, T. H. (1992). The history and development of the fentanyl series. *J Pain Symptom Manage*, 7(3 Suppl), S3-7.

Stansley, B., Post, J., & Hensley, K. (2012). A comparative review of cell culture systems for the study of microglial biology in Alzheimer's disease. *J Neuroinflammation*, 9:115.(doi), 10.1186/1742-2094-1189-1115.

Stein, C., Schafer, M., & Machelska, H. (2003). Attacking pain at its source: new perspectives on opioids. *Nat Med*, 9(8), 1003-1008.

Stein, M., Keshav, S., Harris, N., & Gordon, S. (1992). Interleukin 4 potently enhances murine macrophage mannose receptor activity: a marker of alternative immunologic macrophage activation. *J Exp Med*, 176(1), 287-292.

Stevens. (2009). The evolution of vertebrate opioid receptors. *Front Biosci (Landmark Ed)*, 14, 1247-1269.

Stevens, Aravind, Das, & Davis. (2013). Pharmacological characterization of LPS and opioid interactions at the toll - like receptor 4. *British journal of pharmacology*, 168(6), 1421-1429.

Stewart, C. R., Stuart, L. M., Wilkinson, K., van Gils, J. M., Deng, J., Halle, A., et al. (2010). CD36 ligands promote sterile inflammation through assembly of a Toll-like receptor 4 and 6 heterodimer. *Nat Immunol*, 11(2), 155-161. doi: 110.1038/ni.1836.

Suh, H. S., Zhao, M. L., Choi, N., Belbin, T. J., Brosnan, C. F., & Lee, S. C. (2009). TLR3 and TLR4 are innate antiviral immune receptors in human microglia: role of IRF3 in modulating antiviral and inflammatory response in the CNS. *Virology*, 392(2), 246-259.

Suresh, S., & Anand, K. J. (1998). Opioid tolerance in neonates: mechanisms, diagnosis, assessment, and management. *Semin Perinatol*, 22(5), 425-433.

Suzumura, A., Marunouchi, T., & Yamamoto, H. (1991). Morphological transformation of microglia in vitro. *Brain Res*, 545(1-2), 301-306.

Suzumura, A., Sawada, M., Yamamoto, H., & Marunouchi, T. (1990). Effects of colony stimulating factors on isolated microglia in vitro. *J Neuroimmunol*, 30(2-3), 111-120.

Takemori, A. E., Larson, D. L., & Portoghese, P. S. (1981). The irreversible narcotic antagonistic and reversible agonistic properties of the fumaramate methyl ester derivative of naltrexone. *Eur J Pharmacol*, 70(4), 445-451.

Takemori, A. E., & Portoghese, P. S. (1985). Affinity labels for opioid receptors. *Annu Rev Pharmacol Toxicol*, 25, 193-223.

Takeuchi, O., & Akira, S. (2001). Toll-like receptors; their physiological role and signal transduction system. *Int Immunopharmacol*, 1(4), 625-635.

Takeuchi, O., & Akira, S. (2010). Pattern recognition receptors and inflammation. *Cell*, 140(6), 805-820.

Tan, J., Town, T., Mori, T., Wu, Y., Saxe, M., Crawford, F., et al. (2000). CD45 opposes beta-amyloid peptide-induced microglial activation via inhibition of p44/42 mitogen-activated protein kinase. *J Neurosci*, 20(20), 7587-7594.

Tian, B., Nowak, D. E., & Brasier, A. R. (2005). A TNF-induced gene expression program under oscillatory NF-kappaB control. *BMC Genomics*, 6, 137.

Tobias, P. S., Mathison, J. C., & Ulevitch, R. J. (1988). A family of lipopolysaccharide binding proteins involved in responses to gram-negative sepsis. *J Biol Chem*, 263(27), 13479-13481.

Trescot, A. M., Datta, S., Lee, M., & Hansen, H. (2008). Opioid pharmacology. *Pain Physician*, 11(2 Suppl), S133-153.

Uematsu, S., & Akira, S. (2008). Toll-Like receptors (TLRs) and their ligands. *Handb Exp Pharmacol*, (183), 1-20.

Vallejo, R., de Leon-Casasola, O., & Benyamin, R. (2004). Opioid therapy and immunosuppression: a review. *Am J Ther*, 11(5), 354-365.

Varvel, N. H., Grathwohl, S. A., Baumann, F., Liebig, C., Bosch, A., Brawek, B., et al. (2012). Microglial repopulation model reveals a robust homeostatic process for replacing

CNS myeloid cells. *Proc Natl Acad Sci U S A*, 109(44), 18150-18155. doi: 18110.11073/pnas.1210150109. Vaughan, D. W., & Peters, A. (1974). Neuroglial cells in the cerebral cortex of rats from young adulthood to old age: an electron microscope study. *J Neurocytol.*, 3(4), 405-429.

Volpi, N. (2003). Separation of Escherichia coli 055:B5 lipopolysaccharide and detoxified lipopolysaccharide by high-performance capillary electrophoresis. *Electrophoresis*, 24(17), 3097-3103.

Waldhoer, M., Bartlett, S. E., & Whistler, J. L. (2004). Opioid receptors. *Annu Rev Biochem*, 73, 953-990.

Wang, Friedman, E., Olmstead, M. C., & Burns, L. H. (2005). Ultra-low-dose naloxone suppresses opioid tolerance, dependence and associated changes in mu opioid receptor-G protein coupling and Gbetagamma signaling. *Neuroscience*, 135(1), 247-261.

Wang, Loram, L. C., Ramos, K., de Jesus, A. J., Thomas, J., Cheng, K., et al. (2012a). Morphine activates neuroinflammation in a manner parallel to endotoxin. *Proceedings of the National Academy of Sciences*, 109(16), 6325-6330.

Wang, J., Shao, Y., Bennett, T. A., Shankar, R. A., Wightman, P. D., & Reddy, L. G. (2006). The functional effects of physical interactions among Toll-like receptors 7, 8, and 9. *J Biol Chem*, 281(49), 37427-37434. Epub 32006 Oct 37413.

Wang, P., You, S. W., Yang, Y. J., Wei, X. Y., Wang, Y. Z., Wang, X., et al. (2014). Systemic injection of low-dose lipopolysaccharide fails to break down the blood-brain barrier or activate the TLR4-MyD88 pathway in neonatal rat brain. *Int J Mol Sci*, 15(6), 10101-10115.

Wang, X., Loram, L. C., Ramos, K., de Jesus, A. J., Thomas, J., Cheng, K., et al. (2012b). Morphine activates neuroinflammation in a manner parallel to endotoxin. *Proc Natl Acad Sci U S A*, 109(16), 6325-6330.

Wang, Y., Li, Y., & Shi, G. (2013). The regulating function of heterotrimeric G proteins in the immune system. *Arch Immunol Ther Exp (Warsz)*, 61(4), 309-319.

Ward, S. J., Portoghese, P. S., & Takemori, A. E. (1982). Pharmacological characterization in vivo of the novel opiate, beta-funaltrexamine. *J Pharmacol Exp Ther*, 220(3), 494-498.

Webster, L. R., Butera, P. G., Moran, L. V., Wu, N., Burns, L. H., & Friedmann, N. (2006). Oxytrex minimizes physical dependence while providing effective analgesia: a randomized controlled trial in low back pain. *J Pain*, 7(12), 937-946.

Wee Yong, V. (2010). Inflammation in neurological disorders: a help or a hindrance? *Neuroscientist*, 16(4), 408-420.

Wei, R., & Jonakait, G. M. (1999). Neurotrophins and the anti-inflammatory agents interleukin-4 (IL-4), IL-10, IL-11 and transforming growth factor-beta1 (TGF-beta1) down-regulate T cell costimulatory molecules B7 and CD40 on cultured rat microglia. *J Neuroimmunol*, 95(1-2), 8-18.

Weiss, J. (2003). Bactericidal/permeability-increasing protein (BPI) and lipopolysaccharide-binding protein (LBP): structure, function and regulation in host defence against Gram-negative bacteria. *Biochem Soc Trans*, 31(Pt 4), 785-790.

Westphal, O., Luderitz, O., Rietschel, E. T., & Galanos, C. (1981). Bacterial lipopolysaccharide and its lipid A component: some historical and some current aspects. *Biochem Soc Trans*, 9(3), 191-195.

Whistler, J. L., Enquist, J., Marley, A., Fong, J., Gladher, F., Tsuruda, P., et al. (2002). Modulation of postendocytic sorting of G protein-coupled receptors. *Science*, 297(5581), 615-620.

Williams, J. T., Ingram, S. L., Henderson, G., Chavkin, C., von Zastrow, M., Schulz, S., et al. (2013). Regulation of mu-opioid receptors: desensitization, phosphorylation, internalization, and tolerance. *Pharmacol Rev*, 65(1), 223-254.

Wollmer, M. A., Lucius, R., Wilms, H., Held-Feindt, J., Sievers, J., & Mentlein, R. (2001). ATP and adenosine induce ramification of microglia in vitro. *J Neuroimmunol*, 115(1-2), 19-27.

Wright, S. D., Ramos, R. A., Tobias, P. S., Ulevitch, R. J., & Mathison, J. C. (1990). CD14, a receptor for complexes of lipopolysaccharide (LPS) and LPS binding protein. *Science*, 249(4975), 1431-1433.

Wu, C. F., Bi, X. L., Yang, J. Y., Zhan, J. Y., Dong, Y. X., Wang, J. H., et al. (2007). Differential effects of ginsenosides on NO and TNF-alpha production by LPS-activated N9 microglia. *Int Immunopharmacol*, 7(3), 313-320.

Yamamoto, M., Sato, S., Mori, K., Hoshino, K., Takeuchi, O., Takeda, K., et al. (2002). Cutting edge: a novel Toll/IL-1 receptor domain-containing adapter that preferentially activates the IFN-beta promoter in the Toll-like receptor signaling. *J Immunol*, 169(12), 6668-6672.

Yoon, H. M., Jang, K. J., Han, M. S., Jeong, J. W., Kim, G. Y., Lee, J. H., et al. (2013). Ganoderma lucidum ethanol extract inhibits the inflammatory response by suppressing the NF-kappaB and toll-like receptor pathways in lipopolysaccharide-stimulated BV2 microglial cells. *Exp Ther Med*, 5(3), 957-963. Epub 2013 Jan 2015.

Zanoni, I., Ostuni, R., Marek, L. R., Barresi, S., Barbalat, R., Barton, G. M., et al. (2011). CD14 controls the LPS-induced endocytosis of Toll-like receptor 4. *Cell*, 147(4), 868-880. doi: 10.1016/j.cell.2011.1009.1051.

Zhang, D., Zhang, G., Hayden, M. S., Greenblatt, M. B., Bussey, C., Flavell, R. A., et al. (2004). A toll-like receptor that prevents infection by uropathogenic bacteria. *Science*, 303(5663), 1522-1526.

Zhang, W., Wang, T., Pei, Z., Miller, D. S., Wu, X., Block, M. L., et al. (2005a). Aggregated alpha-synuclein activates microglia: a process leading to disease progression in Parkinson's disease. *Faseb J*, 19(6), 533-542.

Zhang, X., Wang, F., Chen, X., Li, J., Xiang, B., Zhang, Y. Q., et al. (2005b). Beta-arrestin1 and beta-arrestin2 are differentially required for phosphorylation-dependent and -independent internalization of delta-opioid receptors. *J Neurochem*, 95(1), 169-178.

Zipp, F., & Aktas, O. (2006). The brain as a target of inflammation: common pathways link inflammatory and neurodegenerative diseases. *Trends Neurosci*, 29(9), 518-527.

## VITA

Leandra K. Figueroa-Hall

Doctor of Philosophy

Thesis: TLR4 NEUROINFLAMMATORY SIGNALING AND THE ANTI-INFLAMMATORY EFFECTS OF FENTANYL AND MORPHINE IN CHME-5 MICROGLIAL CELLS

Major Field: Biomedical Sciences

Biographical:

Education:

Completed the requirements for the Doctor of Philosophy in Biomedical Sciences at Oklahoma State University-Center for Health Sciences, Tulsa, Oklahoma in July 2017.

Completed the requirements for the Master of Science in Biomedical Research at the University of Maryland, School of Medicine, Baltimore, MD in December 2011.

Completed the requirements for the Bachelor of Science in Biology at the University of the Virgin Islands, St. Thomas, USVI in June 2008.

Experience:

Graduate Research Assistant in the Laboratory of Dr. Randall L. Davis at Oklahoma State University-Center for Health Sciences from 2011 to 2017

Graduate Research Assistant in the Laboratory of Dr. Andrei E. Medvedev at the University of Maryland, School of Medicine from 2009 to 2011.

Professional Memberships:

American Association of Immunologists (AAI), Society for Neuroscience (SFN), The American Physiological Society (APS), American Society for Pharmacology and Experimental Therapeutics (ASPET), Society for the Advancement of Chicanos/Hispanics and Native Americans in Science (SACNAS)